



2

**SYNTHESIS AND STRUCTURAL CHARACTERIZATION OF  
NEW HIGH-VALENT INORGANIC FLUORINE COMPOUNDS  
AND THEIR OXIDIZING PROPERTIES:**

**VOLUME 3.**

**Prof. G.J. Schrobilgen**

**Mc Master University  
Department of Chemistry  
Hamilton, Ontario L8S 4M1  
Canada**

**DTIC**  
**S ELECTE D**  
**A JUN 16 1992**

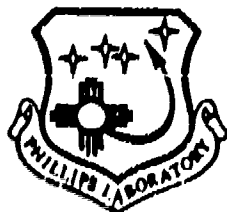
**February 1992**

**Final Report**

**APPROVED FOR PUBLIC RELEASE; DISTRIBUTION UNLIMITED**

**92 6 15 065**

**92-15526**



**PHILLIPS LABORATORY  
Propulsion Directorate  
AIR FORCE SYSTEMS COMMAND  
EDWARDS AIR FORCE BASE CA 93523-5000**

## NOTICE

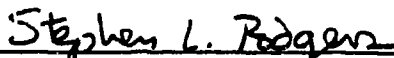
When U.S. Government drawings, specifications, or other data are used for any purpose other than a definitely related Government procurement operation, the fact that the Government may have formulated, furnished, or in any way supplied the said drawings, specifications, or other data, is not to be regarded by implication or otherwise, or in any way licensing the holder or any other person or corporation, or conveying any rights or permission to manufacture, use or sell any patented invention that may be related thereto.

## FOREWORD


This final report was prepared by McMaster University, Hamilton, Ontario, Canada under contract F49620-87-C-0049 for Operating Location AC, Phillips Laboratory (AFSC), Edwards AFB CA 93523-5000. OLAC PL Project Manager was 1Lt Robert A. mantz.

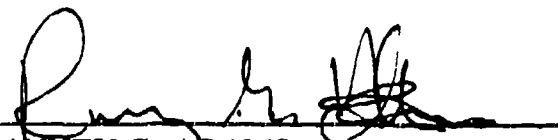
This report has been reviewed and is approved for release and distribution in accordance with the distribution statement on the cover and on the SF Form 298.

  
\_\_\_\_\_  
ROBERT A. MANTZ, 1Lt, USAF  
Project Manager

  
\_\_\_\_\_  
STEPHEN L. RODGERS  
Chief, Emerging Technologies Branch

### FOR THE COMMANDER

  
\_\_\_\_\_  
DAVID W. LEWIS, Major, USAF  
Acting Director,  
Fundamental Technologies Division

  
\_\_\_\_\_  
RANNEY G. ADAMS  
Public Affairs Director

REPORT DOCUMENTATION PAGE			Form Approved OMB No. 0704-0188	
<small>Public reporting burden for this collection of information is estimated to average 1 hour per response, including the time for reviewing instructions, searching existing data sources, gathering and maintaining the data needed, and completing and reviewing the collection of information. Send comments regarding this burden estimate or any other aspect of this collection of information, including suggestions for reducing this burden, to Washington Headquarters Services, Directorate for Information Operations and Reports, 1215 Jefferson Davis Highway, Suite 1204, Arlington, VA 22202-4302, and to the Office of Management and Budget, Paperwork Reduction Project (0704-0188), Washington, DC 20503</small>				
1. AGENCY USE ONLY (Leave blank)	2. REPORT DATE February 1992	3. REPORT TYPE AND DATES COVERED Final-1 May 1987 to 30 April 1991		
4. TITLE AND SUBTITLE SYNTHESIS AND STRUCTURAL CHARACTERIZATION OF NEW HIGH-VALENT INORGANIC FLUORINE COMPOUNDS AND THEIR OXIDIZING PROPERTIES		5. FUNDING NUMBERS C - F49620-87-C-0049 PR- 5730 TA- 007G		
6. AUTHOR(S) G.J. Schrobilgen				
7. PERFORMING ORGANIZATION NAME(S) AND ADDRESS(ES) McMaster University Department of Chemistry Hamilton, Ontario L8S 4M1 Canada		8. PERFORMING ORGANIZATION REPORT NUMBER		
9. SPONSORING/MONITORING AGENCY NAME(S) AND ADDRESS(ES) Phillips Laboratory (AFSC) OLAC PL/RKFE Edwards AFB CA 93523-5000		10. SPONSORING/MONITORING AGENCY REPORT NUMBER PL-TR-91-3108 Volume		
11. SUPPLEMENTARY NOTES Phillips Laboratory, Edwards is the former Astronautics Laboratory. COSATI Code: 07/02				
12a. DISTRIBUTION/AVAILABILITY STATEMENT Approved for Public Release; Distribution is unlimited.			12b. DISTRIBUTION CODE	
13. ABSTRACT (Maximum 200 words)  Noble gas fluorine oxidizers of Neon, Krypton, Argon, and Xenon have been synthesized and characterized. $KrF^+$ and $XeF^+$ cations have been made with neutral organic bases. Kr-N and Kr-O bonded molecules are also synthesized and characterized. The hypervalent compounds $ClF_6^-$ and $XeF_5^-$ are made. The anions $IF_6O^-$ , $TeF_6O^{2-}$ , $TeF_7^-$ and $TeF_8^{2-}$ anions are also made. Proof that the $ClF_6^-$ anion exists is also presented. The photoelectron spectra of $XeF_2$ , $XeF_4$ , and $XeF_6$ are obtained using monochromatized synchrotron radiation. The synthesis and characterization of $Sb(OTeF_5)_6^- Et_4N^+$ , and $Bi(OTeF_5)_6^- Et_4N^+$ salts is completed. Radiotracer experiments involving $^{18}F$ are also accomplished to show the inability to synthesize $NF_5$ is due to mainly steric reasons.				
14. SUBJECT TERMS  fluorine, oxidizers, noble gas, NMR, photoelectron, HEDM.			15. NUMBER OF PAGES 166	
			16. PRICE CODE	
17. SECURITY CLASSIFICATION OF REPORT UNCLASSIFIED	18. SECURITY CLASSIFICATION OF THIS PAGE UNCLASSIFIED	19. SECURITY CLASSIFICATION OF ABSTRACT UNCLASSIFIED	20. LIMITATION OF ABSTRACT SAR	

## PART IX

### HIGH-RESOLUTION PHOTOELECTRON SPECTRA OF $\text{XeF}_2$ , $\text{XeF}_4$ AND $\text{XeF}_6$ ; EVIDENCE FOR NON-OCTAHEDRAL $\text{XeF}_6$

Accession For	
NTIS CRAB	<input checked="" type="checkbox"/>
DTIC TAB	<input type="checkbox"/>
Unannounced	<input type="checkbox"/>
Justification	
By	
Distribution /	
Availability Codes	
Dist	Avail and/or Special
A-1	



LIGAND FIELD SPLITTING ON THE Xe 4d CORE  
LEVELS IN XeF<sub>x</sub> (x = 2, 4, 6) COMPOUNDS FROM  
HIGH RESOLUTION GAS PHASE PHOTOELECTRON  
SPECTRA: THE STRUCTURE OF XeF<sub>6</sub>

J.N. Cutler, G.M. Bancroft, J.D. Bozek and R.H. Tan

Department of Chemistry and Centre for Chemical Physics  
University of Western Ontario  
London, Ontario  
Canada N6A 5B7

and

Canadian Synchrotron Radiation Facility  
Synchrotron Radiation Centre  
University of Wisconsin  
Stoughton, Wisconsin 53589  
U.S.A.

and

G.J. Schrobilgen

Department of Chemistry  
McMaster University  
Hamilton, Ontario  
Canada L8S 4M1

## ABSTRACT

Using monochromatized synchrotron radiation, high resolution (total linewidths of  $\sim 0.2$  eV) Xe 4d photoelectron spectra are reported for the three xenon fluorides,  $\text{XeF}_x$  ( $x = 2, 4, 6$ ). The splitting of the Xe  $4d_{3/2}$  and  $4d_{5/2}$  core levels is due to the ligand field splitting on the Xe 4d ion state. The splitting is due to the asymmetric  $C_2^0$  crystal field term, which transforms like the electric field gradient as normally measured by Mössbauer spectroscopy or NQR.

The appreciable ligand field splitting in  $\text{XeF}_6$  shows immediately that  $\text{XeF}_6$  is considerably distorted from octahedral symmetry. Quantitatively, we have derived the bond angles for the  $C_{3v}$ ,  $\text{XeF}_6$  structure using the  $C_2^0$  for  $\text{XeF}_6$  and an additive treatment which has been shown to work well for  $e^2qQ$  values, giving estimates of  $\theta_{1,2,3} = 50 \pm 2^\circ$  and  $\theta_{4,5,6} = 76 \pm 4^\circ$ . These values are in good agreement with the latest theoretical determinations for these angles.



## INTRODUCTION

Since the discovery of the first noble-gas compounds in 1962<sup>1</sup>, the xenon fluorides ( $\text{XeF}_2$ ,  $\text{XeF}_4$ , and  $\text{XeF}_6$ ) have been of great chemical interest. The geometric and electronic structures of  $\text{XeF}_2$  and  $\text{XeF}_4$  have been investigated by different spectroscopic<sup>1-4</sup> and theoretical techniques.<sup>1,5-10</sup> A model based on a three-center four electron bond, similar to that applied to  $\text{CO}_2$ , has been used to explain the bonding in the hypervalent structures of  $\text{XeF}_2$  ( $D_{\infty h}$ , linear) and  $\text{XeF}_4$  ( $D_{4h}$ , square planar).<sup>11,12</sup>

Although the structures and bonding for  $\text{XeF}_2$  and  $\text{XeF}_4$  have been widely accepted for many years, the structure of  $\text{XeF}_6$  in the gas phase has remained a puzzle for theoreticians and experimentalists to this day. (The complex solid state structure has been determined<sup>13</sup>: a cubic unit cell contains 24 tetramers and 9 hexamers of  $\text{XeF}_6$  in which  $\text{XeF}_5^+$  units are bound through fluorine bridges). According to the three-center four electron model, gas phase  $\text{XeF}_6$  should have an octahedral structure. On the other hand, simple valence-shell electron repulsion rules (VSEPR)<sup>14,15</sup> predict that  $\text{XeF}_6$  should be a monocapped octahedron with a sterically lone pair of electrons.

Early electron diffraction work on  $\text{XeF}_6$  by Gavin and Bartell<sup>16</sup> and Pitzer and Bernstein<sup>17</sup> was explained by a single  $C_{3v}$  configuration with large non-bonded vibrational amplitudes which distorted the molecule from an octahedral structure along a soft  $t_{1u}$  bending mode. This structure was supported by infrared and Raman studies of Claassen et al<sup>18</sup> who reported many more vibrational frequencies than should be expected of an  $O_h$  molecule vibrating harmonically.

Later electric field deflection results<sup>19</sup> showed a substantially smaller dipole moment ( $\approx$



O D) than should be observed in the structure determined by Gavin and Bartell<sup>16</sup>. This was explained by a second order Jahn-Teller pseudorotation along a large amplitude  $T_{1u}$  bending mode which was coupled with the  $T_{2g}$  bending mode.

Several theoretical calculations have been undertaken in an attempt to clarify the structure of  $\text{XeF}_6$ . Rothman et al<sup>20</sup> did a pseudopotential SCF-MO study which showed that  $\text{XeF}_6$  was distorted from  $O_h$  symmetry along the  $t_{1u}$  bending mode, to give a  $C_{3v}$  structure with the long bonds adjacent to the lone pair. This calculation supported the VSPER model and showed that the molecule existed in a single ground state configuration with unusual physical properties. A more recent calculation by Klobukowski et al<sup>21</sup> reported that  $\text{XeF}_6$  had two local minima which were stabilized by 20 kcal mol<sup>-1</sup> when the symmetry of the molecule was lowered from  $O_h$  to  $C_{3v}$  and  $C_{2v}$ .

Experimental and theoretical work has proven that  $\text{XeF}_6$  is a non-rigid molecule with local minima giving  $C_{3v}$  and  $C_{2v}$  geometries via a pseudorotation mechanism.<sup>22,23</sup> The determination of the exact structures at each of these minima is currently unresolved and can only be determined by techniques which are fast compared to the fluxionality of the molecule. The time scale of photoelectron spectroscopy ( $< 10^{-15}$  sec) is several orders of magnitude faster than the rate of pseudorotation in  $\text{XeF}_6$  making it an excellent potential tool for the study of the structure. Indeed, the distorted  $C_{3v}$  ground state was recently supported by an analysis of the very broad (2.63 eV linewidth) F 1s core level photoelectron spectrum of  $\text{XeF}_6$ .<sup>24,25</sup> This linewidth was initially attributed solely to vibrational broadening in an octahedral structure but Gustev and Boldyrev<sup>24</sup> showed that this broad line could be explained qualitatively by the presence of two chemically shifted F 1s peaks of width ~1.8 eV due to two inequivalent fluorines in  $C_{3v}$  symmetry.

We felt that a photoelectron study of the ligand field splittings on the Xe 4d level could give more quantitative information on the  $\text{XeF}_6$  structure, if high resolution spectra (total width  $< 0.2$  eV) could be obtained. Indeed, we have already used high-resolution HeI and HeII photoelectron spectroscopy of low lying (binding energy  $< 30$  eV) core d levels, to characterize bonding and structure in gas phase compounds of main-group elements such as Zn, Cd, Ga and In.<sup>26-32</sup> The observed ligand field splittings in the core  $d^9$  ion states are analogous to the much better known splittings of valence d levels in transition metal compounds.<sup>33-35</sup> The splitting is characterized using the usual crystal field and spin-orbit Hamiltonian<sup>32</sup> and results in five peaks. The core level splittings are dominated by the asymmetric component of the crystal field,  $C_2^0$  (or  $D_s$ ),<sup>32-34</sup> which is proportional to the electric field gradient,  $eq_n$ , at the nucleus measured by Mössbauer spectroscopy, NQR and perturbed angular correlation.<sup>32,36</sup> As with valence level ligand field splittings, and nuclear field gradients, the core level  $C_2^0$  values have been shown to be sensitive to the metal, the bonding properties of the ligand, and the structure of the compound.<sup>32</sup>

Additive models, such as the partial quadrupole splitting model,<sup>36</sup> have been successfully applied to determine structure from quadrupole splittings: for example, to distinguish 4, 5 and 6 coordinate organometallic Sn compounds and obtain C-Sn-C bond angles.<sup>37</sup> In addition, this model gave  $^{129}\text{Xe}$  quadrupole splittings for solid  $\text{XeF}_6$  which are consistent with the solid state structure.<sup>13,38</sup> Because  $C_2^0$  and  $eq_n$  are proportional, such additive models should be very useful for obtaining the structure of  $\text{XeF}_6$  from Xe 4d ligand field splittings.

There have been three previous attempts to measure Xe 4d splittings in the xenon fluorides,<sup>39-41</sup> including  $\text{XeF}_6$ .<sup>39</sup> Comes et al<sup>40</sup> were partially successful in observing the Xe 4d ligand field splittings in  $\text{XeF}_2$  and  $\text{XeF}_4$  from a detailed high-resolution gas phase photoabsorption

study of the  $4d \rightarrow 6p$ ,  $7p$  transitions. For example, four of the expected five  $4d \rightarrow 6p$  peaks were resolved for  $\text{XeF}_2$ ; but only two peaks were resolved in the very weak  $\text{XeF}_4$   $4d \rightarrow 6p$  spectrum. These transitions were not even observed for  $\text{XeF}_6$ ,<sup>20</sup> and no estimate of  $C_2^0$  could be made. However, Comes et al observed the broad  $4d^{10}5s^2 \rightarrow 4d^95s^2$  "5p" transition, and stated that the absorption bands behaved exactly like a molecule of  $O_h$  or near  $O_h$  symmetry. Such photoabsorption spectra cannot be generally used to obtain core level ligand field splittings because the core  $\rightarrow$  Rydberg transitions are usually very weak and strongly overlap. In a previous photoelectron study<sup>41</sup> of the Xe 3d and 4d levels of  $\text{XeF}_2$  and  $\text{XeF}_4$  at an instrumental resolution of  $\sim 0.6$  eV, no ligand field splittings of the  $d_{5/2}$  and  $d_{3/2}$  levels were observed. However, these lines were broadened relative to Xe gas. This broadening, when deconvoluted with a Gauss-Lorentz function, allowed for a determination of  $C_2^0$ . The  $C_2^0$  values from this study were in good agreement with those obtained from the earlier photoabsorption study,<sup>40</sup> and consistent with the calculations of Basch<sup>7</sup> on  $\text{XeF}_2$  and  $\text{XeF}_4$ .

It was evident from the above photoabsorption and photoelectron studies that high intensity, high energy ( $\geq 100$  eV), high resolution ( $\sim 0.1$  eV) photon sources, and high electron resolution ( $< 0.05$  eV) would be required to resolve the Xe 4d ligand field splittings in  $\text{XeF}_2$  and  $\text{XeF}_4$ , and to study the splitting in  $\text{XeF}_6$  for the first time. Very recently, we have demonstrated such resolution using monochromatized synchrotron radiation.<sup>42,43</sup>

Using this high instrumental resolution, we report the Xe 4d photoelectron spectra of the three xenon fluorides  $\text{XeF}_x$  ( $x = 2, 4, 6$ ) in the gas phase. We had two objectives: (1) to fully resolve and characterize the ligand field splitting in  $\text{XeF}_2$  and  $\text{XeF}_4$  and (2) the most important, to use the  $C_2^0$  derived from the  $\text{XeF}_6$  spectra to estimate to what extent  $\text{XeF}_6$  is

distorted from octahedral symmetry.

## EXPERIMENTAL

The samples of  $\text{XeF}_2$ ,  $\text{XeF}_4$  and  $\text{XeF}_6$  were prepared using previously reported techniques<sup>44-46</sup> and were ascertained to be pure by Raman spectroscopy. The gas phase Xe 4d spectra of Xe and the  $\text{XeF}_x$  ( $x = 2, 4, 6$ ) compounds were recorded at the Canadian Synchrotron Radiation Facility (CSRF) located on the 1 GeV storage ring Aladdin<sup>47-49</sup>, using a high resolution photoelectron spectrometer.<sup>42-43</sup> The grazing incidence Grasshopper monochromator was equipped with a 900 groove/mm holographic grating, which gave a practical minimum photon resolution of 0.15 Å at 25 µm slits. Xe 4d spectra were obtained at 94 eV photon energy using 25 µm and 50 µm slits, yielding photon resolutions of 0.11 eV and 0.21 eV, respectively. The photoelectron spectrometer is based on the 36 cm mean radius McPherson electron analyzer, mounted at the pseudo-magic angle relative to the polarized synchrotron beam.<sup>42</sup> The electron resolution ( $\Delta E/E = 1/720$ ) was  $\sim 0.035$  eV at the  $\sim 25$  eV kinetic energy used for these spectra.

The volatile samples were leaked into a copper gas cell through a Teflon tube connected directly to the gas cell. Initial spectra showed a prominent band due to Xe gas, which is produced when the xenon fluorides decompose. The samples were allowed to leak into the gas cell until all exposed surfaces were passivated. This passivation process took close to one hour after which time clean, reproducible Xe 4d spectra of the  $\text{XeF}_x$  ( $x = 2, 4, 6$ ) compounds could be readily obtained. At least five high resolution Xe 4d spectra were obtained for each compound. Our spectrometer gives negligible charging shifts. Therefore the standard deviation of the peak positions and peak widths are generally between 5-10 meV and 5-30 meV respectively (Table

1).

The Xe 4d photoelectron spectra were calibrated using the well-characterized Xe  $4d_{3/2}$  and  $4d_{5/2}$  lines of Xe gas at 69.525(10) and 67.541(9) eV binding energies, respectively.<sup>50</sup> The spectra were fitted using a linear combination of Gaussian and Lorentzian lineshapes using an iterative procedure described previously.<sup>51</sup> Except for the three  $4d_{5/2}$  peaks of  $\text{XeF}_6$ , all peak parameters were left unconstrained. In the fitting procedure, the fitted bandwidths at the best photon resolutions gave linewidths at half height of close to 0.2 eV with usually ~ 30% Gaussian and ~ 70% Lorentzian components. These lineshapes reflect the fact that the inherent Lorentzian Xe 4d linewidth of  $\geq 0.13$  eV<sup>42,52</sup> is larger than the total instrumental photon plus electron width (Gaussian) of ~ 0.11 eV.

## RESULTS AND DISCUSSION

### $\text{XeF}_2$ and $\text{XeF}_4$

A typical Xe 4d calibration spectrum of  $\text{XeF}_2$ , taken at 94 eV photon energy and an instrumental resolution of 0.21 eV, is shown in Figure 1. Several general features are immediately apparent: (1) the Xe calibrant spectrum consists of two narrow peaks (of 0.25 eV width), due to the spin-orbit splitting in the  $4d^9$  ion state; (2) in contrast, the chemically shifted  $\text{XeF}_2$  spectrum consists of at least four peaks due to a combination of spin-orbit and ligand field splitting in the ion state; (3) the  $\text{XeF}_2$  linewidths are within 0.01 eV of the Xe linewidths, showing that vibrational broadening is very small indeed in  $\text{XeF}_2$ , as previously assumed;<sup>41</sup> (4) the linewidths in even this "medium" resolution spectrum are much narrower than in the previous best

photoelectron spectrum (see, for example, Figure 3 in ref. 41); and as good as, or better than, the previously published photoabsorption spectrum.<sup>40</sup> The chemical shift for  $\text{XeF}_2$  of  $\sim 2.8$  eV is in excellent agreement with values from the previous low resolution spectra.<sup>8,41,42</sup> Obviously, the increased resolution has dramatically increased the chemical shift sensitivity of the photoelectron technique.

Higher resolution photoelectron spectra (at 0.11 eV instrumental resolution) of  $\text{XeF}_2$  and  $\text{XeF}_4$  are shown in Figure 2. For  $\text{XeF}_2$ , the five peaks are now more apparent than in Figure 1. The small peak at 69.53 eV is due to the  $\text{Xe } 4d_{3/2}$  peak of Xe gas. The  $\text{XeF}_4$  spectrum is qualitatively similar to the  $\text{XeF}_2$  spectrum. The two weak peaks at low binding energy in the  $\text{XeF}_4$  spectrum are due to the  $4d_{3/2}$  peaks of the decomposition product  $\text{XeF}_2$ . Table 1 summarizes the peak positions, widths and standard deviations for peaks 1-5 in the two spectra. Looking more carefully at Figure 2 and Table 1, significant differences between the  $\text{XeF}_2$  and  $\text{XeF}_4$  spectra become apparent. First, the  $4d_{3/2}$  splitting pattern in the two spectra is quite different: in  $\text{XeF}_2$ , peak 5 is well separated and resolved, whereas in  $\text{XeF}_4$ , peak 3 is well resolved. As seen below, this is due to the different sign of  $C_2''$  because of the different structures. Second, while the linewidths of  $\text{XeF}_2$  of  $< 0.24$  eV are within 0.04 eV of Xe gas, the  $\text{XeF}_4$  linewidths - especially peaks 1 and 3 - are significantly broader. Undoubtedly, some of this broadening is vibrational or chemical in origin (see below).

The five observed peaks of  $\text{XeF}_2$  and  $\text{XeF}_4$  in Figure 2 are due to a combination of spin-orbit and ligand field effects which remove the degeneracy of the  $d^9$  final state. The Hamiltonian for the  $d^9$  hole state in  $D_{\infty h}$  ( $\text{XeF}_2$ ),  $D_{4h}$  ( $\text{XeF}_4$ ) and  $C_{3v}$  ( $\text{XeF}_6$ ) symmetries simplifies to Equation 1.<sup>33,34</sup>

$$\begin{aligned}
H = H_0 &+ C_2'' [3L_z^2 - L(L+1)] \\
&+ C_4'' [35L_z^4 - 30L(L+1)L_z^2 - 25L_z^2 - 6L(L+1) + 3L^2(L+1)^2] \\
&+ \lambda [1/2 (L_+S_- + L_-S_+) + L_zS_z]
\end{aligned}$$

Diagonalizing the Hamiltonian in d electron subspace, and treating  $d^9$  and  $d^1$  with the usual sign changes, the eigenvalues and eigenfunctions can be calculated<sup>26,32,33</sup> (Table 2 and Table 3).

The five equations derived from Eq. 1 comprise a non-linear overdetermined system thereby making exact solutions for  $E_{40}$ ,  $C_2''$ ,  $C_4''$  and  $\lambda$  impossible. It was decided that two different techniques should be used to calculate the ligand field parameters reported in Table 2. A non-linear least square fitting procedure and a Monte Carlo simulation were both applied to the five equations so that a global minimum could be obtained. The values calculated by the two techniques are in excellent agreement and the average is reported in Table 2.

The parameters (Table 2) are in remarkably good agreement with those obtained earlier in the lower resolution study,<sup>41</sup> but the errors (standard deviations from ten separate spectra) on  $C_2''$  are much smaller in our present study.  $C_4''$  is insignificant for both compounds. The calculated peak positions using the best-fit parameters in Table 2 are in excellent agreement with the experimental peak positions (Table 3). Indeed, in  $\text{XeF}_2$  and  $\text{XeF}_4$ , the calculated and experimental positions agree to within 0.03 eV. The eigenfunctions in Table 3 are also in remarkably good agreement with those derived from the previous photoabsorption study,<sup>40</sup> especially that only two of the five peaks were resolved in  $\text{XeF}_4$ .<sup>40</sup>

The spin-orbit splittings are slightly larger than the splittings for atomic Xe of 1.984 eV (Table 1). We believe that this increase is real. However, if the splitting is fixed at 1.984 eV in  $\text{XeF}_2$  and  $\text{XeF}_4$ , the  $C_2''$  values do not differ significantly from those in Table 2.

As indicated above by the different splitting pattern for the  $D_{5/2}$  level in  $\text{XeF}_2$  and  $\text{XeF}_4$ , the signs of  $C_2''$  are opposite in the two compounds. The positive and negative signs for  $C_2''$  in linear  $\text{XeF}_2$  and square planar  $\text{XeF}_4$  are expected, and reflected in the wave functions in Table 3. The positive  $C_2''$  (and positive  $e_{q_n}$ ) in  $\text{XeF}_2$  arises because the electronegative F ligands withdraw  $5p_z$  electron density from the Xe atom, and thereby making  $n_{pz} < 1/2(n_{px} + n_{py})$ . There is a depletion of valence p electron density along the molecular z-axis. In  $\text{XeF}_4$ , the opposite is true, and there will obviously be a surplus of valence p electron density along the molecular z-axis. In an octahedral molecule such as  $\text{XeF}_6$ , no splitting would be expected. Precisely these arguments are used in rationalizing positive and negative  $e_{q_n}$  values.<sup>30,54</sup>

The ordering of the d orbitals indicated by the wave functions in Table 3 can be rationalized by simple electrostatic arguments. Because there is a depletion of  $p_z$  valence electron density in  $\text{XeF}_2$ , the z-type 4d orbitals in  $\text{XeF}_2$  will be stabilized, and the energy ordering is  $d_{z^2} < d_{xz}, d_{yz} < d_{xy}, d_{x^2-y^2}$  ( $|0\rangle < |1\rangle < |2\rangle$ ), resulting in the opposite ordering of binding energies,  $|0\rangle > |1\rangle > |2\rangle$  for  $\text{XeF}_4$  as is apparent from Table 3, e.g., the order of binding energies is  $\Sigma_{1/2}$  (majority  $|0\rangle$ )  $>$   $\Pi_{3/2}$  (majority  $|1\rangle$ )  $>$   $\Delta_{5/2}$  (majority  $|2\rangle$ ).

When Table 1 is examined, it is immediately apparent that a line broadening is observed going from Xe gas to  $\text{XeF}_2$  and  $\text{XeF}_4$ . There are two possible mechanisms to account for this behaviour. The first is due to a vibrational broadening of the lines from  $v = 0 \rightarrow v' = 0, 1, 2, \dots$  etc. transitions in the ion state. Previous work on the Zn 3d and Cd 4d levels<sup>26-32</sup> shows that substantial vibrational effects are not generally important on d-levels. More importantly, our unpublished Ge 3d spectrum of  $\text{GeH}_4$  (to be published) shows no hint of vibrational effects; in great contrast to the extensive vibrational effects in the Si 2p levels of  $\text{SiH}_4$ .<sup>42,43</sup> The second



mechanism involves a chemical effect on the linewidths due to a change in Auger decay rates from a loss of Xe valence electron density in the Xenon fluorides relative to atomic Xe. Recent experimental and theoretical work on C 1s levels<sup>55</sup> shows that this chemical effect can be important in changing core level linewidths; and our recent work on the I 4d levels in I compounds show that this effect is much more important than vibrational in I compounds<sup>56</sup> and probably in our Xe compounds. We are observing predominantly  $v = 0 \rightarrow v' = 0$  transitions for all peaks, as is strongly shown by the good agreement between observed and calculated energies in Table 3.

The wavefunctions in Table 3 are important in rationalizing the first broadening mechanism (Table 1). For example, in  $\text{XeF}_2$  none of the 4d lines are broadened greatly relative to the Xe gas 4d lines; but peak 1, which corresponds to the orbital with high  $d_{z^2}$  character pointed towards the F ligands, is broader than peak 2, which corresponds to d orbitals not pointing towards the F ligands. The symmetric stretching frequency,  $\nu_1$ , for  $\text{XeF}_2$  is only  $514.5 \text{ cm}^{-1}$  (64 meV).<sup>56</sup> The lack of appreciable broadening or asymmetry of the lines shows that any vibrational broadening is very small with  $v = 0 \rightarrow v' = 0$  being by far the predominant transition, with perhaps a small  $v = 0 \rightarrow v' = 1$  contribution to peak 1.

In  $\text{XeF}_4$  considerable broadening is observed in peaks 1 and 3 (Table 1). Some vibrational broadening ( $\nu_1 = 554.3 \text{ cm}^{-1}$ , 69 meV)<sup>56</sup> would be expected on the orbitals with d character in the x-y plane (corresponding to peaks 1 and 3) and directed toward the F ligands. The other d orbitals directed away from the F ligands have a FWHM similar to  $\text{XeF}_2$  indicating little or no vibrational broadening.

In the second mechanism, the loss of electron density in the Xe 5p orbitals changes the

rate of Auger decay into the core hole and is reflected by the linewidth increase. McGuire<sup>57</sup> calculated that the lifetime of the Xe  $N_{4,5}$  shells should be substantially narrower ( $\sim 80$  meV) than the surrounding  $N_{4,5}$  shells (Sn:  $\sim 140$  meV). Also, our measured I 4d linewidths<sup>58</sup> of 0.2-0.3 eV are much broader than the atomic Xe 4d linewidths of  $\sim 0.13$  eV.<sup>42,52</sup> This decrease in linewidth in Xe is due to the fact that super-Coster-Kronig transitions are forbidden in Xe atoms.<sup>57</sup> Therefore, when the F ligands withdraw electron density from the Xe 5p shell, several new decay channels open up to fill the 4d core hole. The Auger rate increases which leads to an increase in the linewidths in this case. (This is the opposite trend to that observed and predicted for C 1s and I 4d linewidths<sup>44,58</sup>). When one examines the linewidths of the peaks with a majority of orbital character perpendicular to the Xe-F bond, the linewidths increase from 0.202 eV for Xe, to 0.223 eV for  $\text{XeF}_2$  and 0.255 eV for  $\text{XeF}_4$  as the amount of 5p density withdrawn from the Xe atom increases. These increased linewidths approach I 4d inherent linewidths of 0.20 eV to 0.25 eV for ICl and IBr.<sup>58</sup> Some of the broadening of the peaks 1 and 3 in  $\text{XeF}_2$  and  $\text{XeF}_4$  will also be due to this chemical effect.

### $\text{XeF}_6$

High-resolution Xe 4d spectra of Xe gas and  $\text{XeF}_6$  are shown in Figure 3. A hint of the  $4d_{3/2}$  peaks of  $\text{XeF}_4$ , from decomposition, are also seen at  $\sim 75$  eV binding energy. Although no ligand field splitting is resolved in the  $\text{XeF}_6$  spectrum, the  $\text{XeF}_6$  lines are about double the linewidth of Xe lines (0.36 and 0.40 eV versus 0.20 eV). We attribute this large broadening of the  $\text{XeF}_6$  peaks to unresolved ligand field splitting from a distorted  $C_{3v}$   $\text{XeF}_6$  structure.

Before fitting this spectrum to the characteristic five peaks, it is important to comment

on three other line broadening mechanisms - vibrational broadening, chemical shift broadening due to two (or more)  $\text{XeF}_6$  structures (e.g.  $C_{3v}$  and  $C_{2v}$ ) which are "frozen out" by the fast photoelectron technique and the above chemical effect on the Auger rates due to a decrease in Xe 5p electron density. Vibrational broadening cannot be the major broadening mechanism for three reasons. First, the symmetric ground state vibrational frequency of  $\text{XeF}_6$  ( $\nu = 608 \text{ cm}^{-1}$ )<sup>18</sup> is comparable to those for  $\text{XeF}_2$  and  $\text{XeF}_4$ . Very large vibrational broadening would not be expected for  $\text{XeF}_6$  because substantial vibrational broadening was not observed at all for  $\text{XeF}_2$ , and only on the two peaks of high  $d_{x^2-y^2}$  and  $d_{xy}$  character in  $\text{XeF}_4$  (Table 1). Second, and more significant, vibrational broadening would result in the same  $4d_{3/2}$  and  $4d_{5/2}$  widths, whereas the widths of 0.36 eV and 0.40 eV are substantially different. Two (or more) different structures can also be ruled out as controlling the broadening mechanism. Like vibrational broadening, several structures would lead to the same widths for both 4d lines. In addition, Bristow and Bancroft<sup>25</sup> showed that the observed vibrational features observed on the  $8a_{1g}$  valence band orbital could be explained by a single gas phase structure. Also, the recent analysis of the broad F 1s spectrum<sup>24</sup> of  $\text{XeF}_6$  gives reasonable evidence for the two non-equivalent fluorines in one  $C_{3v}$  structure. Thirdly, a line broadening due to the chemical effect is an unlikely mechanism to account for the substantial increase in linewidths. As was observed in  $\text{XeF}_2$  and  $\text{XeF}_4$ , three of the linewidths increased by only  $\sim 20 \text{ meV}$  and  $\sim 50 \text{ meV}$ , respectively. An increase in linewidth of 160 meV due to a loss of Xe 5p electron density seems very unlikely. If one assumes a linear relationship between linewidths and electron density, a line broadening of only  $\sim 70\text{-}80 \text{ meV}$  would be expected for  $\text{XeF}_6$ . This value is one-half of the measured line broadening which indicates that a chemical effect is only a small component of the observed line broadening.

Unresolved ligand field splitting is the only mechanism that would yield such broad and different Xe  $4d_{3/2}$  and  $4d_{5/2}$  widths. Figure 4 shows the five peaks fits to two spectra (of over 10) taken at the two different photon resolutions. The  $4d_{5/2}$  doublet was fit without any constraints. The two peak positions and widths (peaks 1 and 2, Table 1) are in excellent agreement, and the standard deviation from other spectra at each resolution are small ( $\sim 10$  meV). The  $4d_{3/2}$  splitting of 0.15 eV (which is used below to obtain  $C_2^0$ ) is certainly accurate to  $\pm 0.02$  eV. The three peak fit to the  $4d_{5/2}$  triplet is not unique, so we do not use these positions to calculate  $C_2^0$ . However, reasonable linewidth and lineshape constraints from the  $\text{XeF}_2$  and  $\text{XeF}_4$  fits give good reproducibility for the three peak positions (Table 1).

The derived chemical shift, ligand field and spin-orbit parameters for  $\text{XeF}_6$  are given in Table 2. The chemical shift is very large and in agreement with previous measurement from the Xe 3d levels.<sup>8</sup> The  $C_2^0$  value of  $0.018 \pm 0.002$  eV, derived from the  $4d_{3/2}$  splitting using the following formula,<sup>28</sup>

$$\frac{\Delta E_{3/2} \text{XeF}_6}{\Delta E_{3/2} \text{XeF}_2} = \frac{C_2^0 \text{XeF}_6}{C_2^0 \text{XeF}_2}$$

is less than one-half of those for  $\text{XeF}_2$  and  $\text{XeF}_4$ . Equation 2 is a good approximation when the spin-orbit splitting is large compared to  $C_2^0$  as shown from  $d_{3/2}$  splittings of  $\text{XeF}_2$  and  $\text{XeF}_4$ . A  $C_2^0$  for  $\text{XeF}_4$  of -45.2 meV, determined from the  $d_{3/2}$  splittings of  $\text{XeF}_2$  and  $\text{XeF}_4$  and the  $C_2^0$  of  $\text{XeF}_2$ , is in good agreement with the experimentally determined value of -46.8 meV. The sign of  $C_2^0$  cannot be obtained directly from the spectrum, but we assign a negative sign based on what structure is reasonable (see below).

Qualitatively, the  $C_2^0$  value of  $-0.018 \pm 0.002$  eV shows immediately that  $\text{XeF}_6$  is distorted

considerably from octahedral symmetry. To obtain F-Xe-F bond angles, we can use an adaptation of the additive partial quadrupole splitting (PQS) treatment,<sup>54,59</sup> used to obtain bond angles and structure in Sn compounds<sup>36,37</sup> and solid state XeF<sub>6</sub>.<sup>38</sup> For <sup>129</sup>Xe quadrupole splittings ( $\Delta E_Q$ ) for the xenon fluorides, we can write:<sup>34,54,59</sup>

$$\Delta E_Q = (\text{PQS})_F \sum_F (3\cos^2\Theta - 1)$$

Because the quadrupole and  $C_2^0$  Hamiltonians transform identically, we can write by analogy

$$C_2^0 = (\text{PLFS})_F \sum_F (3\cos^2\Theta - 1)$$

where PLFS is the partial ligand field splitting for F in the xenon fluorides, and  $\Theta$  is the angle between the molecular z-axis and the bond of interest. Before using this model for the first time for ligand-field splittings, it is important to review the assumptions involved and the expected validity and accuracy of the model:<sup>59</sup> we assume (1) that  $C_2^0$ , like  $e^2qQ$ , can be regarded as sum of independent contributions, one from each F bound to Xe; (2) that the PLFS for F is constant in all Xe-F compounds; this implies that each F withdraws the same amount of Xe 5p valence electron density (or the Xe-F bond character is constant), and the Xe-F bond lengths are consistent in all compounds containing Xe-F bonds; (3) that any relaxation contributions to  $C_2^0$  are negligible or constant in all Xe-F compounds and (4) the principal ligand field axis corresponds to the molecular symmetry axis in all compounds.

The first two assumptions could be challenged immediately by the rather large difference in Xe-F bond lengths in two-, four- and six-coordinate Xe compounds<sup>38</sup> (see Table 4). However, there is still considerable evidence that the model can be used quantitatively. Thomas pointed out<sup>8</sup> that the Xe 3d and Xe 4d photoelectron chemical shifts show that each F in XeF<sub>2</sub>, XeF<sub>4</sub> and XeF<sub>6</sub>,

have the same charge, and indeed withdraws the same amount of Xe valence electron density. Perhaps more relevant to the additive model, the  $^{129}\text{Xe}$  quadrupole splittings ( $\Delta E_Q$ ) for a large number of compounds are within  $\pm 4\%$  of that predicted from the additive model regardless of bond lengths. For example, the  $|\Delta E_Q|$  values for linear  $\text{XeF}_2$  and  $\text{XeF}^+\text{Sb}_2\text{F}_{11}^-$  [ $\Theta = 0^\circ$ ,  $\Delta E_Q = 4(\text{PQS})_F$ ] are 39.7 and 41.5  $\text{mm s}^{-1}$ , respectively, while the  $|\Delta E_Q|$  values for square planar  $\text{XeF}_4$  and  $\text{XeF}_3^+\text{BiF}_6^-$  [ $\Theta = 90^\circ$ ,  $\Delta E_Q = -4(\text{PQS})_F$ ] are 41.0 and 41.3  $\text{mm s}^{-1}$ , respectively.

The additive model above indicated that the  $\Delta E_Q$  values for  $\text{XeF}_2$  should be equal to the  $\Delta E_Q$  for  $\text{XeF}_4$ , but the signs should be opposite. The sign of  $^{129}\text{Xe}$   $\Delta E_Q$  cannot be measured readily whereas the signs of  $C_2^0$  can be measured directly, but the  $|\Delta E_Q|$  values for  $\text{XeF}_2$  and  $\text{XeF}_4$  are again within 5% of each other. The above values show that  $\Delta E_Q$  is not sensitive to the individual bond lengths or bond characters as assumed in the model. In addition, the  $\Delta E_Q$  value for the distorted  $\text{XeF}_6$  octahedron in the solid state (7.7  $\text{mm s}^{-1}$ )<sup>38</sup> is rationalized very well by the additive model, demonstrating the strong dependence of  $\Delta E_Q$  on the distortion of the octahedron. The  $^{129}\text{Sn}$  and  $^{57}\text{Fe}$   $\Delta E_Q$  values<sup>37,54,59</sup> also demonstrate that  $\Delta E_Q$  is not sensitive to small changes in metal ligand character but is very sensitive to bond angle changes.<sup>37</sup>

The above evidence strongly indicates that we can use Eq. 4 to obtain bond angles in  $\text{XeF}_6$ . We first derive the  $(\text{PLFS})_F$  value from the  $C_2^0$  values for  $\text{XeF}_2$  and  $\text{XeF}_4$ . The value for  $(\text{PLFS})_F$  from the two compounds are +0.0098 and +0.0117 eV, respectively. Using the average of these two values (+0.0108 eV) and assuming the  $C_{3v}$  structure (Figure 5) for  $\text{XeF}_6$ , we can write

$$C_2^0 = 3(\text{PLFS})_F(3\cos^2\Theta_{1,2,3} - 1) + 3(\text{PLFS})_F(3\cos^2\Theta_{4,5,6} - 1)$$

It was not possible to solve  $\Theta_{1,2,3}$  and  $\Theta_{4,5,6}$  concurrently. Therefore to solve Eq. 5, the

angle  $\Theta_{1,2,3}$  was held constant at different fixed angles ( $48^\circ$ ,  $50^\circ$ ,  $52^\circ$  and  $54.7^\circ$ ) and  $\Theta_{4,5,6}$  was allowed to float. Figure 5 is a plot of  $C_2^0$  versus  $\Theta_{4,5,6}$  while holding  $\Theta_{1,2,3}$  constant. From electron diffraction<sup>16,17</sup> and latest theoretical values<sup>21</sup> for  $\Theta_{1,2,3}$  of  $49^\circ$  and  $52^\circ$ , respectively, we fix  $\Theta_{1,2,3}$  at  $50^\circ$ . The two boxed-in regions refer to the experimentally measured  $C_2^0$  and the size of the boxes gives the estimated error, which we take as 50% greater than the standard deviation in  $C_2^0$ , due to deficiencies in the model.

Since it is not possible to directly determine the sign of  $C_2^0$  for  $\text{XeF}_6$ , two possible angles for  $\Theta_{4,5,6}$  are possible. If  $C_2^0$  is positive, the F-Xe-F angle falls between  $77^\circ - 84^\circ$  indicating that the angle defined by  $\Theta_{4,5,6}$  is closing up and the lone pair of electrons are acting a ring of charge in the x-y plane forcing the ring to close. In the negative  $C_2^0$  case, the F-Xe-F angle is  $111^\circ - 117^\circ$  thereby forcing  $\Theta_{4,5,6}$  to open up, indicating that the lone pairs is directed toward the face of the cone.

The majority of the experimental and latest theoretical results suggest strongly that the latter distortion takes place, and thus  $C_2^0$  is negative. This gives estimates for  $\Theta_{1,2,3}$  and  $\Theta_{4,5,6}$  of  $50 \pm 2^\circ$  and  $76 \pm 4^\circ$ , respectively. These angles are in good agreement with the latest theoretical values of  $49^\circ$  and  $76^\circ$ , respectively,<sup>21</sup> but not in as good agreement with the electron diffraction results of  $52^\circ$  and  $67^\circ$ , respectively.<sup>16,17</sup>

Finally, it is interesting to note that our  $C_2^0$  value is much larger than that expected from the known solid state structure.<sup>13</sup> A  $C_2^0$  value for the solid state structure ( $-0.008$  eV in Table 2) can be estimated readily using the Mössbauer  $e^2qQ$  values in the solid state,<sup>38,60</sup> and using the known proportionality of  $C_2^0$  and  $e^2qQ$ :<sup>28</sup>

$$\frac{(e^2qQ)_{\text{XeF}_6}}{(e^2qQ)_{\text{XeF}_2}} = \frac{(C_2^0)_{\text{XeF}_6}}{(C_2^0)_{\text{XeF}_2}}$$

Using the  $e^2qQ$  values for  $\text{XeF}_2$  and  $\text{XeF}_6$  of  $+39.7 \text{ mm s}^{-1}$  and  $\pm 7.7 \text{ mm s}^{-1}$ , and the  $C_2^0$  value of  $\text{XeF}_2$ , the  $C_2^0$  value of  $\pm 0.008 \text{ eV}$  can be readily calculated. This smaller  $C_2^0$  value for the solid state structure is consistent with the smaller (and different) distortion of  $\text{XeF}_6$  in the solid state.

## CONCLUSIONS

We have resolved ligand field splittings by photoelectron spectroscopy in relatively deep core levels ( $E_B > 30 \text{ eV}$ ) for the first time. To resolve these effects, it required very high resolution not previously attained. The spectra have been characterized using a simple Hamiltonian involving crystal field splitting and spin-orbit splitting.

Of particular interest, we have estimated the gas phase structure of  $\text{XeF}_6$  from the Xe 4d spectra using an additive model similar to that used in Mössbauer spectroscopy. It has been shown that for a  $C_{4v}$   $\text{XeF}_6$  structure,  $\Theta_{1/2} = 50^\circ$  and  $\Theta = 76 \pm 4^\circ$ . This is perhaps the best experimental evidence of the distorted gas phase  $\text{XeF}_6$ , and it is shown to be in excellent agreement with the recent calculations of Klobukowski et al.<sup>21</sup>



## ACKNOWLEDGEMENTS

The authors would like to thank Dr. John Tse for many helpful and thought provoking discussions and the staff at the Synchrotron Radiation Center (Stoughton) for their technical support. We are grateful to the National Research Council (NRC) of Canada, the Natural Sciences and Engineering Research Council (NSERC) of Canada and to the U.S. Air Force Astronautics Laboratory, Edwards AFB, California (GJS) for financial support.

## REFERENCES

1. Hyman, H.H. (ed) Noble Gas Compounds, University of Chicago Press: Chicago, IL, 1963 and references therein.
2. Agron PA; Begun, G.M.; Levy, H.A.; Mason, A.A.; Jones, C.G.; Smith, D.F. *Science* **1963**, 139, 842-843; Reichmann, S.; Schreiner F. *J. Chem. Phys.* **1969**, 51, 2355-2358.
3. Siegel, S.; Gebert, E. *J. Am. Chem. Soc.* **1963**, 85, 240; Templeton, D.H.; Zalkin, A.; Forester, J.D.; Williamson, S.M. *J. Am. Chem. Soc.* **1963**, 85, 242.
4. Levy, H.A.; Agron, P.A. *J. Am. Chem. Soc.* **1963**, 85, 241-242.
5. Lohr, Jr., L.L.; Lipscomb, W.N. *J. Am. Chem. Soc.* **1963**, 85, 240-241.
6. Coulson, C.A. *J. Chem. Soc.* **1964**, 1442-1454.
7. Basch, H.; Moskowitz, J.W.; Hollister, C.; Hankin, D.J. *Chem. Phys.* **1971**, 55, 1922-1933.
8. Carroll, T.X.; Shaw, Jr., R.W.; Thomas, T.D.; Kindle, C.; Bartlett, N. *J. Am. Chem. Soc.* **1974**, 96, 1989-1996.
9. Bartell, L.S.; Rothman, M.J.; Ewig, C.S.; Van Wazer, J.R. *J. Chem. Phys.* **1980**, 73, 367-374.
10. Hemdon, W.C. *J. Mol. Struct. (Theochem)* **1988**, 169, 389-401 and references therein.
11. Lombardi, E.; Ritter, R.; Jansen, L. *Int. J. Quantum Chem.* **1973**, 7, 155-171.
12. Lombardi, E.; Pirola, L.; Tarantini, G.; Jansen, L.; Ritter R. *Int. J. Quantum Chem.* **1974**, 8, 335-345.
13. Burbank, R.D.; Jones, G.R. *J. Am. Chem. Soc.* **1974**, 96, 43-48.

14. Gillespie, R.J.; Nyholm, R.S. *Q. Rev. Chem. Soc.* **1957**, 11, 339-380.
15. Gillespie, R.J.; Hargitti, I. *The VSEPR Model of Molecular Geometry*, Allyn and Bacon, Boston, 1991.
16. Gavin, Jr., R.M.; Bartell, L.S. *J. Chem. Phys.* **1968**, 48, 2460-2465; Bartell, L.S.; Gavin, Jr., R.M. *J. Chem. Phys.* **1968**, 48, 2466-2483.
17. Pitzer, K.S.; Bernstein, L.S. *J. Chem. Phys.* **1975**, 63, 3849-3856.
18. Claassen, H.H.; Goodman, G.L.; Kim, H. *J. Chem. Phys.* **1972**, 56, 5042-5053.
19. Bernstein, L.S.; Pitzer, K.S. *J. Chem. Phys.* **1975**, 62, 2530-2534.
20. Rothmann, M.J.; Bartell, L.S.; Ewig, C.S.; Van Wazer, J.R. *J. Chem. Phys.* **1980**, 73, 375-381.
21. Klobukowski, M.; Hazinaga, S.; Seijo, L.; Barandiaran, Z. *Theor. Chim. Acta.* **1987**, 71, 237-245.
22. Strauss, H.L. *Ann. Rev. Phys. Chem.* **1983**, 34, 301-328.
23. Christe, K.O.; Wilson, W.W. *Inorg. Chem.* **1989**, 28, 3275-3277.
24. Gustev, G.L.; Boldyrev, A. I. *Russ. J. Inorg. Chem.* **1989**, 34, 598-599.
25. Bristow, D.J.; Bancroft, G.M. *J. Am. Chem. Soc.* **1983**, 105, 5634-5638.
26. Bancroft, G.M.; Creber, D.K.; Basch, H. *J. Chem. Phys.* **1977**, 67, 4891-4897.
27. Creber, D.K.; Bancroft, G.M. *Inorg. Chem.* **1980**, 19, 643-648 and references.
28. Gupta, R.P.; Tse, J.S.; Bancroft, G.M. *Philos. Trans. Roy. Soc.* **1980**, 293, 535-569.
29. Bancroft, G.M.; Bristow, D.J.; Tse, J.S. *J. Chem. Phys.* **1983**, 75, 277-296.
30. Bancroft, G.M.; Bristow, D.J. *Can. J. Chem.* **1983**, 61, 2669-2678.
31. Edgell, R.G. "Electronic Structure and Magnetism of Inorganic Compounds", The Royal

- Society of Chemistry, **1982**, 1, 117-120.
32. Bancroft, G.M.; Tse, J.S. *Comments Inorg. Chem.* **1986**, 5, 89-118 and references.
  33. Ballhausen, C.J. *Introduction to Ligand Field Theory*; McGraw-Hill: New York 1962.
  34. Jørgensen, C.K. *Modern Aspects of Ligand Field Theory*, North-Holland: Amsterdam, 1971.
  35. Cotton, F.A.; Wilkinson, G. *Advanced Inorganic Chemistry* 5th Edition; John Wiley and Sons: New York, 1987.
  36. Bancroft G.M. *Mössbauer Spectroscopy: An Introduction for Inorganic Chemists and Geochemists*; McGraw-Hill: London, 1973.
  37. Sham, T.K.; Bancroft, G.M. *Inorg. Chem.* **1975**, 14, 2281-2283.
  38. de Waard, H.; Bukshpan, S.; Schrobilgen, G.J.; Holloway, J.H.; Martin, D. J. *Chem. Phys.* **1979**, 70, 3247-3253 and references therein.
  39. Nielsen, U.; Haensel, R.; Schwarz, W.H.E. *J. Chem. Phys.* **1974**, 61, 3581-3586.
  40. Comes, F.J.; Haensel, R.; Nielsen, U.; Schwarz, W.H.E. *J. Chem. Phys.* **1973**, 58, 516-529.
  41. Bancroft, G.M.; Malmquist, P.-Å.; Svensson, S.; Basilier, E.; Gelius, U.; Siegbahn K. *Inorg. Chem.* **1978**, 17, 1595-1599.
  42. Bozek, J.D.; Cutler J.N.; Bancroft, G.M.; Coatsworth, L.L.; Tan, K.H.; Yang, D.S.; Cavell, R.G. *Chem. Phys. Lett.* **1990**, 165, 1-5.
  43. Bozek, J.D.; Bancroft, G.M.; Cutler, J.N.; Tan, K.H. *Phys. Rev. Lett.* **1990**, 65, 2757-2760; Bozek, J.D.; Bancroft, G.M.; Tan, K.H. *Phys. Rev. A* **1991**, 43, 3597-3608.
  44. Syvret, R.G. Ph.D. Thesis: McMaster University: Hamilton, 1987.

45. Malm, J.G.; Chernick, C.L. *Inorg. Synth.* **1966**, 8, 254-258.
46. Chernick, C.L.; Malm, J.G. *Inorg. Synth.* **1966**, 8, 258-260.
47. Bancroft, G.M.; Bozek, J.D.; Cutler, J.N.; Tan, K.H. *J. Electron. Spectrosc. Relat. Phenom.* **1988**, 47, 187-196.
48. Yates, B.W.; Tan, K.H.; Coatsworth, L.L.; Bancroft, G.M. *Phys. Rev. A* **1985**, 31, 1529-1534.
49. Bancroft, G.M.; Bozek, J.D.; Tan, K.H. *Phys. Can.* **1987**, 43, 113-120.
50. Krause, M.O.; *Synchrotron Radiation Research*, edited by Winick, H.; Doniach, S; Plenum press: New York, 1980; pp 101-158.
51. Bancroft, G.M.; Adams, I.; Coatsworth, L.L.; Bennewitz, C.D.; Brown, J.D.; Westwood, W.D. *Anal. Chem.* **1975**, 47, 586-588.
52. King, G.C.; Tronc, M.; Read, F.H.; Bradford, R.C. *J. Phys. B* **1977**, 10, 2479-2495.
53. Siegbahn, K. et al *ESCA Applied to Free Molecules*; North Holland Publishing Co.: New York, 1971; pp 132-136.
54. Bancroft, G.M.; Platt, R.H. *Advan. Inorg. Radiochem.* **1972**, 15, 59-258.
55. Coville, M.; Thomas, T.D. *Phys. Rev. A*, to be published and references therein.
56. Tsao, P.; Cobb, C.C.; Claassen, H.H. *J. Chem. Phys.* **1971**, 54, 5247-5253.
57. McGuire, E.J. *Phys. Rev. A* **1974**, 9, 1840-1851.
58. Cutler, J.N.; Bancroft, G.M.; Sutherland, D.G.; Tan, K.H. *Phys. Rev. Lett.*, to be submitted.
59. Bancroft, G.M. *Coord. Chem. Rev.* **1973**, 11, 247-262.
60. Perlow, G.J.; Perlow, M.R. *J. Chem. Phys.* **1968**, 48, 955-961.

**Table 1:** Photoelectron experimental data for Xe, XeF<sub>2</sub>, XeF<sub>4</sub>, and XeF<sub>6</sub> (eV). The values in the brackets are the standard deviations of the positions and widths.

Compound		Peak Position (eV)	Peak Width (eV)
Xe	1	69.525(10)	0.207(4)
	2	67.541(9)	0.202(4)
XeF <sub>2</sub>	1	72.568(6)	0.248(8)
	2	72.248(6)	0.223(10)
	3	70.601(13)	0.264(26)
	4	70.421(9)	0.256(27)
	5	70.179(6)	0.214(19)
XeF <sub>4</sub>	1	75.098(6)	0.319(8)
	2	74.729(7)	0.255(8)
	3	73.140(2)	0.392(1)
	4	72.816(10)	0.210(27)
	5	72.661(5)	0.225(26)
XeF <sub>6</sub> <sup>a</sup>	1	77.450(13)	0.35(4)
	2	77.317(11)	0.30(3)
	3	75.51	0.34
	4	75.37	0.28
	5	75.24	0.28
XeF <sub>6</sub> <sup>b</sup>	1	77.462(13)	0.32(4)
	2	77.321(11)	0.25(3)
	3	75.53	0.33
	4	75.38	0.25
	5	75.25	0.25

<sup>a</sup> and <sup>b</sup> refer to Figures 4a and 4b, respectively, which were taken at experimental resolutions of 0.21 eV and 0.11 eV, respectively.

**Table 2: Ligand field and spin-orbit splitting parameters for  $\text{XeF}_2$ ,  $\text{XeF}_4$  and  $\text{XeF}_6$  (eV).  
The values in the brackets are the standard deviations.**

	$\text{XeF}_2$		$\text{XeF}_4$		$\text{XeF}_6$
	This work	Bancroft et al <sup>11</sup>	This work	Bancroft et al <sup>11</sup>	
$C_2^0$	+0.0391(2)	+0.041(4)	-0.0468(10)	-0.045(4)	-0.018(2) -0.008*
$C_4^0$	+0.0010(2)	--	-0.0003(10)	--	--
$\lambda$	0.814(3)		0.822(3)		0.807(4)
$5/2\lambda$	2.035(3)	1.98(2)	2.055(3)	2.00(1)	2.018(4)
$E_{4d}$	71.212(3)	71.13(2)	73.679(3)	73.60(1)	76.118(4)
$\Delta E_{4d}$	2.877(3)	2.84(1)	5.344(3)	5.30(1)	7.783(4)
$\Delta E_{3d}^0$		2.87		5.41	7.64

\* Values for solid state  $\text{XeF}_6$  are predictions based on quadrupole splittings obtained from Mössbauer data. See body of text.

**Table 3:** One-electron eigenfunctions and eigenvalues for the Xe 4d levels in XeF<sub>2</sub> and XeF<sub>4</sub> <sup>†</sup>

	$M_j$	Term	Eigenfunction	Energy(eV)	
				Expt.	Calc.
XeF <sub>2</sub>	1/2	$\Pi_{1/2}$	$0.74  1\beta\rangle - 0.68  0\alpha\rangle$	72.568	72.597
	3/2	$\Delta_{3/2}$	$0.86  2\beta\rangle - 0.50  1\alpha\rangle$	72.248	72.276
	1/2	$\Sigma_{1/2}$	$0.68  1\beta\rangle + 0.74  0\alpha\rangle$	70.601	70.602
	3/2	$\Pi_{3/2}$	$0.50  2\beta\rangle + 0.86  1\alpha\rangle$	70.421	70.402
	5/2	$\Delta_{5/2}$	$ 2\alpha\rangle$	70.179	70.175
XeF <sub>4</sub>	3/2	$e''_{g3/2}$	$0.92  2\beta\rangle - 0.38  1\alpha\rangle$	75.098	75.120
	1/2	$e'_{g1/2}$	$0.80  1\beta\rangle - 0.60  0\alpha\rangle$	74.729	74.719
	5/2	$e''_{g5/2}$	$ 2\alpha\rangle$	73.140	73.134
	3/2	$e''_{g3/2}$	$0.38  2\beta\rangle + 0.92  1\alpha\rangle$	72.816	72.800
	1/2	$e'_{g1/2}$	$0.60  1\beta\rangle + 0.80  0\alpha\rangle$	72.661	72.624

<sup>†</sup>  $|0\rangle$ ,  $|1\rangle$  and  $|2\rangle$  refer to  $(d_{x^2})$ ,  $(d_{xz}, d_{yz})$  and  $(d_{xy}, d_{x^2-y^2})$ , respectively.

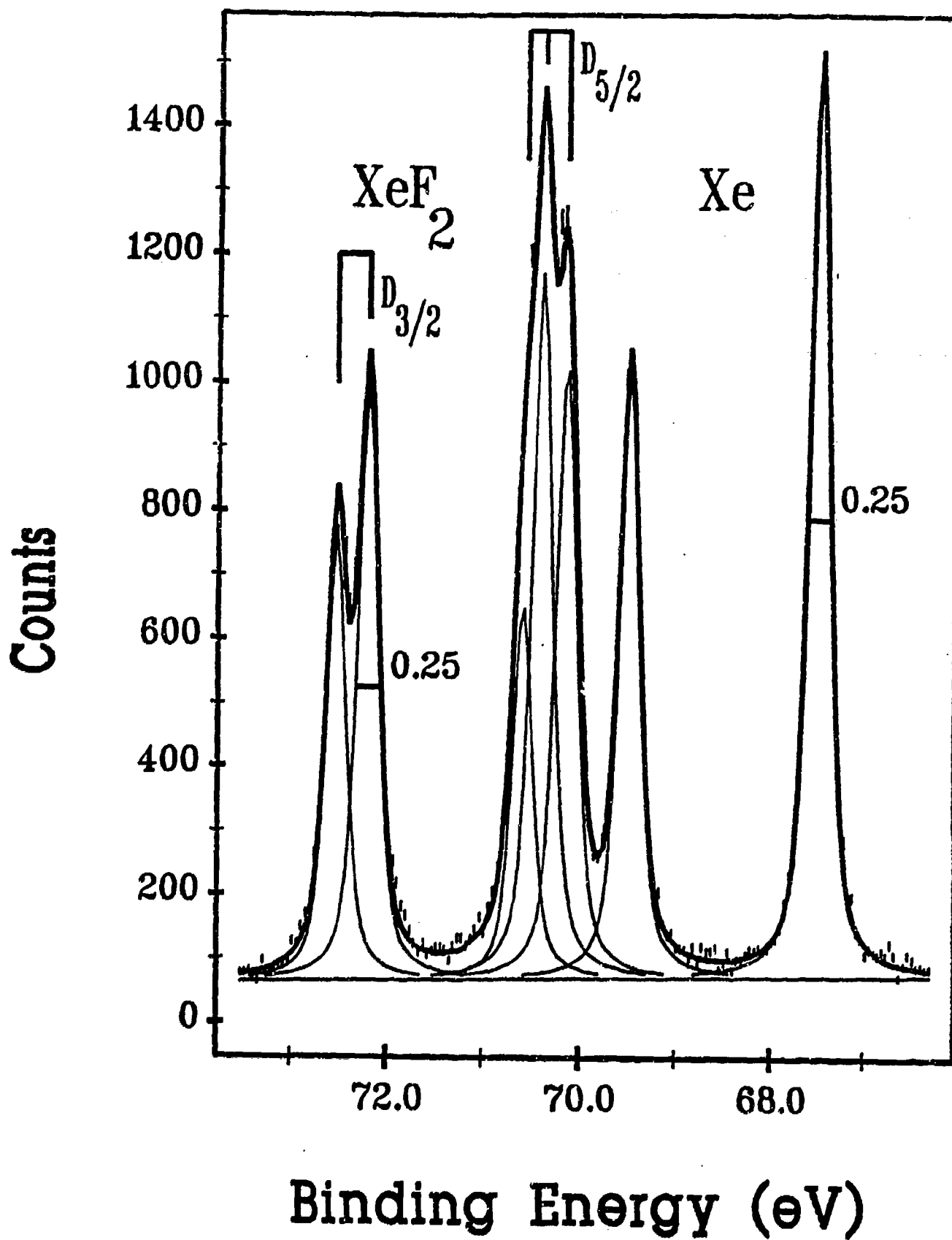


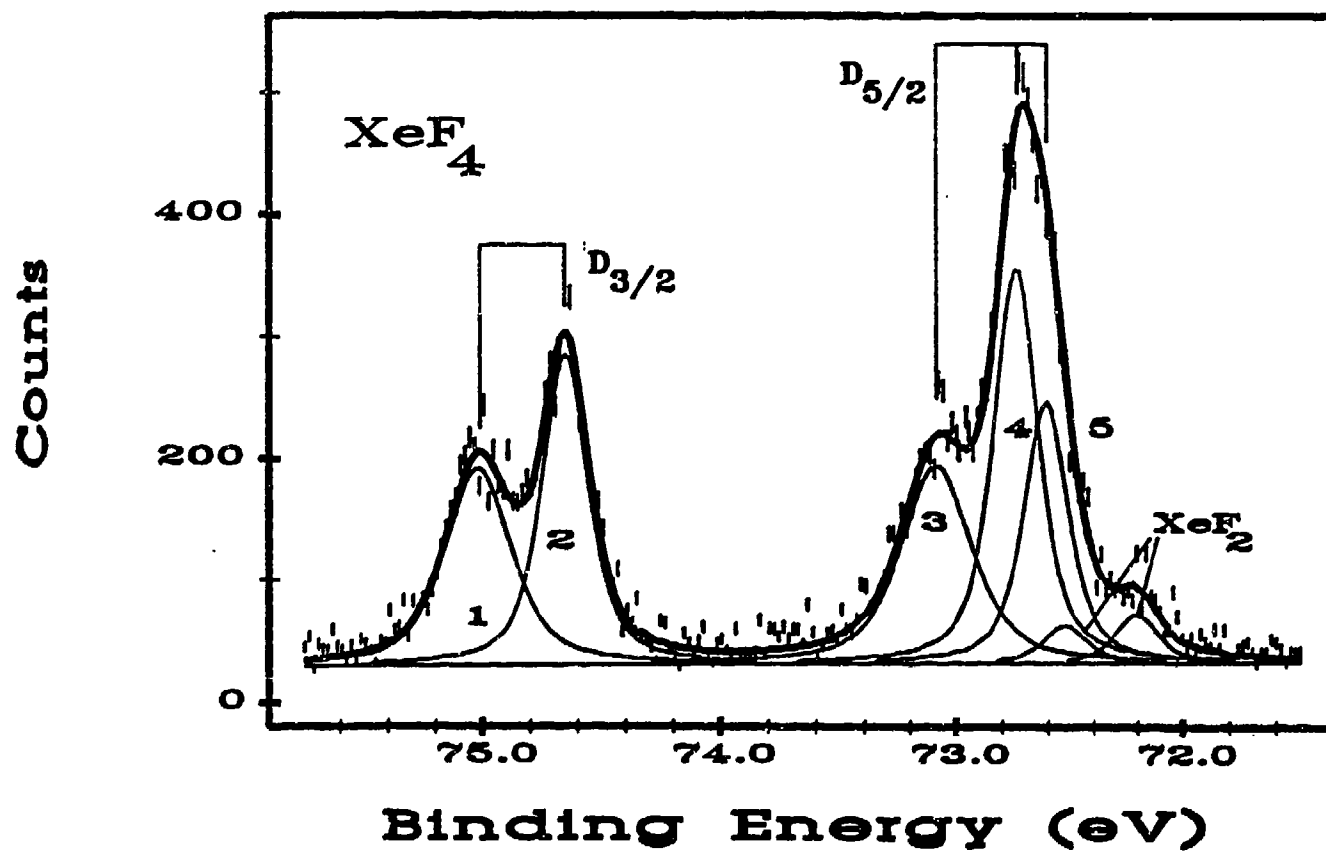
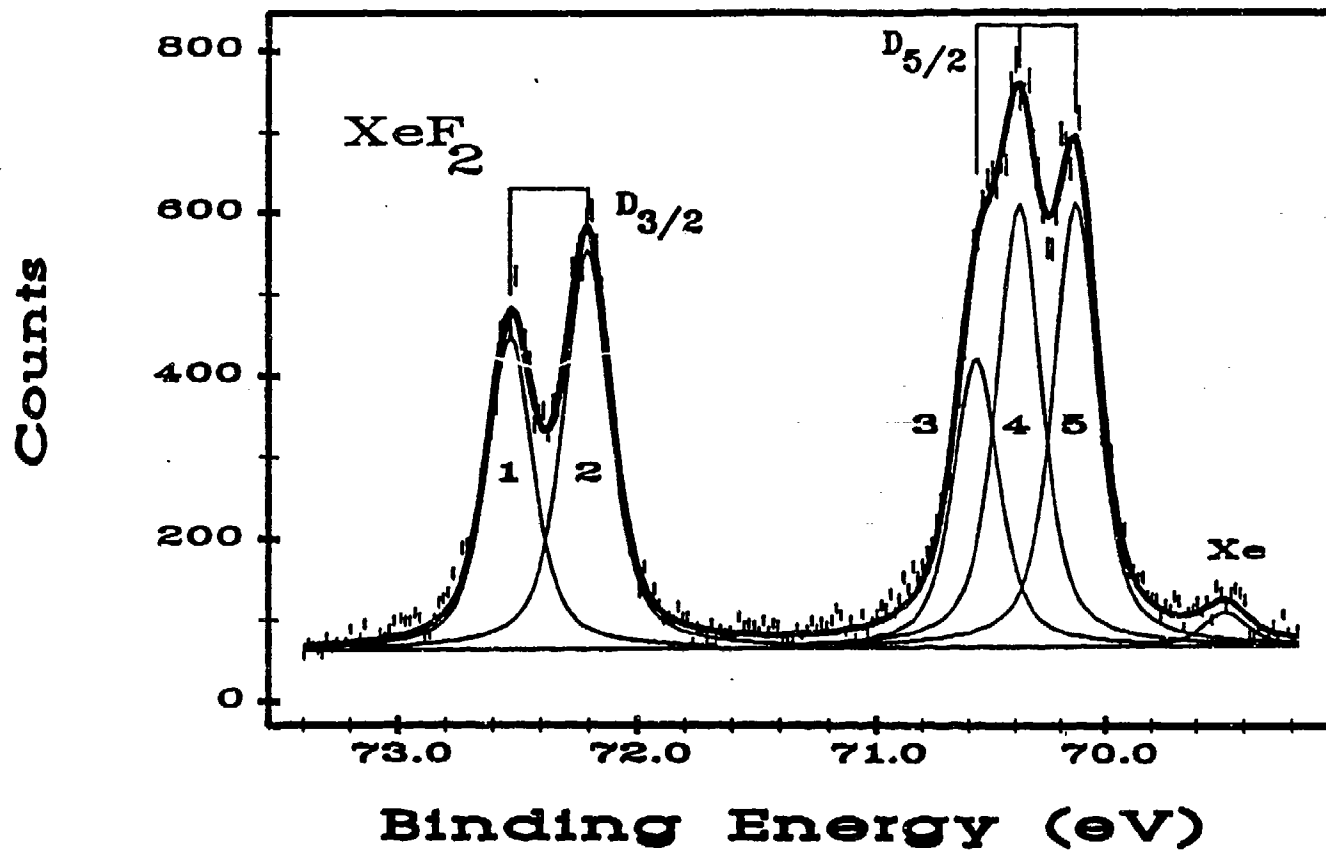
**Table 4:** Bond lengths and  $^{129}\text{Xe}$  quadrupole splittings of selected xenon compounds in the +2, +4 and +6 oxidation states.

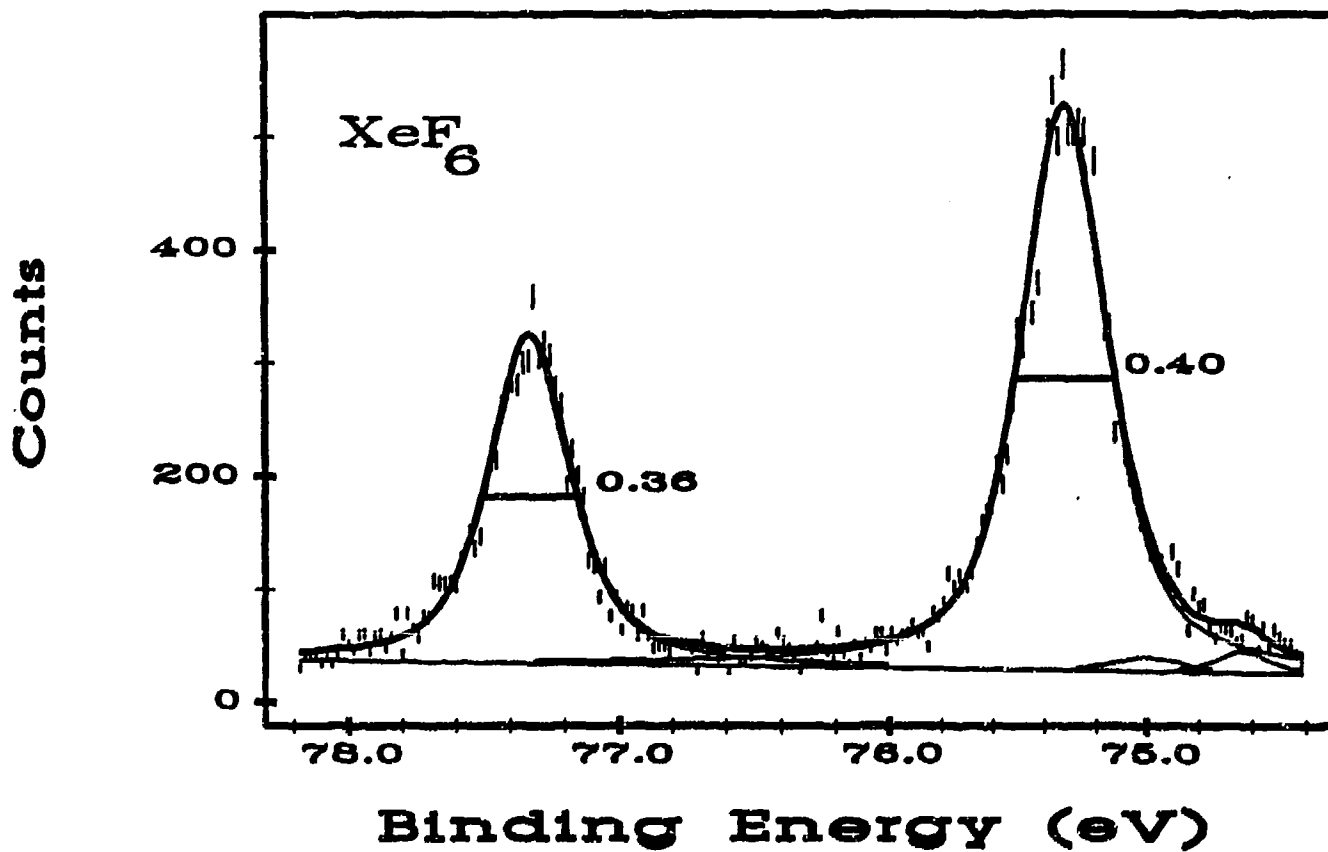
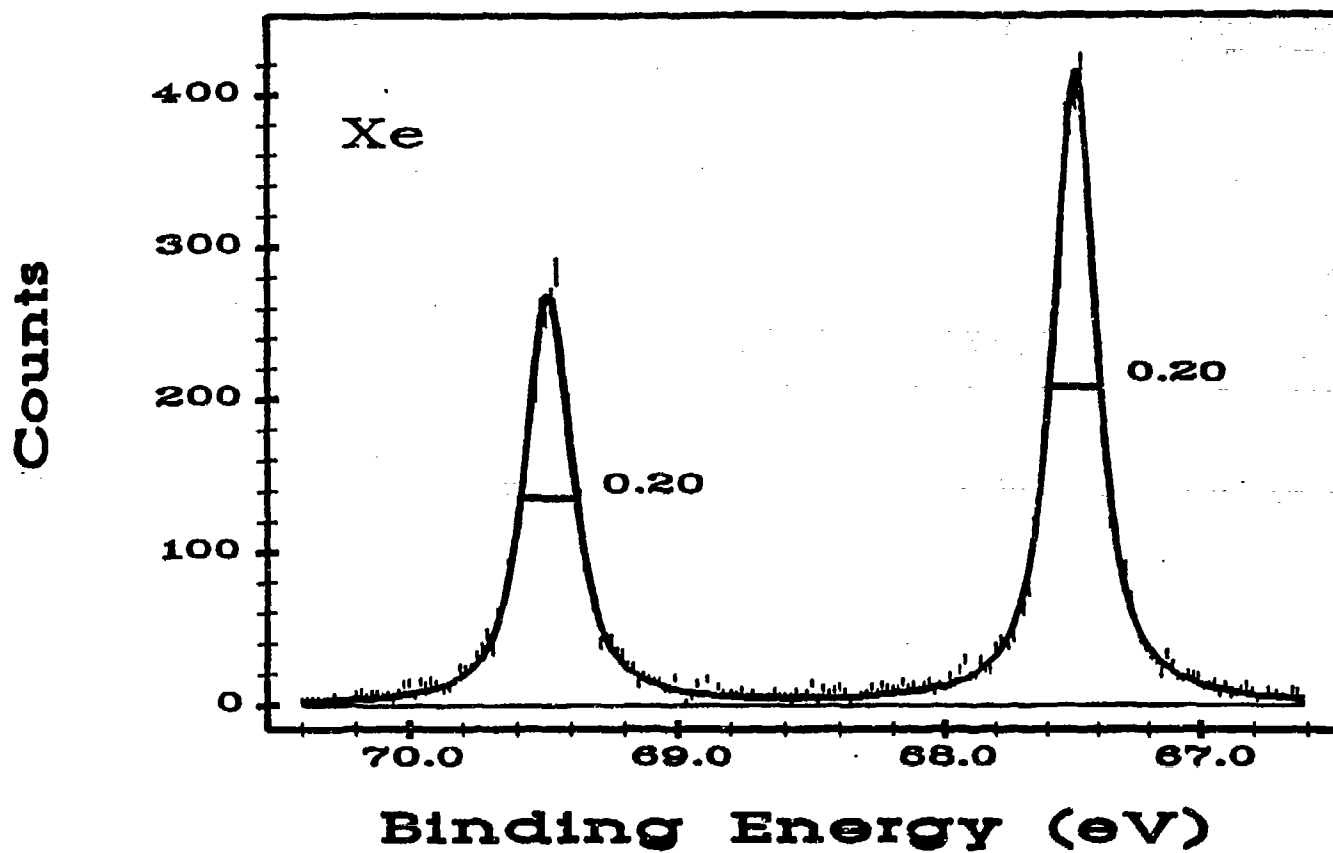
Compound	Xe-F Bridging Å	Xe-F Terminal Å	$\Delta E_Q$ mm s <sup>-1</sup>	Ref
$\text{XeF}_2$		2x2.00	39.7(4)	2
$\text{XeF}_2 \cdot 2\text{WOF}_4$	2.04	1.89	41.0(3)	38
$\text{XeF}^+\text{Sb}_2\text{F}_{11}^-$	2.35	1.84	41.5(2)	38
$\text{Xe}_2\text{F}_3^+\text{AsF}_6^-$	2.14	2x1.90	41.3(2)	38
$\text{XeF}_4$		4x1.953	41.04(7)	38
$\text{XeF}_3^+\text{BiF}_6^-$	2.25	1.81; 2x1.93	41.3(1)	38
$\text{XeF}_6$ (Tetramer)	2.23/2.60(3)	1.86(3); 1.84(3)	7.7(2)	13
(Hexamer)	2.56(2)	1.76(3); 1.96(2)		

## FIGURE CAPTIONS

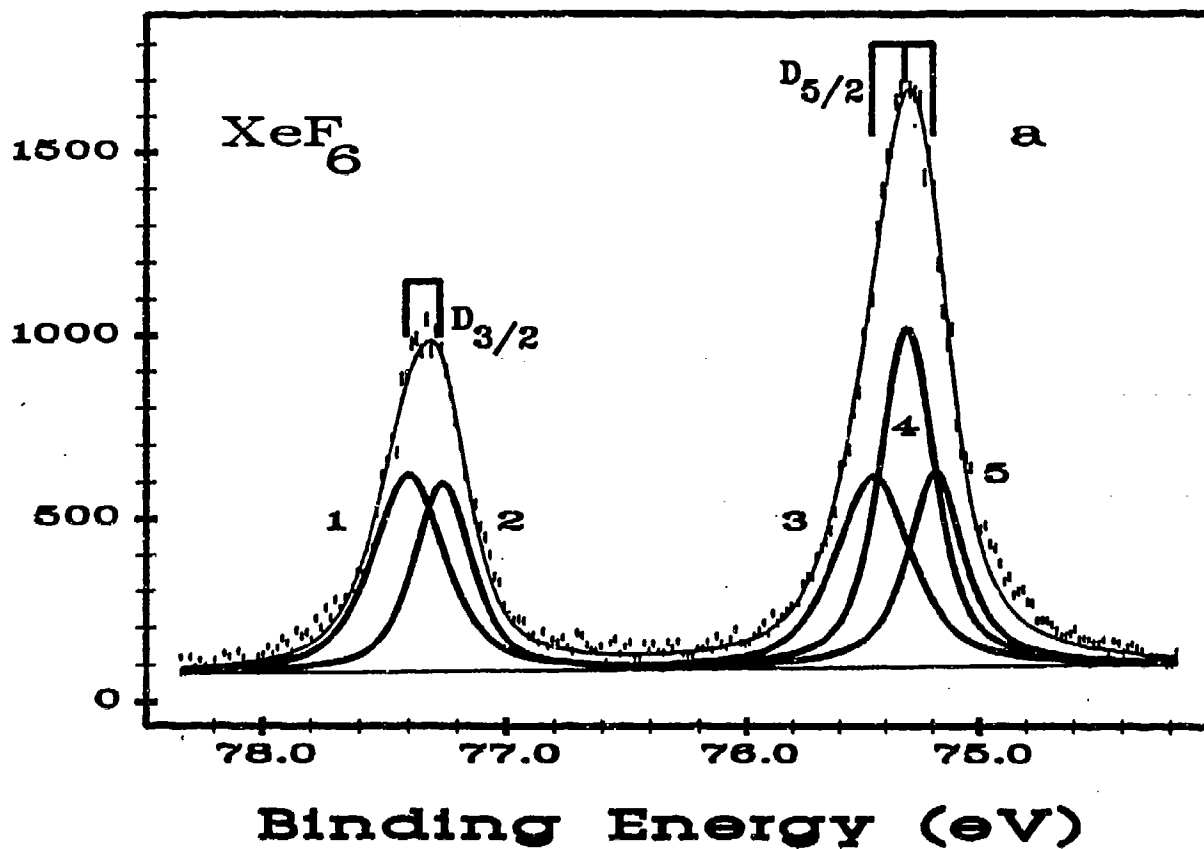
- (1) A calibration spectrum of the 4d level in Xe and XeF<sub>2</sub> showing the similar FWHM in both species.
- (2) The ligand field splitting in XeF<sub>2</sub> and XeF<sub>4</sub>. These spectra show the resolved splitting patterns. The thin lines are a best fit to the spectra.
- (3) A comparison of the 4d region of Xe and XeF<sub>6</sub>. It is apparent that XeF<sub>6</sub> has substantially broader lines than in Xe. This broadening is due to ligand field splitting of the core 4d level.
- (4) The best five peak fits to the gas phase 4d spectrum of XeF<sub>6</sub> taken at two different resolutions; a) was taken at 50  $\mu\text{m}$  ( $\Delta E = 0.21\text{eV}$ ) and b) was taken at 25  $\mu\text{m}$  ( $\Delta E = 0.11\text{eV}$ ). The five peak fit of spectra (b) are statistically better than the single band fit in Figure 3.
- (5) Plot of  $C_2^0$  versus  $\theta_{4,5,6}$  (and F-Xe-F bond angle) for different  $\theta_{1,2,3}$  values (48° —, 50° — — —, 52° •••, 54.7° — • — • —).  $\circ$  represents the position of XeF<sub>6</sub> if it is perfectly octahedral. (The F-Xe-F angles are 90° and  $\theta_{1,4}$  is 54.7°.) In the case of  $\theta_{1,2,3}$  being 50°, the errors on  $C_2^0$  and  $\theta_{4,5,6}$  are given by the dimensions of the box.



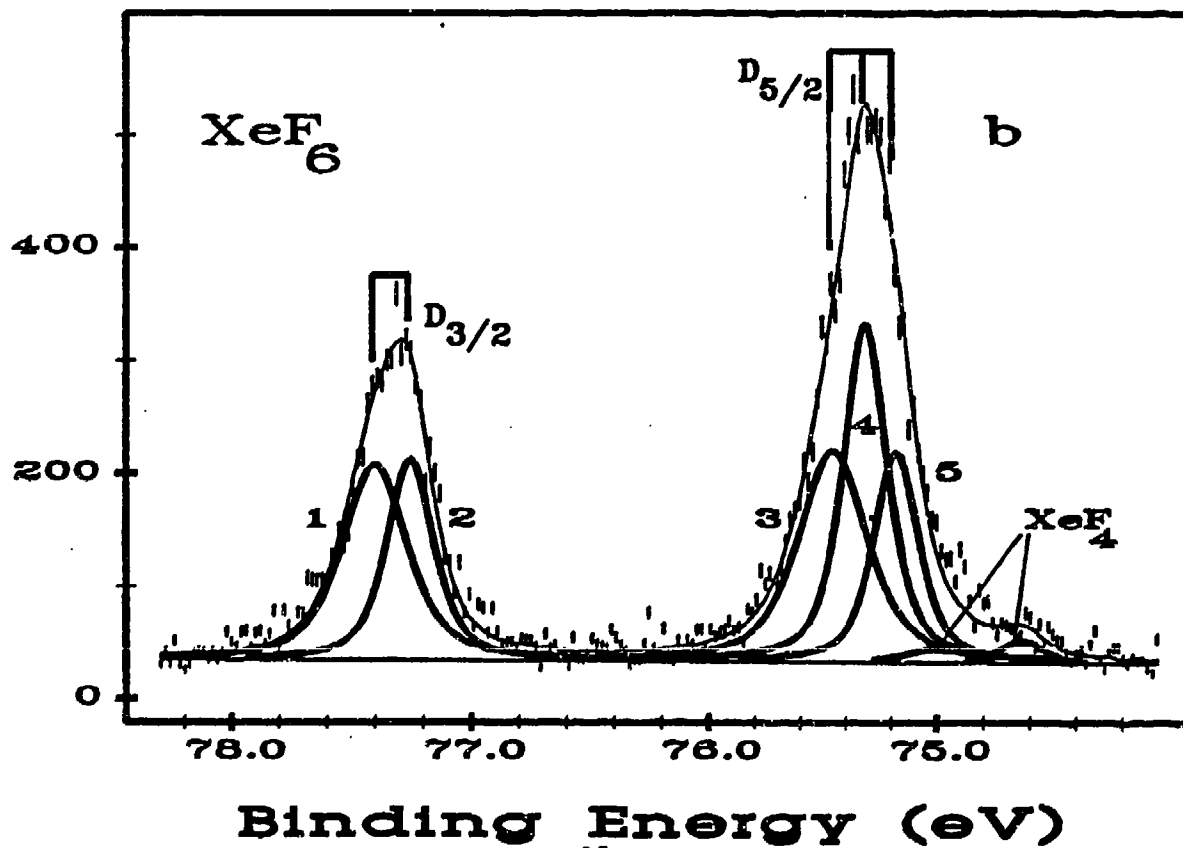


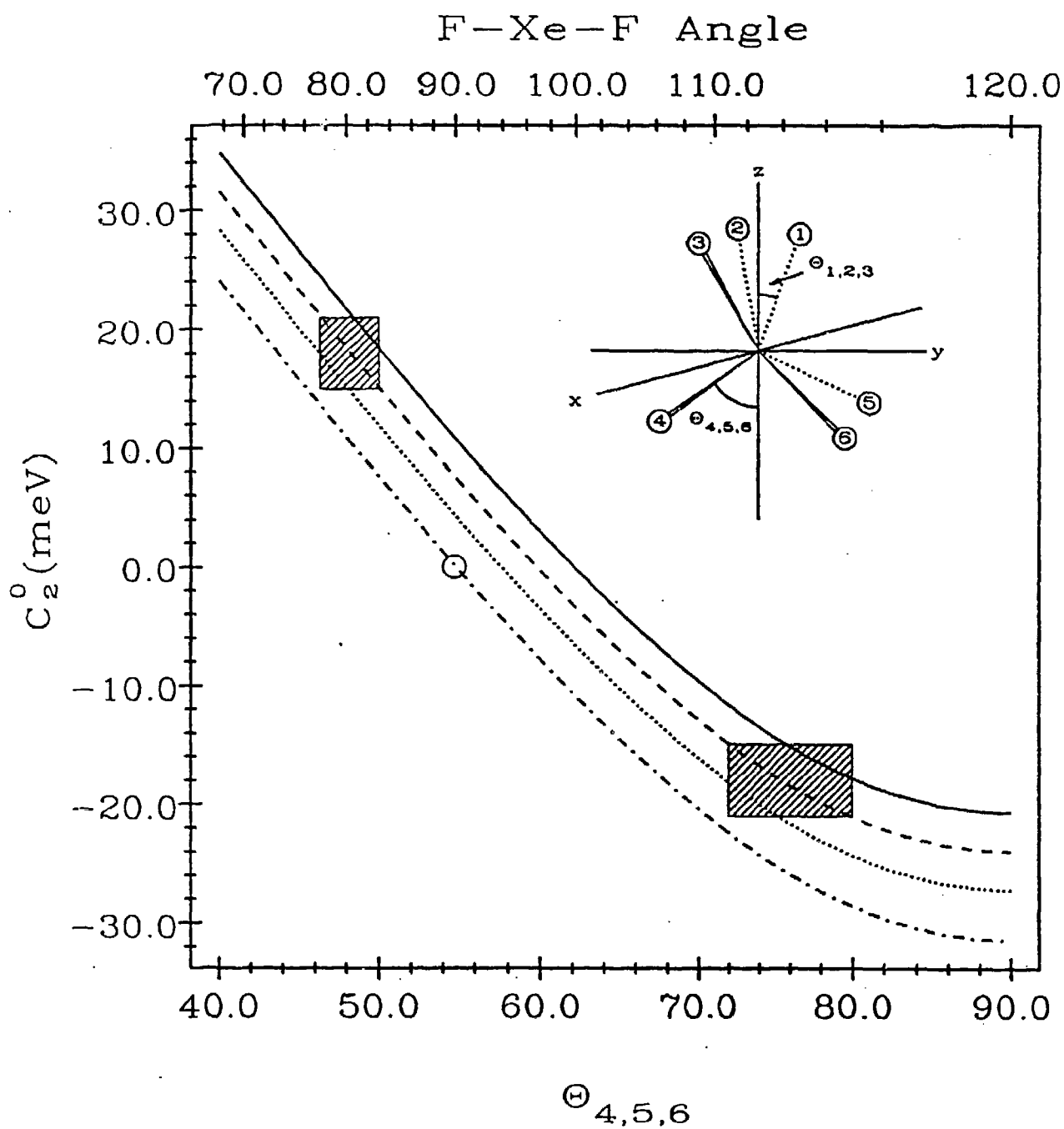


Counts



Counts





## PART X

THE SYNTHESIS AND CHARACTERIZATION OF THE WEAKLY  
COORDINATING ANIONS  $\text{Sb}(\text{OTeF}_5)_6^-$ ,  $\text{Bi}(\text{OTeF}_5)_6^-$  AND  $\text{Pb}(\text{OTeF}_5)_6^-$





## SUMMARY

In this study the interest lies in preparing derivatives of Sb and Bi in their +5 oxidation state. Characterization of these species relied upon NMR spectroscopy involving  $^{19}\text{F}$  ( $I=1/2$ ), and the little studied quadrupolar nuclei  $^{121}\text{Sb}$  ( $I=5/2$ ), and  $^{209}\text{Bi}$  ( $I=9/2$ ).

$\text{Et}_4\text{N}^+\text{Sb}(\text{OTeF}_5)_4^-$  was prepared and found to be stable at room temperature. The  $\text{Sb}(\text{OTeF}_5)_5$  was not isolated. The  $\text{Sb}(\text{OTeF}_5)_4^-$  was characterized using  $^{121}\text{Sb}$  and  $^{19}\text{F}$  NMR spectroscopy in acetonitrile solution.

The  $\text{Bi}(\text{OTeF}_5)_4^-$  anion was also prepared as the  $\text{Et}_4\text{N}^+$  salt and was found to decompose slowly in acetonitrile at room temperature. The salt was prepared using the same basic method as for the analogous  $\text{Sb}(\text{OTeF}_5)_4^-$  anion. However, in this case the  $\text{Bi}(\text{OTeF}_5)_5$  formed in the reaction of  $\text{BiF}_5$  and  $\text{B}(\text{OTeF}_5)_3$  was isolated. The  $\text{Bi}(\text{OTeF}_5)_4^-$  anion was characterized by  $^{209}\text{Bi}$  and  $^{19}\text{F}$  NMR in  $\text{SO}_2\text{ClF}$  and  $\text{CH}_3\text{CN}$  solutions.

The  $\text{Bi}(\text{OTeF}_5)_4^-$  anion is unique in that it is only the second octahedral  $\text{Bi(V)}$  species known and gives only the second  $\text{Bi(V)}$  NMR resonance known; the other being  $\text{BiF}_6^-$ .

## INTRODUCTION

### The $\text{OTeF}_5$ Ligand

The  $\text{OTeF}_5$  group is a highly electronegative ligand which is capable of stabilizing high positive oxidation states of the atom to which it is bonded.<sup>1-6</sup> Moreover, the ligand is capable of forming stable derivatives whose analogs are fluorine compounds. Examples include  $\text{TeF}_6$ ,  $\text{Te}(\text{OTeF}_5)_4$ ;<sup>3,4,5</sup>  $\text{UF}_6$ ,  $\text{U}(\text{OTeF}_5)_4$ ;<sup>6,7</sup> and  $\text{O}=\text{XeF}_4$ ,

$O=Xe(OTeF_5)_4$ .<sup>3,6,7</sup> The  $OTeF_5$  group stabilizes many derivatives and has a wide range of applications. Seppelt has prepared a review of the  $OTeF_5$  group which includes tables listing many of these derivatives.<sup>1</sup>

The  $OTeF_5$  ligand has two analogs,  $OSeF_5$  and  $OSF_5$ , and the reactivities of the derivatives of these ligands differ somewhat. The  $OSF_5$  derivatives are relatively unstable and are obtained in only a few cases.<sup>1</sup> There are a large number of  $OSeF_5$  derivatives, although  $OSeF_5$  chemistry is not as extensive as  $OTeF_5$  chemistry. This is in part because  $OSeF_5$  derivatives are thermally less stable than  $OTeF_5$  derivatives and also because  $OSeF_5$  derivatives are more difficult to prepare than their  $OTeF_5$  analogs. This is due to the highly oxidizing nature of  $HOSeF_5$ , and the fact that the selenium analog of  $B(OTeF_5)_3$ , the major ligand transfer reagent for  $OTeF_5$ , is not stable.<sup>1</sup>

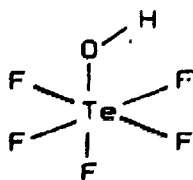
#### Pentafluorooxotelluric Acid, $HOTeF_5$

The starting material for  $OTeF_5$  derivatization is the moderately strong, monoprotic acid  $HOTeF_5$  and is best prepared from  $Te(OH)_6$  according to equation (1)

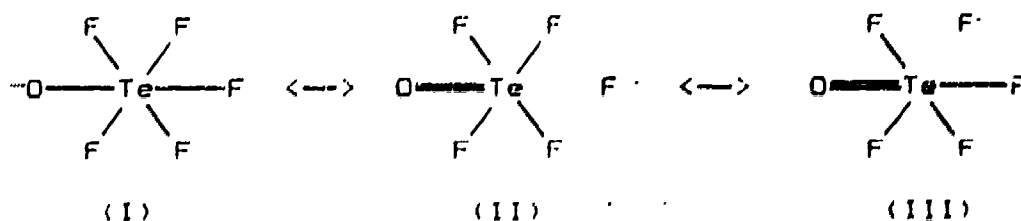


Pentafluorooxotelluric acid,  $HOTeF_5$ , is found to have an acid strength between  $HCl$  and  $HNO_3$  when measured in glacial acetic acid<sup>1</sup> and is easily converted into  $OTeF_5^-$  salts.<sup>1</sup>

The structure of  $HOTeF_5$  has been shown to be pseudo-octahedral<sup>1</sup>.



Thus, the  $^{125}\text{Te}$  NMR spectra of  $\text{OTeF}_5$  groups are generally  $\text{AB}_4$  spin systems (vide infra).<sup>1</sup> The vibrational spectra of alkali metal salts of  $\text{HOTeF}_6$  are consistent with  $\text{OTeF}_5^-$  anion formation and can be rationalized in terms of three resonance structures.<sup>11</sup>



From the low frequency of the  $\text{Te-F}$  stretch and the high frequency of the  $\text{O-Te}$  stretch, it is assumed that resonance structures (II) and (III) are dominant, which can be accounted for in terms of the higher electronegativity of F when compared to that of O.

#### Electronegativity of the $\text{OTeF}_5$ Group

The high electronegativity of the  $\text{OTeF}_5$  ligand is one of its most important properties. Several studies have developed a qualitative comparison between the  $\text{OTeF}_5$  group and F.<sup>1,11,12,14</sup> Studies have shown, through the use of NMR and Mössbauer spectroscopy, that the electronegativity of  $\text{OTeF}_5$  is less than that of F. It has been quoted as 3.88 versus 4.01 for F (Pauling Scale).<sup>2</sup> The high electronegativity of the group is due to the powerful negative inductive

effect of the five fluorines, and this is possibly enhanced by some backbonding from the oxygen to tellurium.<sup>2,4</sup> The earlier apparent contradiction to the VSEPR rules, which suggested that  $\text{OTeF}_6$  was more electronegative than F, can be explained by noting that the differences between the equatorial and axial positions of the pseudo-octahedral  $\text{F}_{n+1}(\text{OTeF}_6)_{5-n}$  series (square based pyramidal structure) are not great. In contrast, the barriers to rotation are significant in bipyramidal structures.

#### Derivatives of the $\text{OTeF}_6$ Group

Most of the derivatives are produced by the replacement of F in simple substitution reactions. The  $\text{OTeF}_6$  derivatives can be placed in three main classes; s-block main-group (alkali and alkaline earth salts), transition metal, and p-block main-group derivatives. The salts are usually formed by the reaction of  $\text{HOTeF}_6$  and alkali metal halides other than fluorides.



The derivatives formed with transition metals are not as abundant as those for the main-group elements. This is not necessarily an indication that the derivatives are not as stable, but is presumed to be an indication of less research in this area. These derivatives are mainly formed by reactions of  $\text{B}(\text{OTeF}_6)_3$  with the first transition period fluorides. Some examples include  $\text{Ti}(\text{OTeF}_6)_4$ ,<sup>12,14</sup>  $\text{O}=\text{V}(\text{OTeF}_6)_3$ ,<sup>12,17</sup> and  $\text{W}(\text{OTeF}_6)_6$ .<sup>17</sup>

Main-group  $\text{OTeF}_6$  chemistry is extensive, including compounds from

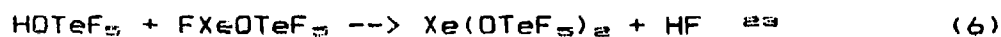
every period.<sup>1</sup> Many of the covalent derivatives have measureable vapour pressures and have a tendency to sublime, indicating that OTeF<sub>5</sub> groups cause very little intermolecular interaction, in contrast to their F analogs. The OTeF<sub>5</sub> group also rarely forms bridges, which is also in contrast with the F derivatives. This leads to interesting comparisons between the F and OTeF<sub>5</sub> derivatives. For example, SbF<sub>5</sub> tends to adopt octahedral symmetry by forming cis-F bridges and polymerizing to (SbF<sub>5</sub>)<sub>n</sub>, whereas the pentakis OTeF<sub>5</sub> analog, even though it has oxygen lone pairs, will not bridge, which is partially due to steric hindrance effects. Thus, the structure of the five coordinate Sb(OTeF<sub>5</sub>)<sub>5</sub> compound may be expected to exhibit either trigonal bipyramidal or square-based pyramidal symmetry around the Sb atom.

Noble-gas (xenon) derivative formation is indicative of the high effective group electronegativity of the OTeF<sub>5</sub> ligand and its resistance to oxidative attack by xenon in its positive oxidation states. It yields the most stable covalent derivative of XeF<sub>2</sub> and the only other fully substituted covalent derivatives of XeF<sub>4</sub> and XeOF<sub>4</sub>.<sup>1</sup> The Xe derivatives provide an important route for the oxidative addition of the OTeF<sub>5</sub> ligand (vide infra).<sup>1</sup>

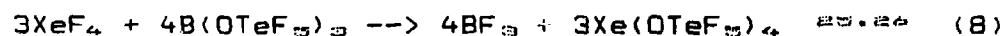
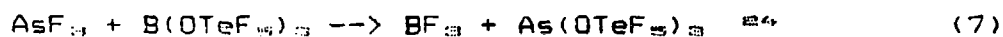
#### Methods of Preparation for Main-Group OTeF<sub>5</sub> Derivatives

There are several methods of preparation of OTeF<sub>5</sub> derivatives. The most direct involve reactions of a halide with HOTeF<sub>5</sub> leading to the elimination of volatile hydrogen halides; for example





The second reaction is of particular importance as  $\text{B}(\text{OTeF}_5)_3$  is the starting material for the majority of  $\text{OTeF}_5$  derivatives. A few examples of this preparative approach include



The latter routes are particularly attractive in that  $\text{BF}_3$  is readily removed under vacuum.

The latter two reactions are both substitution reactions of F by  $\text{OTeF}_5$ . The bis-derivative,  $\text{Xe}(\text{OTeF}_5)_2$ , can be used to cleanly introduce  $\text{OTeF}_5$  oxidatively



#### Multinuclear Magnetic Resonance Spectroscopy of $\text{OTeF}_5$ Derivatives

In order to characterize the compounds synthesized in this work, the NMR spectra of three nuclides were studied;  $^{19}\text{F}$ ,  $^{121}\text{Sb}$ , and

$^{209}\text{Bi}$ . The  $^{19}\text{F}$  nucleus has a spin of  $1/2$ , 100% abundance, and a high sensitivity of 0.833 relative to  $^1\text{H}$ . The  $\text{OTeF}_5$  group exhibits an  $\text{AB}_4$  pattern, which, in the first-order limit, is observed as a strong doublet (the  $\text{X}_4$  part) and a weaker quintet (the A part). However, the  $\text{AB}_4$  pattern is never that simple, and in extreme cases can even appear as a single peak. As the chemical shifts of the A and  $\text{B}_4$  fluorines ( $\delta_A$  and  $\delta_B$ ) approach similar values the resolution between the two sets of peaks decreases until the point when  $\delta_A = \delta_B$  and the two sets of peaks overlap completely. The  $\text{B}_4$  portion of this group belongs to the  $\text{D}_4$  symmetry group, which yields thirty-two symmetrised spin product functions. The  $\text{AB}_4$  system involves twenty-five possible transitions, and thus twenty-five possible bands. Therefore, the  $\text{AB}_4$  patterns tend to be very complex.<sup>127</sup> Another observable feature of the  $^{19}\text{F}$  NMR spectra of the  $\text{OTeF}_5$  groups are the  $^{125}\text{Te}$  satellites. They appear as small sets of peaks (approximately 3.5% of total intensity) on either side of the  $^{19}\text{F}$ - $^{19}\text{F}$  coupling peaks and their shapes resemble those of the central peaks. Occasionally  $^{123}\text{Te}$  (0.89% abundant) satellites can be observed although these are often too weak to be seen over the base-line noise.

In the present work, the anions,  $\text{MF}_6^-$  and  $\text{M}(\text{OTeF}_5)_2^-$  ( $\text{M} = \text{Sb}, \text{Bi}$ ), were also studied by  $^{121}\text{Sb}$  and  $^{209}\text{Bi}$  NMR. These nuclei both have high nuclear spin quantum numbers ( $^{121}\text{Sb}$ ,  $I=5/2$ ;  $^{209}\text{Bi}$ ,  $I=9/2$ ) and good sensitivity, but they both have large quadrupole moments (Table 1), thus making antimony and bismuth NMR spectra difficult to obtain in cases where the electronic symmetry at the nucleus is less than cubic.



Table 1. NMR Parameters for  $^{121}\text{Sb}$  and  $^{209}\text{Bi}$

<u>PARAMETER</u>	<u><math>^{121}\text{Sb}</math></u>	<u><math>^{209}\text{Bi}</math></u>
$I^a$	5/2	9/2
$C$ (%) <sup>b</sup>	57.25	100
$(10^7 \text{ rad T}^{-1} \text{ s}^{-1})^c$	6.4355	4.2988
$Q$ ( $10^{-28} \text{ m}^2$ ) <sup>d</sup>	-0.28	-0.38
$\nu$ (MHz) <sup>e</sup>	24.056	16.070
$f$ ( $10^{-10} \text{ s} / \text{m}^2$ ) <sup>f</sup>	$2.5 \times 10^{-10}$	$1.1 \times 10^{-10}$
$D_{\text{rel}}^g$	527	777

<sup>a</sup> $^{123}\text{Sb}$  is also NMR active; 25.92% abundant,  $I = 7/2$ ; but is less sensitive than  $^{121}\text{Sb}$ .

<sup>b</sup>Nuclear spin quantum number.

<sup>c</sup>Natural abundance.

<sup>d</sup>Magnetogyric ratio.

<sup>e</sup>Quadrupole moment.

<sup>f</sup>Resonance frequency at 2.3488T.

<sup>g</sup>Linewidth factor  $= (2I + 3)Q^2 / I^2(2I - 1)$ .

<sup>h</sup>Receptivity relative to  $^{13}\text{C}$ .

Quadrupole relaxation broadens spectral lines, where the linewidth is defined by the equation (10)

$$w_q = \frac{3\pi^2 (2I + 3)}{10 I^2 (2I - 1)} \left[ \frac{[e^2 q_{zz} - Q]}{h^2} \right]^2 (1 + \eta^2/3) \tau_c \quad (10)$$

where  $I$  is the spin of the nucleus,  $e$  is the charge of the electron,  $q_{zz}$  is the largest component of the electric field gradient at the nucleus,  $Q$  is the quadrupole moment,  $\eta$  is the asymmetry parameter for  $q$ , and  $\tau_c$  is the isotropic correlation time.<sup>19</sup> Thus, in order to obtain reasonably narrow  $^{121}\text{Sb}$  or  $^{209}\text{Bi}$  linewidths, a small to zero electric field gradient at the quadrupolar nucleus, along with a small correlation (tumbling) time, are required. Observation of the resonance of a quadrupolar nucleus thus requires that the ligands be symmetrically arranged around the quadrupolar nucleus and that the sample be run dilute in a low-viscosity solvent in order to minimize  $\tau_c$ .

NMR studies involving  $^{209}\text{Bi}$  are rare; there are only two previously reported  $^{209}\text{Bi}$  resonances,  $\text{BiF}_6^-$ <sup>20</sup> and  $\text{Bi}(\text{NO}_3)_3$ .<sup>21</sup> Aqueous solutions of  $\text{Bi}(\text{NO}_3)_3$  give broad resonances ( $w_q = 3200$  Hz). The  $^{209}\text{Bi}$  spectrum of  $\text{BiF}_6^-$  consists of a 1:6:15:20:15:6:1 septet with an observed  $^{209}\text{Bi}$ - $^{19}\text{F}$  coupling constant of  $3823 \pm 3$  Hz and a linewidth of 44 Hz.<sup>20</sup>

Antimony-121 NMR has been used more extensively than  $^{209}\text{Bi}$  NMR, but it too has a large quadrupole moment which consequently limits the number of Sb compounds which exhibit a  $^{121}\text{Sb}$  resonance. The  $^{121}\text{Sb}$  linewidths range from 35 Hz for octahedral  $\text{SbF}_6^-$  in  $\text{Et}_4\text{N}^+\text{SbF}_6^-$  (0.1 M in  $\text{CH}_3\text{CN}$ ),<sup>21</sup> to as high as 8000 Hz for  $\text{SbCl}_3$  (neat liquid).<sup>22</sup>

### Purpose of Present Research

The research outlined in this section of our report is aimed at expanding our knowledge of the group 5 (15) OTeF<sub>5</sub> derivatives. Several derivatives have been isolated and characterized previous to this work, including P(OTeF<sub>5</sub>)<sub>3</sub>, As(OTeF<sub>5</sub>)<sub>3</sub>, and Sb(OTeF<sub>5</sub>)<sub>3</sub> in the +3 oxidation state; and As(OTeF<sub>5</sub>)<sub>5</sub>,<sup>32</sup> As(OTeF<sub>5</sub>)<sub>4</sub><sup>-</sup>,<sup>32</sup> SbF<sub>5</sub>(OTeF<sub>5</sub>)<sub>2</sub>,<sup>32</sup> and SbF<sub>4</sub>OTeF<sub>5</sub><sup>32</sup> in the +5 oxidation state. The compound Sb(OTeF<sub>5</sub>)<sub>5</sub> has also been claimed and has been reported to decompose rapidly at room temperature.<sup>1</sup>

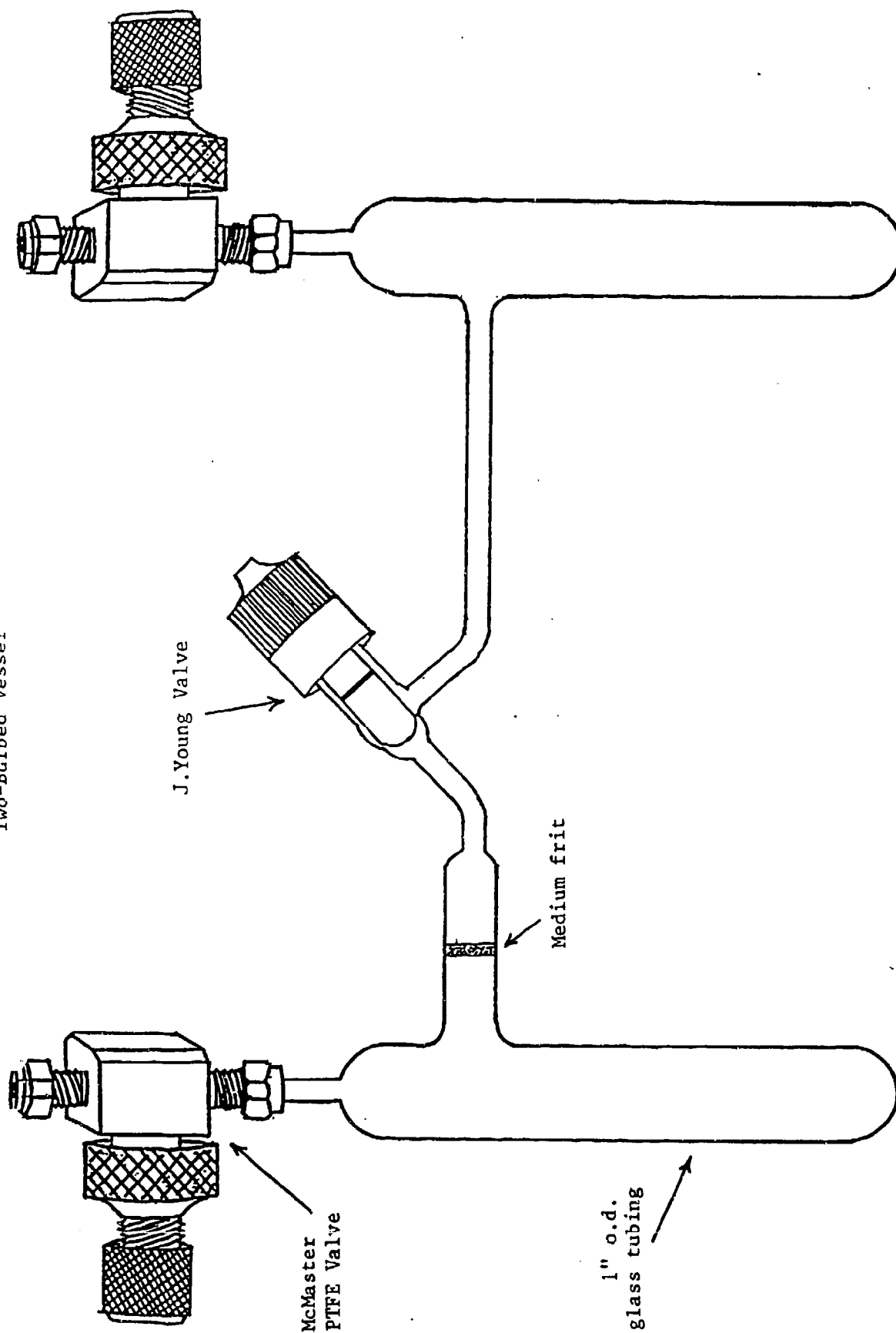
The work involved the preparation of OTeF<sub>5</sub> derivatives of Sb(V) and Bi(V). The aim of this research was to prepare both the M(OTeF<sub>5</sub>)<sub>5</sub> and M(OTeF<sub>5</sub>)<sub>4</sub><sup>-</sup> species where M = Sb or Bi. The purpose was two-fold; there is intrinsic value in the knowledge gained of the chemistry of Sb and Bi in their highest oxidation states, and these compounds can be used as precursors for other work. The OIF<sub>4</sub>=O group, which is of greater electronegativity than OTeF<sub>5</sub>, can be introduced by the reaction of the acid HOIF<sub>4</sub>=O with an OTeF<sub>5</sub> derivative



Also, the formation of Xe(OTeF<sub>5</sub>)<sub>n</sub><sup>+</sup> cations can be explored by using these compounds as OTeF<sub>5</sub> group acceptors.



Figure 1  
Two-Bulbed Vessel



$\text{SO}_2\text{ClF}$  (Columbia Organic Chemicals) was purified according to literature technique.<sup>35</sup> The chlorofluorocarbon solvents,  $\text{CFCl}_3$  and  $\text{CClF}_2\text{CClF}_2$  (Freon 114; Aldrich), were dried over  $\text{P}_2\text{O}_5$ . Anhydrous HF (Harshaw), which was used as both a solvent and a reactant, was purified by storing it under 5 atm. of  $\text{F}_2$  for at least one month as previously described.<sup>34</sup>

#### Preparation of Starting Materials

$\text{Et}_4\text{N}^+[\text{F}^--(\text{HF})_n]$  Hydrogen fluoride solvated tetraethylammonium fluoride was prepared by directly mixing  $\text{Et}_4\text{NCl}$  (2.4221 g, 14.617 mmol) and excess HF in an FEP tube. The HCl that was produced and the excess HF were pumped off under vacuum to leave a white solid.

$\text{Me}_4\text{N}^+[\text{F}^--(\text{HF})_n]$  Hydrogen fluoride solvated tetramethylammonium fluoride was prepared by allowing  $\text{Me}_4\text{NBr}$  (.9701 g, 5.854 mmol) to react with excess anhydrous HF in an FEP tube. The excess HF and the HBr that was produced by the reaction were pumped off under vacuum to leave a light brown sticky solid.

$\text{Et}_4\text{N}^+\text{OTeF}_5^-$  The first attempt to prepare tetraethylammonium pentafluorooxotellurate(VI) involved the neat reaction of  $\text{Et}_4\text{N}^+\text{Cl}$  (3.3998 g, 20.5171 mmol) and  $\text{HOTeF}_5$  (4.9987 g, 20.863 mmol). Hydrogen chloride gas was evolved during the reaction, and the product obtained was an opaque, bright yellow, viscous mass. This was inconsistent with previous literature observations<sup>14</sup> and thus a second method was attempted.

The second attempt involved allowing equimolar portions of  $\text{HOTeF}_5$

(4.5281 g, 18.8985 mmol) and  $\text{Et}_4\text{N}^+\text{Cl}^-$  (3.0386 g, 18.3373 mmol) to react in  $\text{CH}_2\text{Cl}_2$  solvent. The reaction was carried out in a two-bulb reaction vessel (Fig. 1). This yielded a clear yellow solution and  $\text{HCl}$  gas. The solvent was pumped off under vacuum to leave a yellow solid which was extracted three times with ethyl acetate. This was done by adding ethyl acetate to the product and then filtering it off through the frit to the second bulb. The impurities were soluble in the solvent but the product was not. The solvent was redistilled onto the product and refiltered twice, and then the solvent was pumped off both bulbs yielding 5.7430 g of slightly yellow solid,  $\text{Et}_4\text{N}^+\text{OTeF}_6^-$  (84.9% yield), and a bright yellow insoluble fraction (not characterized).

$\text{Et}_4\text{N}^+\text{SbF}_6^-$  Tetraethylammonium hexafluoroantimonate(V) was prepared by the reaction of equimolar quantities of  $\text{Et}_4\text{N}^+\text{F}^-$  (14.617 mmol) and  $\text{SbF}_5$  (3.1661 g, 14.608 mmol) in  $\text{HF}$  solvent. The  $\text{Et}_4\text{N}^+\text{F}^-$  and the  $\text{SbF}_5$  were both dissolved in  $\text{HF}$  in the set-up shown in Figure 2. The reactants were then allowed to mix and they were left to react. The product solution in  $\text{HF}$  was a yellow low-viscosity liquid. The solvent was then removed and the substance was pumped under vacuum for 5½ hours at 60 °C. This gave 5.1336 g (96% yield) of colorless crystals. A 0.1 M NMR sample was prepared in acetonitrile in a 10 mm FEP tube.

$\text{Me}_4\text{N}^+\text{BiF}_6^-$  Tetramethylammonium hexafluorobismuthate(V) was prepared by the reaction of  $\text{Me}_4\text{N}^+\text{F}^-$  (4.4239 mmol) with  $\text{BiF}_5$  (1.3427 g, 4.4172 mmol) in  $\text{HF}$  solvent. The reactants were dissolved in  $\text{HF}$  in two separate FEP tubes, and then joined as shown in Figure 2. They were allowed to mix at liquid  $\text{N}_2$  temperature by pouring the  $\text{Me}_4\text{N}^+\text{F}^-$  in  $\text{HF}$

## EXPERIMENTAL

### Vacuum Procedures

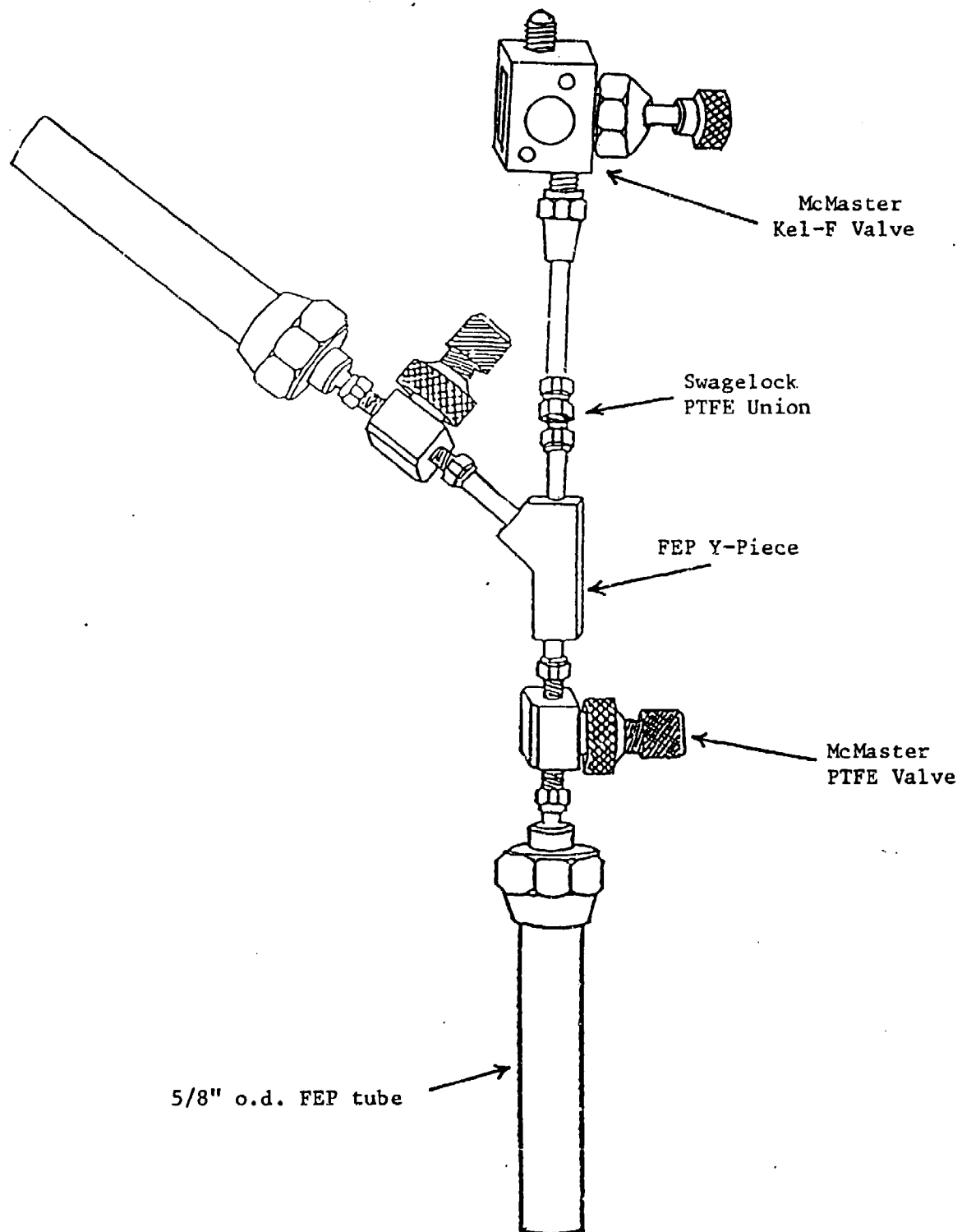
Most of the compounds used in the course of this research were air and moisture sensitive and required the use of drybox and vacuum line techniques. Those compounds with low vapour pressures were transferred and manipulated directly in the drybox, which had an atmosphere of less than 0.01 ppm of  $O_2$  and  $H_2O$ , and those compounds with high vapour pressures were transferred on a metal vacuum line.

### Starting Materials

Many of the starting materials were present in pure state in the lab, and were ready for use. The compounds  $HO\text{TeF}_5$  and  $B(OTeF_5)_3$ , had been prepared and purified according to literature techniques previously described by Sladky et al.<sup>20</sup> and Engelbrecht and Sladky respectively.<sup>19</sup> The antimony pentafluoride (Ozark Mahoning) had been purified by techniques previously described.<sup>24</sup> The  $BiF_5$  was supplied by Dr. K.O. Christie (Rocketdyne Division, North American Rockwell, Canoga Park, California) and the purity was checked by Raman spectroscopy.  $Et_4NCl$  (Aldrich) and  $Me_4NBr$  (BDH Chemicals), were dried under vacuum at 100 °C overnight or longer, and no further purification was needed.

The solvents  $CH_3CN$  (Baker Chemicals) and  $SO_2$  (Matheson) were dried over  $P_2O_5$  (BDH Chemicals) at least overnight.  $CH_2Cl_2$  (BDH Chemicals) was dried over  $CaH_2$  (BDH Chemicals), and ethyl acetate (Fisher Chemicals) was dried over molecular sieves (Davidson, Fisher, Type 4A).

Figure 2  
Y-Piece Apparatus





onto the  $\text{BiF}_3$  under HF and then allowed to warm slowly to room temperature. The reaction vessel contained a white powder at all times, since the reactant,  $\text{BiF}_3$ , and the product,  $\text{Me}_4\text{N}^+\text{BiF}_6^-$ , were both insoluble in HF. The solvent was removed and the product obtained was a fine white powder. A 0.1 M NMR sample was prepared in acetonitrile and was used as the  $^{209}\text{Bi}$  standard.

$\text{Et}_4\text{N}^+\text{SbF}_6^- / \text{B}(\text{OTeF}_5)_3$  This reaction, the first attempt at preparing  $\text{Sb}(\text{OTeF}_5)_4^-$ , was carried out by combining stoichiometric amounts of  $\text{Et}_4\text{N}^+\text{SbF}_6^-$  (0.6235 g, 1.704 mmol) and  $\text{B}(\text{OTeF}_5)_3$  (2.5487 g, 3.508 mmol) in the solvent  $\text{CFCl}_3$ . The reactants were combined at  $-196^\circ\text{C}$  and then allowed to warm to room temperature. No reaction occurred until the mixture was heated above room temperature with a hot-air gun, at which point  $\text{BF}_3$  gas was evolved. After allowing the mixture to react for a little over an hour the solvent was removed and the product obtained was a light brown viscous liquid. The  $^{121}\text{Sb}$  NMR of the product indicated that  $\text{Sb}(\text{OTeF}_5)_4^-$  had not been formed, rather a mixture of  $\text{SbF}_6^-$  and intermediate species such as  $\text{SbF}_5(\text{OTeF}_5)^-$  was indicated.

$\text{Et}_4\text{N}^+\text{Sb}(\text{OTeF}_5)_4^-$  The second attempt at preparing the  $\text{Sb}(\text{OTeF}_5)_4^-$  anion followed the same synthetic route as outlined for the preparation of  $\text{As}(\text{OTeF}_5)_4^-$ .<sup>38</sup> Stoichiometric amounts of  $\text{B}(\text{OTeF}_5)_3$  (6.3241 g, 8.70388 mmol) and  $\text{SbF}_5$  (0.9899 g, 4.5672 mmol) were added to separate sides of a two bulbed container (Figure 1). The solvent,  $\text{SO}_2$ , was then added to each bulb of the container, and the  $\text{B}(\text{OTeF}_5)_3$  in  $\text{SO}_2$  in the one bulb was poured through the frit onto the  $\text{SbF}_5$  in the other bulb.

The reaction was kept at 0 °C, and very little gas appeared to be evolved. The SO<sub>2</sub> was then pumped off and a white tacky solid remained. This was presumed to be Sb(OTeF<sub>5</sub>)<sub>3</sub>·SO<sub>2</sub>, but it was not isolated. The bulb containing the "Sb(OTeF<sub>5</sub>)<sub>3</sub>" was isolated and kept at -196 °C to prevent possible decomposition. The reaction vessel was then taken into a glove bag and an equimolar amount of Et<sub>4</sub>N<sup>+</sup>OTeF<sub>5</sub><sup>-</sup> (1.6771 g, 4.60113 mmol) was added to the second bulb. The vessel was then returned to the vacuum line and the Et<sub>4</sub>N<sup>+</sup>OTeF<sub>5</sub><sup>-</sup> was dissolved in SO<sub>2</sub>, and poured through the frit onto the Sb(OTeF<sub>5</sub>)<sub>3</sub>. Everything dissolved and the SO<sub>2</sub> was pumped off. The product remaining was a light brown tacky solid which formed a yellowish liquid when dissolved in acetonitrile. This solution exhibited <sup>121</sup>Sb NMR resonance indicating the presence of the desired anion, Sb(OTeF<sub>5</sub>)<sub>4</sub><sup>-</sup>.

Et<sub>4</sub>N<sup>+</sup>BiF<sub>4</sub><sup>-</sup>/B(OTeF<sub>5</sub>)<sub>3</sub> This reaction, the first attempt at preparing Bi(OTeF<sub>5</sub>)<sub>4</sub><sup>-</sup>, involved the combination of stoichiometric amounts of Et<sub>4</sub>N<sup>+</sup>BiF<sub>4</sub><sup>-</sup> (0.6803 g, 1.7131 mmol) and B(OTeF<sub>5</sub>)<sub>3</sub> (2.6475 g, 3.64376 mmol) in CH<sub>2</sub>Cl<sub>2</sub> solvent. A pale yellow substance formed in small amounts which was soluble in the solvent, although the majority of the product was a white insoluble powder. The powder was extracted several times with the solvent to remove impurities and allowed to dry. The contaminated solvent was pumped off the other bulb of the reaction vessel and a bright yellow solid remained, which turned brown when left sitting for several days at room temperature. An NMR sample of the white product was prepared that was approximately 0.1 M in acetonitrile, but it yielded no <sup>209</sup>Bi resonance, indicating that no Bi(OTeF<sub>5</sub>)<sub>4</sub><sup>-</sup> was formed.

Bi(OTeF<sub>5</sub>)<sub>5</sub> Bismuth pentakis(pentafluoroxotellurate) was prepared by the reaction of BiF<sub>3</sub> with B(OTeF<sub>5</sub>)<sub>3</sub>. In this reaction, finely powdered BiF<sub>3</sub> (0.5226 g, 1.7192 mmol) and excess B(OTeF<sub>5</sub>)<sub>3</sub> (2.7076 g, 3.7265 mmol) were added to separate sides of a two-bulbed vessel. The solvent CClF<sub>3</sub>CClF<sub>3</sub> (Freon 114) was distilled on to the B(OTeF<sub>5</sub>)<sub>3</sub> at -196 °C and then allowed to warm to room temperature to effect dissolution of the B(OTeF<sub>5</sub>)<sub>3</sub>. The B(OTeF<sub>5</sub>)<sub>3</sub> solution was poured on to the BiF<sub>3</sub>, held at -196 °C. BF<sub>3</sub> was evolved rapidly and a yellow coloration developed in the solution. The BF<sub>3</sub> was pumped off when the reaction subsided and the reaction mixture left to stand at room temperature for 3 days. The solvent was pumped off at 0 °C leaving the Bi(OTeF<sub>5</sub>)<sub>5</sub> as a pale yellow powder, (2.3981 g, 99%). The <sup>129</sup>F NMR spectrum in Freon 114 indicated the presence of unreacted B(OTeF<sub>5</sub>)<sub>3</sub>. This was removed by pumping the sample at room temperature for 5 hours.

Et<sub>4</sub>N<sup>+</sup>Bi(OTeF<sub>5</sub>)<sub>5</sub> Several attempts were made to prepare this compound. The same technique was used in each case, but the solvent was changed. The reaction procedure involved was the same as the preparation of Sb(OTeF<sub>5</sub>)<sub>5</sub><sup>-</sup>, that is Bi(OTeF<sub>5</sub>)<sub>3</sub> was allowed to react with a stoichiometric amount of Et<sub>4</sub>N<sup>+</sup>OTeF<sub>5</sub><sup>-</sup>. In the first attempt, the solvent used was acetonitrile. Both Bi(OTeF<sub>5</sub>)<sub>3</sub> and Et<sub>4</sub>N<sup>+</sup>OTeF<sub>5</sub><sup>-</sup> were dissolved in CH<sub>3</sub>CN, and they were combined and allowed to warm to room temperature. It appeared that the Bi(OTeF<sub>5</sub>)<sub>3</sub> reacted with the acetonitrile and a brownish liquid was formed. The final product was a brown sticky solid which showed no <sup>209</sup>Bi NMR resonance when redissolved in acetonitrile.

In a second attempt,  $\text{CH}_3\text{CN}$  was still used as the solvent, although the sample was not allowed to warm above  $0^\circ\text{C}$ . The reaction solution turned yellow when the substance was warmed to  $-50^\circ\text{C}$  but the color faded when the reaction solution was warmed to  $0^\circ\text{C}$ . This also did not exhibit a  $^{209}\text{Bi}$  NMR resonance in acetonitrile.

The third attempt involved the use of  $\text{SO}_2\text{ClF}$  as the solvent since it is not as basic as acetonitrile and thus it was thought that the products and reactants would be stable. The reactants were both put into a 10mm thin-walled glass NMR tube at  $-196^\circ\text{C}$  in the drybox. The tube was then put on the vacuum line and  $\text{SO}_2\text{ClF}$  was added. As the reaction mixture was allowed to warm, a yellow color appeared, which disappeared when the mixture reached room temperature. This solution seemed stable at room temperature and exhibited a  $^{209}\text{Bi}$  NMR resonance. The compound was then isolated and redissolved in the lower viscosity solvent  $\text{CH}_3\text{CN}$  in order to obtain a better resolved  $^{209}\text{Bi}$  NMR spectrum. However, the compound decomposed quite rapidly at room temperature in this solvent (see Results and Discussion section).

### Instrumentation

All spectra were recorded on commercial pulse spectrometers and the free-induction decays were accumulated in 16K or 32K of memory. Spectra (5.8719 T) were recorded on a Bruker WM-250 spectrometer with observing frequencies of 59.854, 40.201, and 235.360 MHz for  $^{121}\text{Sb}$ ,  $^{209}\text{Bi}$ , and  $^{19}\text{F}$ , respectively. The high-field (11.744 T) spectra were recorded on Bruker AM-500 at 470.600 and 80.380 MHz for  $^{19}\text{F}$ , and  $^{209}\text{Bi}$ , respectively. Some of the  $^{209}\text{Bi}$  and  $^{121}\text{Sb}$  spectra were resolution enhanced through the use of line broadening techniques and by

multiplying the free induction decay by a Gaussian function, which enhances the latter part of the FID. Pulse widths corresponding to bulk magnetization tip angles of  $\sim 90^\circ$  were 60  $\mu$ s ( $^{121}\text{Sb}$ ), 1  $\mu$ s ( $^{19}\text{F}$ ), and 40  $\mu$ s ( $^{209}\text{Bi}$ ) for the low-field spectra, and 1  $\mu$ s ( $^{19}\text{F}$ ) and 29  $\mu$ s ( $^{209}\text{Bi}$ ) for the high field spectra. The NMR samples were prepared in precision thin-wall glass NMR tubes (Wilmad, 5 mm and 10 mm o.d.) for those samples not containing HF, and FEP NMR tubes (10mm and 5mm) for those samples which might have contained HF. The tubes were all vacuum sealed and stored in a dry ice/acetone bath until the spectra could be run.

## RESULTS AND DISCUSSION

### Synthesis and Characterization of $\text{Et}_4\text{N}^+\text{SbF}_6^-$

The compound,  $\text{Et}_4\text{N}^+\text{SbF}_6^-$ , was prepared as both a precursor for further reactions and as a  $^{121}\text{Sb}$  NMR standard according to equation (13)

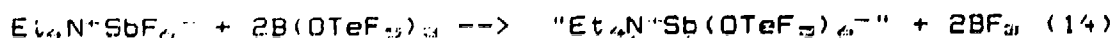


A  $^{121}\text{Sb}$  NMR spectrum was obtained for the product, which yielded a septet corresponding to the relative intensities 1:6:15:20:15:6:1. The multiplet arises from  $^1J(^{121}\text{Sb} - ^{19}\text{F})$  with a coupling constant of 1904 Hz. The middle line of the septet was defined to have a chemical shift of zero, and was subsequently used to reference the chemical shift of  $\text{Sb}(\text{OTeF}_5)_6^-$ . The  $^{19}\text{F}$  NMR spectrum was also obtained and

consisted of a well-resolved sextet and octet. The equal intensity multiplets arise from the two spin active isotopes of Sb;  $^{121}\text{Sb}$  ( $I = 1/2$ , 57.25%) and  $^{123}\text{Sb}$  ( $I = 7/2$ , 24.92%). The  $\text{SbF}_6^-$  anion has a  $^{19}\text{F}$  chemical shift of -123 ppm relative to  $\text{CFCl}_3$ , (literature value of -123 ppm)<sup>34</sup>, and coupling constants of  $J(^{19}\text{F}-^{121}\text{Sb}) = 1909$  Hz and  $J(^{19}\text{F}-^{123}\text{Sb}) = 1065$  Hz. These values compare well with previously reported values of  $1934 \pm 15$  Hz and  $1047 \pm 25$  Hz, respectively.<sup>34</sup>

#### Synthesis and Characterization of $\text{Et}_4\text{N}^+\text{Sb}(\text{OTeF}_5)_4^-$

The first attempt at preparing  $\text{Sb}(\text{OTeF}_5)_4^-$  involved the reaction of  $\text{Et}_4\text{N}^+\text{SbF}_6^-$  with  $\text{B}(\text{OTeF}_5)_3$  according to equation (14)



using  $\text{CFCl}_3$  as the solvent. The product was a thick, light brown viscous material which indicated that the product was probably not a homogeneous mixture and that  $\text{OTeF}_5$  ligand substitution was incomplete. The  $^{121}\text{Sb}$  NMR indicated that a major component of the mixture was  $\text{SbF}_6^-$ , although a second multiplet was present (Fig. 3). As the sample was warmed to 70 °C, the second multiplet increased in intensity and became more and more predominant indicating that the substitution reaction was still occurring. The second set of peaks appears to be a sextet which would indicate that the monosubstituted product  $\text{SbF}_5(\text{OTeF}_5)^-$  was being formed. The increased width of the second multiplet arises from the decreased local symmetry at the  $^{121}\text{Sb}$  nucleus. That is, as the symmetry decreases, the electric field gradient,  $q_{zz}$ , increases; and this increases the linewidth according to equation (10). One also notes that with increasing  $\text{OTeF}_5$  group

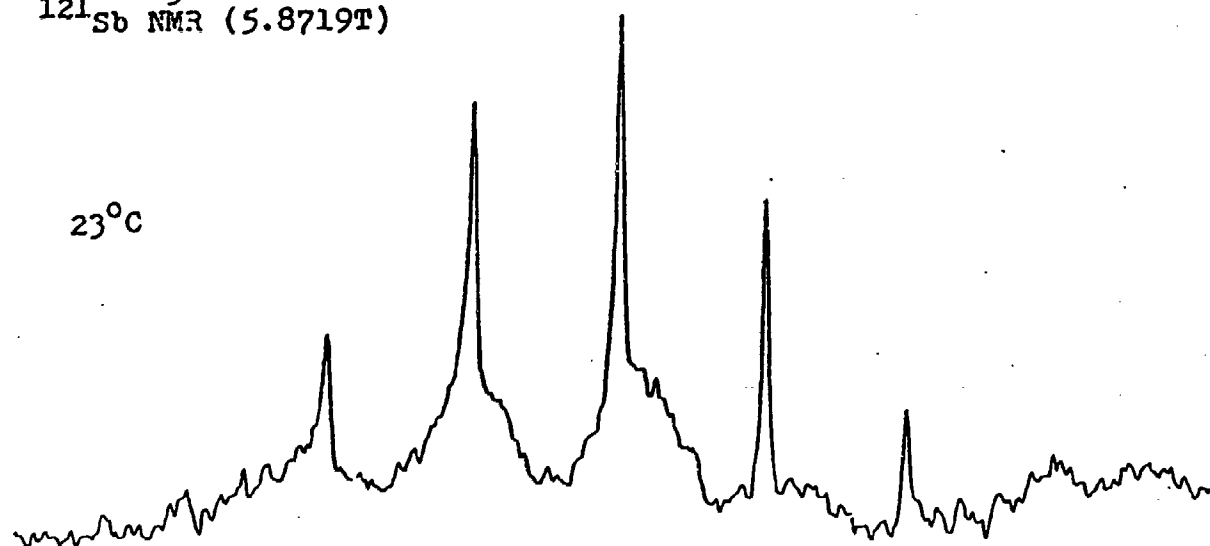
$\text{SbF}_6^- / \text{B}(\text{OTeF}_5)_3$  reaction mixture

Figure 3

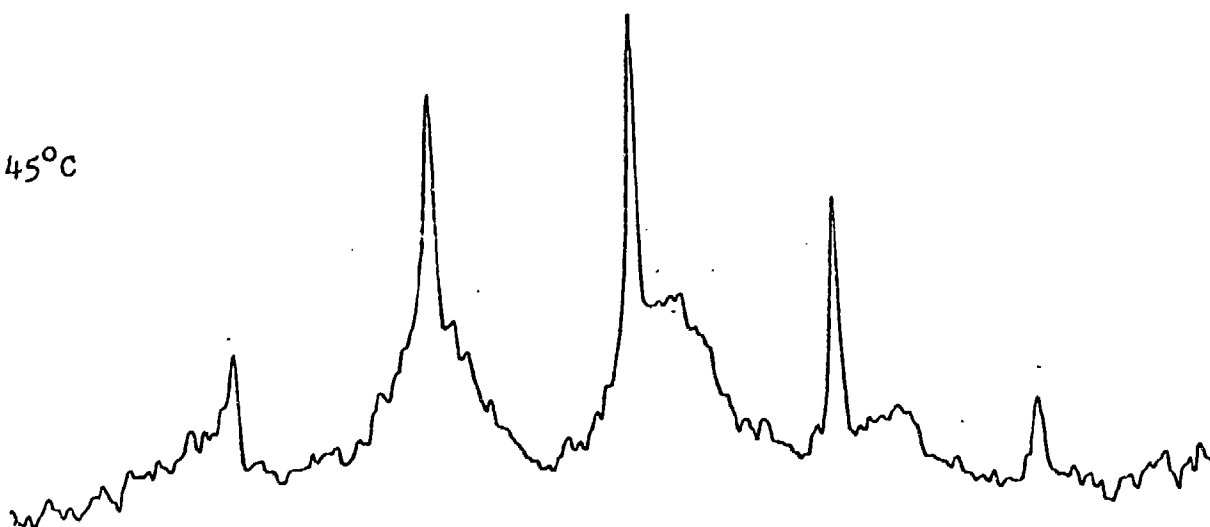
0.1M  $\text{CH}_3\text{CN}$

$^{121}\text{Sb}$  NMR (5.8719T)

23°C



45°C



70°C

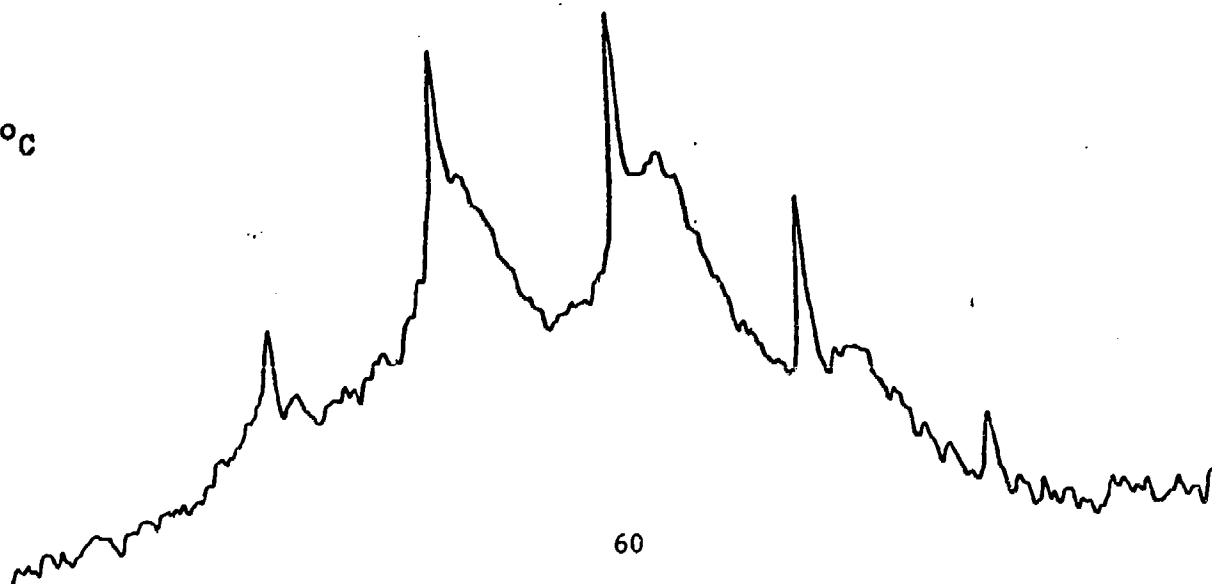


FIGURE 4:  $\text{SbF}_6^- / \text{B}(\text{OTeF}_5)_3$  reaction mixture  
0.1M  $\text{CH}_3\text{CN}$   
 $^{19}\text{F}$  NMR (5.8719)

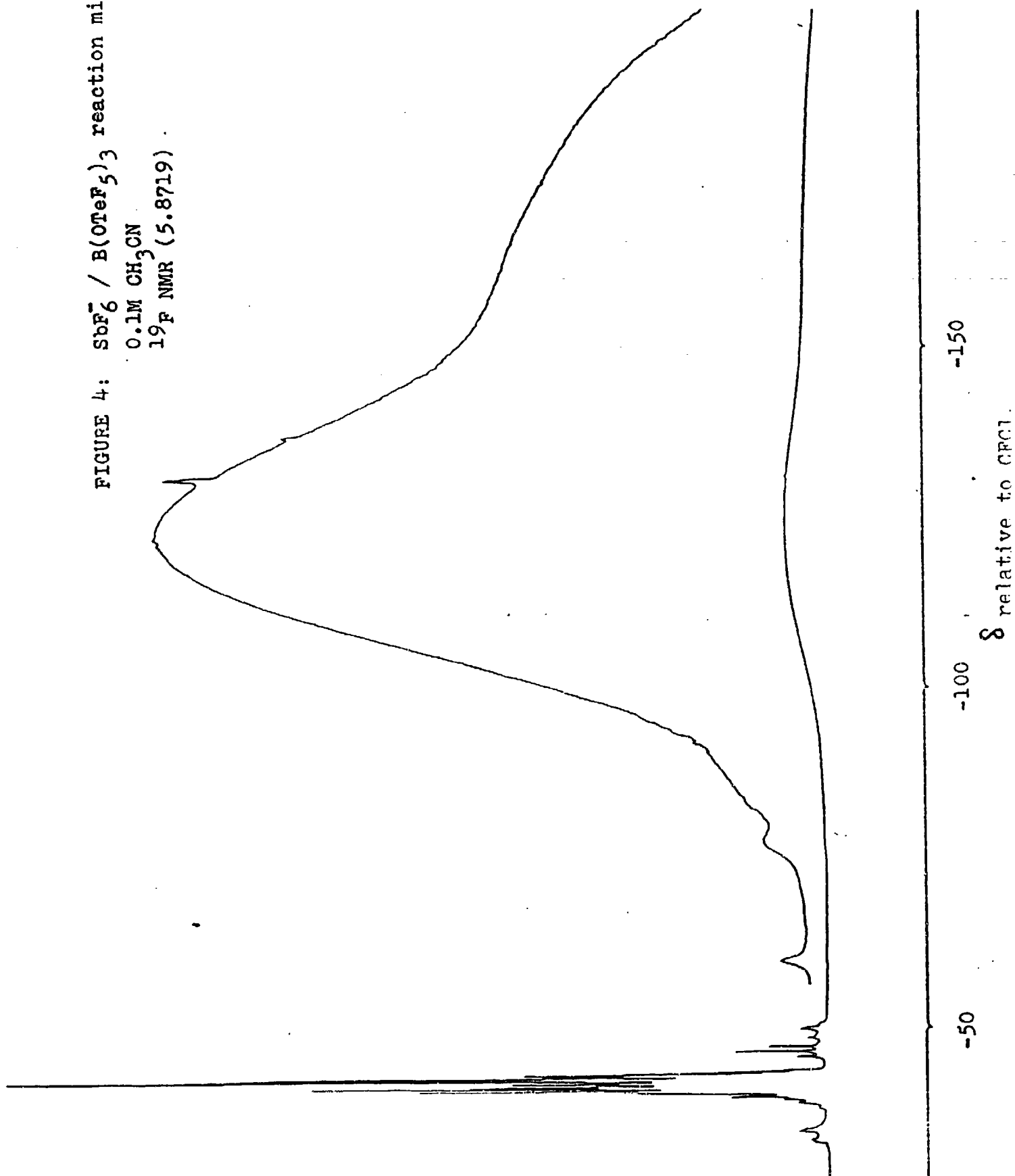




Figure 5:  $\text{SbF}_6^-/\text{B}(\text{OTeF}_5)_3$  reaction product  
0.1M in  $\text{CH}_3\text{CN}$

$^{19}\text{F}$  NMR Spectrum (5.8719T)  
Expansion of high-frequency region.

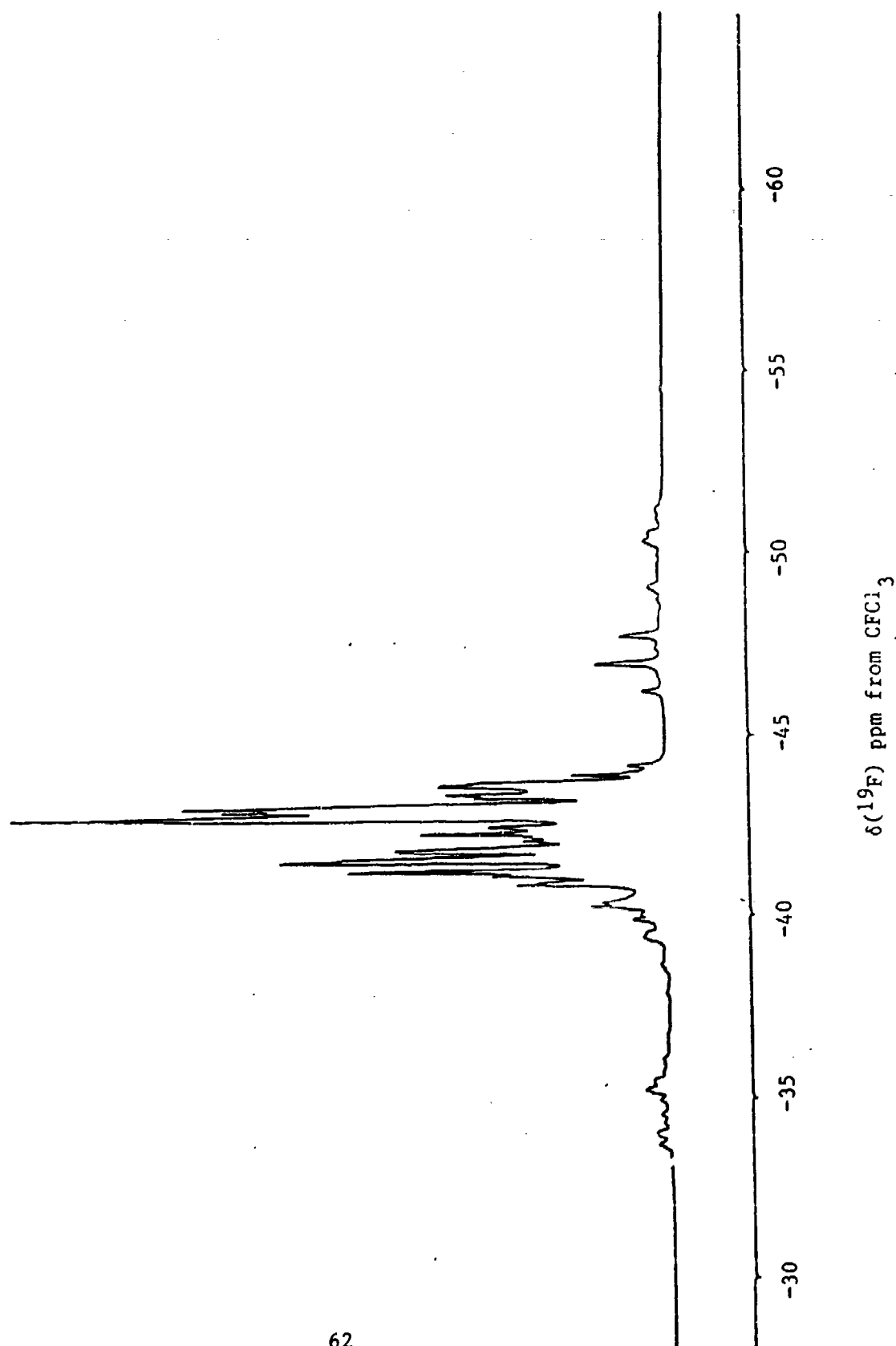
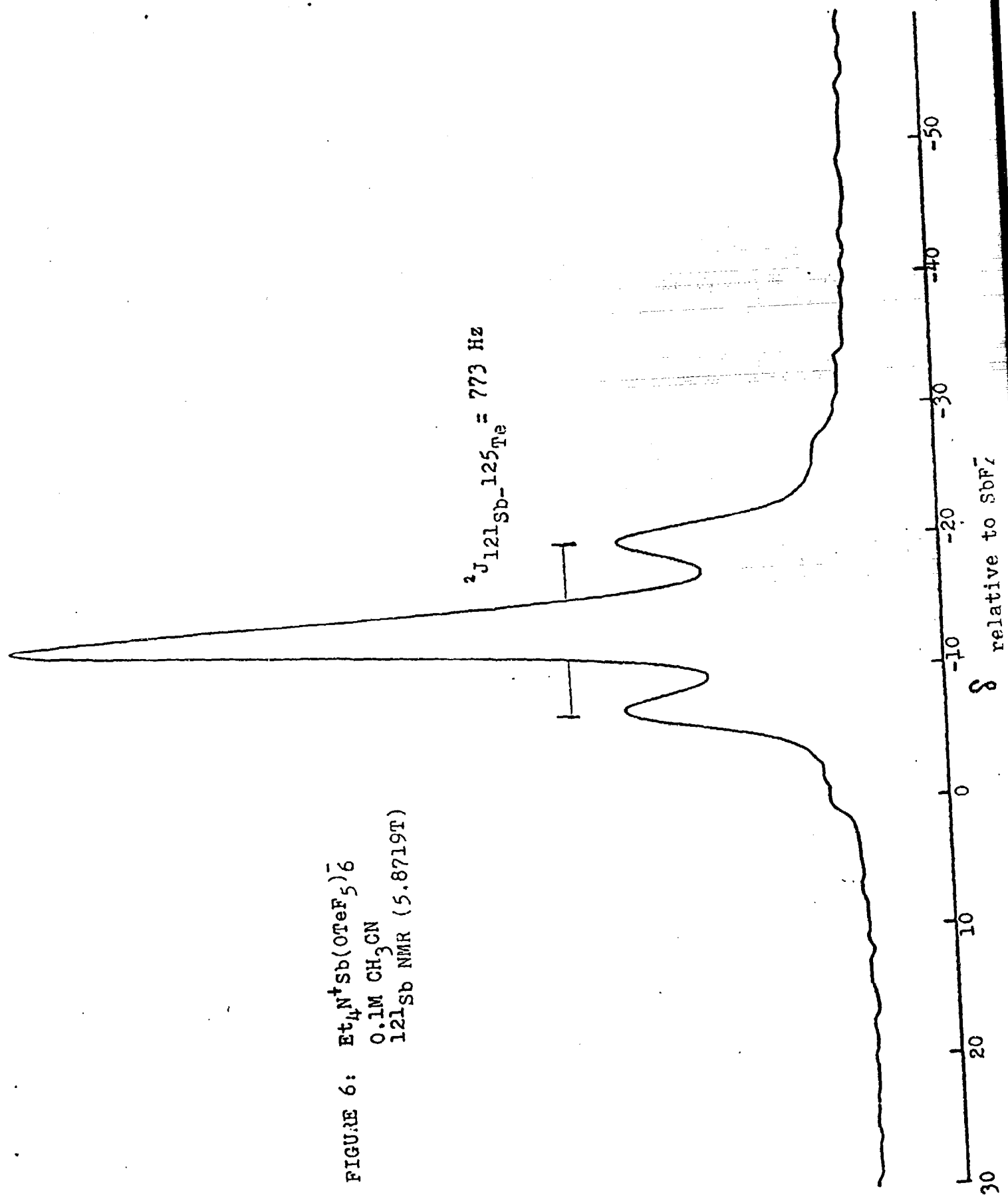


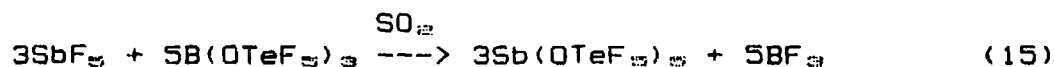
FIGURE 6:  $\text{Et}_4\text{N}^+\text{Sb}(\text{OTeF}_5)_6^-$   
 0.1M  $\text{CH}_3\text{CN}$   
 $^{121}\text{Sb}$  NMR (5.8719T)



substitution, the  $^{121}\text{Sb}$  chemical shift moves to progressive lower frequency, which is consistent with the lower electronegativity of the  $\text{OTeF}_5$  group.

The  $^{19}\text{F}$  NMR spectrum of this sample is complex (Fig. 4). The large broad peaks in the -100 ppm region are assigned to F bonded to  $\text{Sb(V)}$ . They are broad because of partial quadrupole collapse of the  $^{121}\text{Sb}$ - $^{19}\text{F}$  and  $^{123}\text{Sb}$ - $^{19}\text{F}$  spin coupling. Figure 5 shows an expansion of the  $^{19}\text{F}$  spectrum, focusing on the complex set of peaks, which includes the  $^{19}\text{F}$  resonances of  $\text{OTeF}_5$  bonded to both  $\text{Sb(V)}$  and  $\text{B(III)}$ . However, it is too complex to assign any values to the various components of the reaction mixture.

The second attempt at preparing the  $\text{Sb}(\text{OTeF}_5)_6^-$  anion involved a two-step reaction and the formation of  $\text{Sb}(\text{OTeF}_5)_5$  according to equation (15)



The pentakis-compound,  $\text{Sb}(\text{OTeF}_5)_5$ , was not isolated in this reaction and was allowed to react with  $\text{Et}_4\text{N}^+\text{OTeF}_5^-$  according to equation (16)



Again the product was a light brown, viscous liquid, however, the  $^{121}\text{Sb}$  NMR spectrum in  $\text{CH}_3\text{CN}$  at room temperature yielded a single peak with  $^{125}\text{Te}$  satellites (Fig. 6). This indicated that the product contained little or no  $\text{SbF}_6^-$  and that it contained a  $^{121}\text{Sb}$  nucleus in a highly symmetric environment. This indicated that  $\text{Sb}(\text{OTeF}_5)_6^-$  had been formed and that the ligands were arranged in octahedral symmetry

around the Sb. No  $^3J(^{121}\text{Sb}-^{19}\text{F})$  coupling was observed probably because it is too small to be resolved within the constraint of the  $^{121}\text{Sb}$  linewidth and the distance between the  $^{121}\text{Sb}$  and  $^{19}\text{F}$  nuclei is too great to allow interaction. The  $^{121}\text{Sb}$  can couple with the two spin active Te isotopes,  $^{125}\text{Te}$  and  $^{123}\text{Te}$ . Table 2 indicates the percent abundance and the multiplet fine structure that can be expected for each isotopic species. Although the  $^{123}\text{Te}$  has a spin of  $1/2$ , it is only 0.87% abundant and therefore is present in a sufficiently small proportion to be disregarded in any coupling treatment (Table 2). The nucleus  $^{125}\text{Te}$  ( $I = 1/2$ ) has a natural abundance of 6.99% and thus  $^2J(^{121}\text{Sb}-^{125}\text{Te})$  can be observed. The singlet and doublet can be plainly observed on the  $^{121}\text{Sb}$  spectrum with the outer components of the triplet also distinguishable from the baseline.

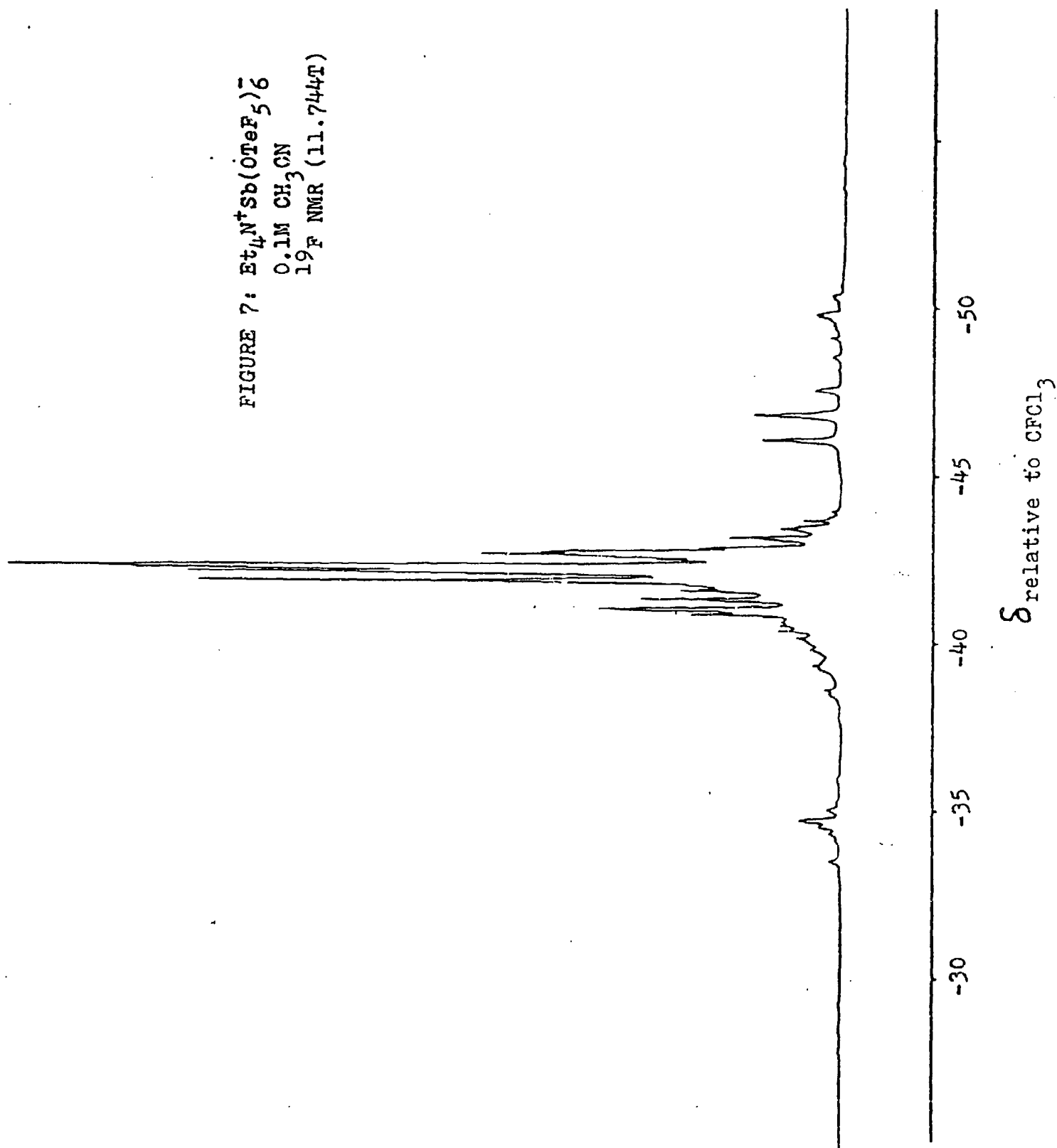
The  $^{121}\text{Sb}$  chemical shift value of  $\text{Sb}(\text{OTeF}_5)_4^-$  is -13.5 ppm with respect to  $\text{SbF}_6^-$ . The increased shielding of the  $^{121}\text{Sb}$  nucleus is expected since the  $\text{OTeF}_5$  group is less electronegative than the F ligand. A linewidth value of 275 Hz is observed which is also expected, since the quadrupolar relaxation of the  $^{121}\text{Sb}$  nucleus will have the effect of broadening the resonance line. The  $^{121}\text{Sb}-^{125}\text{Te}$  coupling constant is found to be 773 Hz.

The  $^{19}\text{F}$  NMR of  $\text{Et}_4\text{N}^+\text{Sb}(\text{OTeF}_5)_4^-$  yielded a very complex second order  $\text{AB}_4$  pattern (Fig. 7). The chemical shift values for A and  $\text{B}_4$  appear to be approximately equal ( $\delta_A \approx \delta_{\text{B}_4} = -42$  ppm), making analysis difficult.

Table 2. Statistical Distribution of Different Isotopic Species  
of  $M(\text{OTeF}_5)_4^-$  ( $M = \text{Sb or Bi}$ )

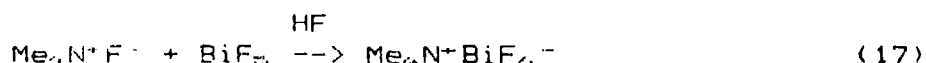
<u>Species</u>	<u>Percent</u> <u>Abundance</u>	<u>Multiplet</u>
$M(\text{OTeF}_5)_4^-$	61.2	singlet
$M(\text{OTeF}_5)_3(\text{O}^{129}\text{TeF}_5)^-$	27.8	doublet
$M(\text{OTeF}_5)_4(\text{O}^{129}\text{TeF}_5)_2^-$	5.3	triplet
$M(\text{OTeF}_5)_3(\text{O}^{129}\text{TeF}_5)_3^-$	0.5	quartet
$M(\text{OTeF}_5)_3(\text{O}^{131}\text{TeF}_5)^-$	3.5	doublet
$M(\text{OTeF}_5)_4(\text{O}^{131}\text{TeF}_5)_2^-$	0.1	triplet
Remaining isotopic species	1.6	

FIGURE 7:  $\text{Et}_4\text{N}^+\text{Sb}(\text{OteF}_5)_6^-$   
0.1M  $\text{CH}_3\text{CN}$   
 $^{19}\text{F}$  NMR (11.744T)



### Synthesis and Characterization of $\text{Me}_4\text{N}^+\text{BiF}_6^-$

The salt  $\text{Me}_4\text{N}^+\text{BiF}_6^-$  was prepared both as a precursor for further reactions and as an NMR reference for  $^{209}\text{Bi}$  (equation (17)). One of the starting materials for the preparation was  $\text{BiF}_3$ , which is an extremely powerful oxidizing agent.<sup>27</sup> The  $\text{Me}_4\text{N}^+$  cation was used as the counterion since  $\text{Me}_4\text{N}^+$  is more difficult to oxidize than  $\text{Et}_4\text{N}^+$ .



The removal of HF under vacuum yielded a white powder. The NMR sample (0.1 M acetonitrile) exhibited a well-resolved  $^{209}\text{Bi}$  resonance (Fig.8). The  $^{209}\text{Bi}$  couples to  $^{19}\text{F}$  yielding a 1:6:15:20:15:6:1 septet, with a  $^{209}\text{Bi}$ - $^{19}\text{F}$  coupling constant of 3810 Hz, and a linewidth of 28 Hz. The previously reported  $^{209}\text{Bi}$  resonance of  $\text{BiF}_6^-$  yielded comparable values of  $3823 \pm 3$  Hz for the coupling constant and a linewidth of 44 Hz.<sup>28</sup> The linewidth of the present sample is less than the previously reported value owing to solvent viscosity effects. In the previous study the spectra were recorded in acetone, which is more viscous than acetonitrile. Thus, the sample in acetone has a slower isotropic tumbling rate and therefore a wider linewidth according to equation (10). The chemical shift of the central component of the septet was defined to be 0 ppm for  $\text{Me}_4\text{N}^+\text{BiF}_6^-$  in acetonitrile at room temperature and was used as the standard for  $^{209}\text{Bi}$  in this study.

In the  $^{19}\text{F}$  NMR spectrum an equal intensity decet was observed (Fig. 9). The coupling constant  $^1J(^{19}\text{F}-^{209}\text{Bi}) = 3810$  Hz and agrees with the value measured in the  $^{209}\text{Bi}$  spectrum. The  $^{19}\text{F}$  chemical shift of  $\text{BiF}_6^-$  in the present study was -44.0 ppm with respect to  $\text{CFCl}_3$ , compared to

$\text{Me}_4\text{N}^+\text{BiF}_6^-$   
0.1M  $\text{CH}_3\text{CN}$

FIGURE 8:  $^{209}\text{Bi}$  NMR (5.8719T)

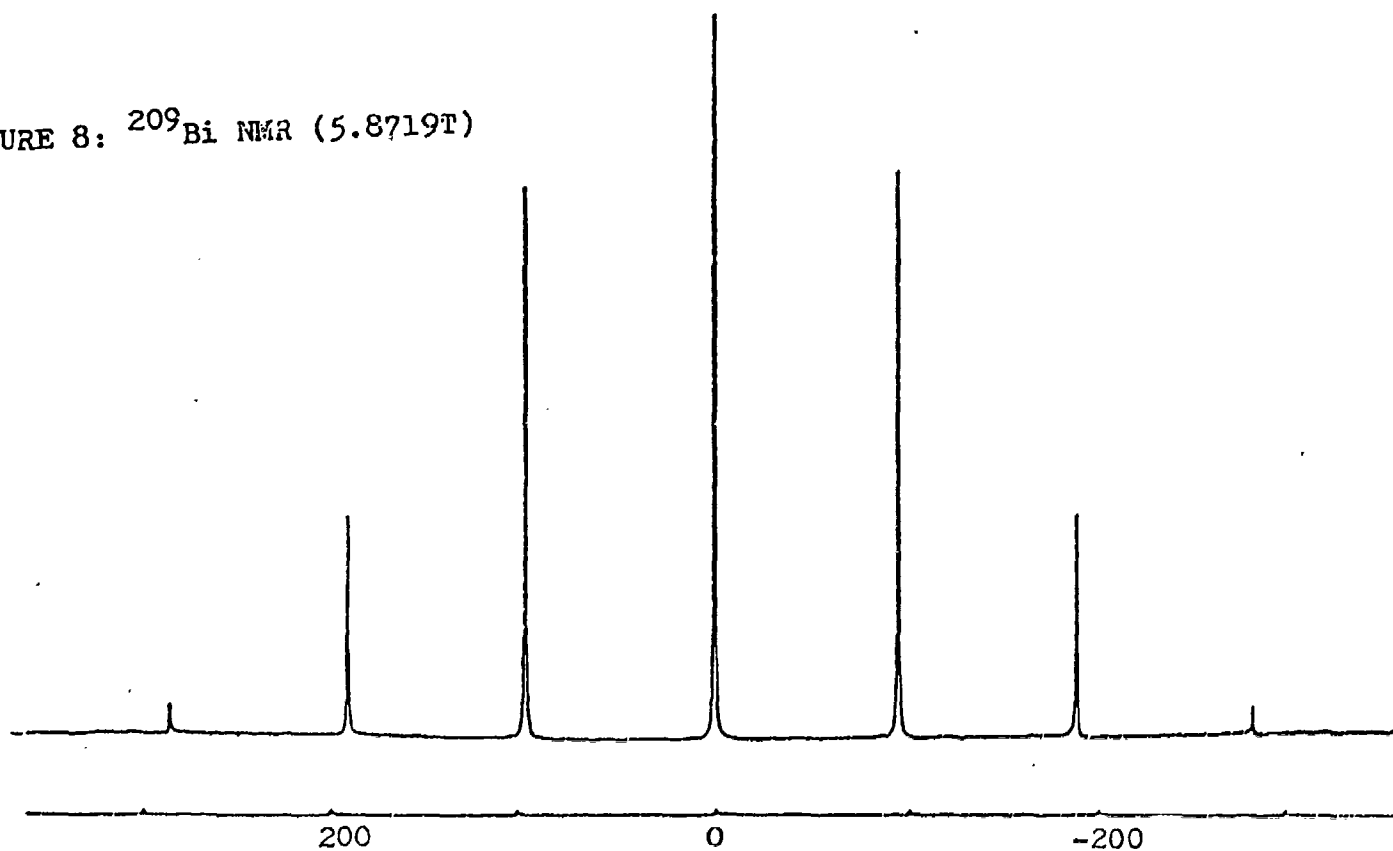
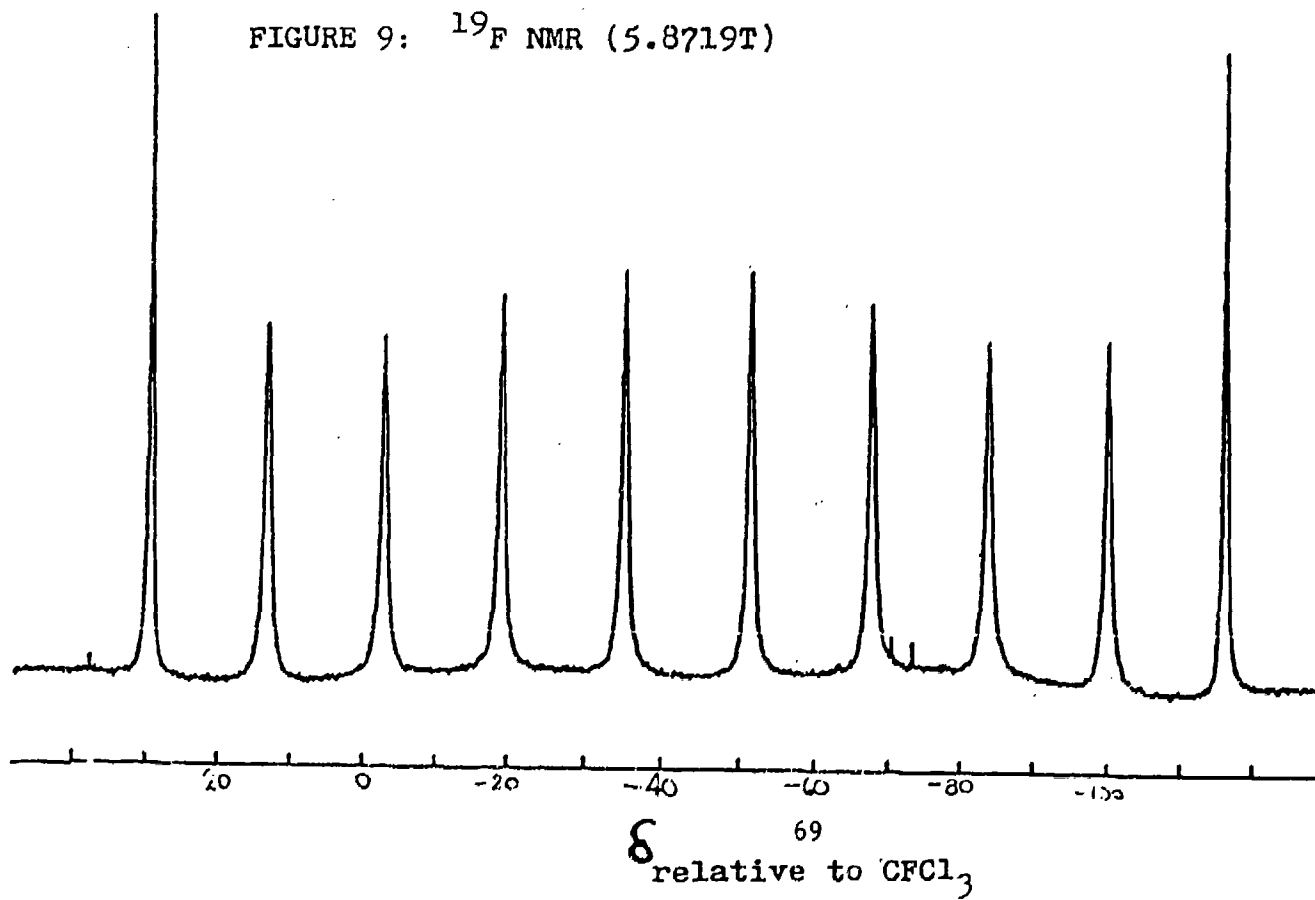


FIGURE 9:  $^{19}\text{F}$  NMR (5.8719T)

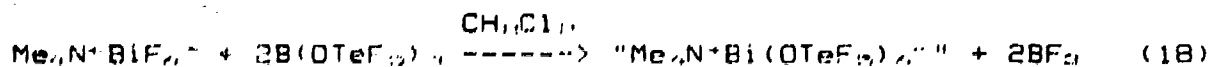




-42.6 ppm previously reported for  $\text{BiF}_6^-$  in acetone.<sup>20</sup>

$\text{Me}_4\text{N}^+\text{Bi}(\text{OTeF}_5)_4^-$  and  $\text{Et}_4\text{N}^+\text{Bi}(\text{OTeF}_5)_4^-$

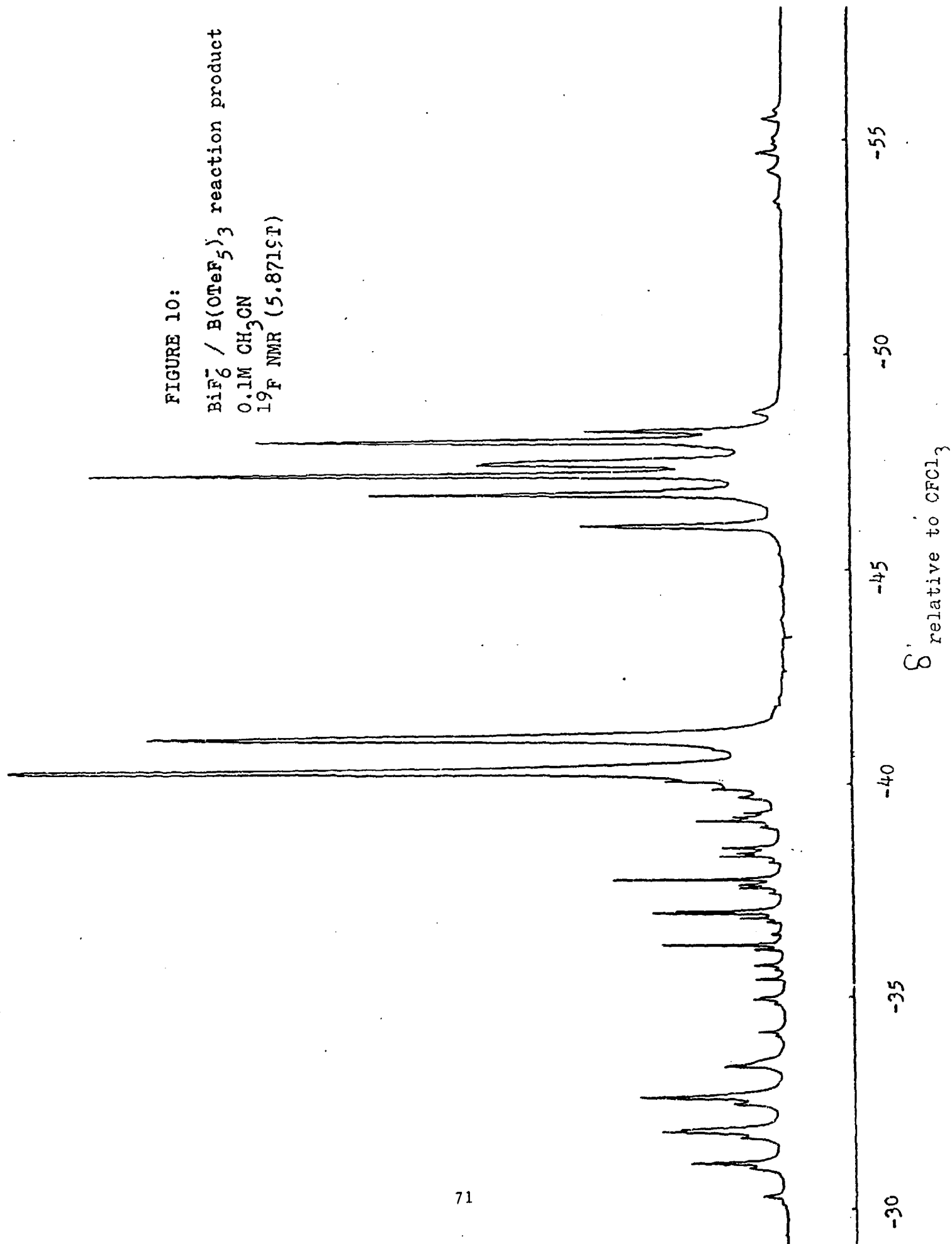
The first attempt to prepare  $\text{Bi}(\text{OTeF}_5)_4^-$  was carried out according to equation (18).



The product obtained was a white solid which did not exhibit a  $^{209}\text{Bi}$  resonance when dissolved in acetonitrile. This indicated that  $\text{BiF}_6^-$  was no longer present and that the product did not contain  $^{209}\text{Bi}$  in a symmetrical environment, i.e.  $\text{Bi}(\text{OTeF}_5)_4^-$  was presumably not present. The  $^{19}\text{F}$  NMR showed the presence of many overlapping  $\text{AB}_4$  patterns (Fig. 10), which indicated that the product obtained was not pure. When this spectrum was compared to the  $^{19}\text{F}$  NMR spectrum of  $\text{As}(\text{OTeF}_5)_5\text{Cl}^-$  in the literature,<sup>21</sup> it was found that the predominant  $\text{AB}_4$  pattern of the product was very similar to the  $\text{AB}_4$  pattern observed in  $\text{As}(\text{OTeF}_5)_5\text{Cl}^-$ . That is the quintet ( $\delta_{\text{A}} = -32$  ppm) and the doublet ( $\delta_{\text{B}} = -40.5$  ppm) for the sample spectrum are in the same relative positions as in the  $^{19}\text{F}$  spectrum of  $\text{As}(\text{OTeF}_5)_5\text{Cl}^-$ . The peaks are, however, shifted to lower frequency compared with those of the  $\text{As}(\text{III})$  species ( $\delta_{\text{A}} = -32.5$ ,  $\delta_{\text{B}} = -38$  ppm) which could be the result of many things such as solvent effects or different counterions. This suggested that the product contained Bi which had been reduced to the +3 oxidation state. There are also other  $\text{AB}_4$  patterns apparent, indicating that there is more than one product which have yet to be identified.

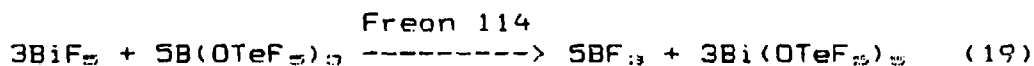
FIGURE 10:

$\text{BiF}_3$  /  $\text{B}(\text{OTeF}_5)_3$  reaction product  
0.1M  $\text{CH}_3\text{CN}$   
 $^{19}\text{F}$  NMR (5.8715T)



### Bi(OTeF<sub>5</sub>)<sub>5</sub>

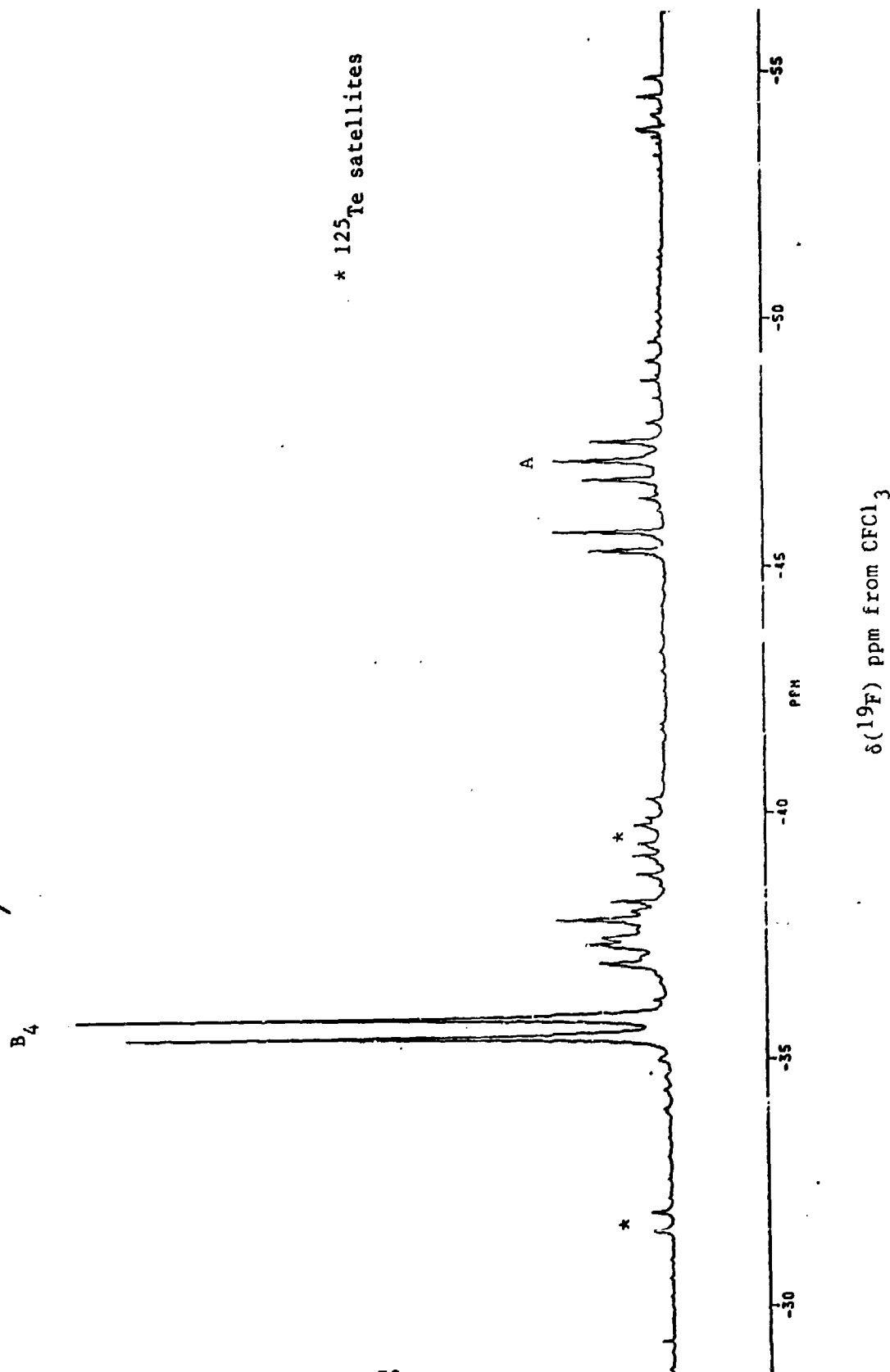
The second attempt at preparing Bi(OTeF<sub>5</sub>)<sub>5</sub><sup>-</sup> involved the preparation of Bi(OTeF<sub>5</sub>)<sub>5</sub> according to the equation (19)



In this procedure, unlike in the preparative procedure for Sb(OTeF<sub>5</sub>)<sub>5</sub><sup>-</sup>, the Bi(OTeF<sub>5</sub>)<sub>5</sub> was isolated. It is a light yellow solid which is stable at room temperature and is only the second Group V (Group 15) pentakis-derivative of OTeF<sub>5</sub> to have been isolated. The <sup>19</sup>F NMR spectrum (Fig. 11) of Bi(OTeF<sub>5</sub>)<sub>5</sub> dissolved in Freon 114 (CCl<sub>2</sub>F<sub>2</sub>CCl<sub>2</sub>F<sub>2</sub>) was obtained at -50 °C. The dominant feature of this spectrum was a well-resolved AB<sub>4</sub> pattern (δ<sub>A</sub> = -47.1; δ<sub>B</sub> = -35.6; <sup>2</sup>J(F<sub>A</sub>-F<sub>B</sub>) = 181 Hz and <sup>1</sup>J(<sup>19</sup>F<sub>B</sub>-<sup>125</sup>Te) = 3696 Hz) which could be attributed to Bi(OTeF<sub>5</sub>)<sub>5</sub>. The Bi(OTeF<sub>5</sub>)<sub>5</sub> molecule would be expected to have a trigonal bipyramidal structure which should give rise to two OTeF<sub>5</sub> environments in the <sup>19</sup>F NMR spectrum. That only one is observed indicates that Bi(OTeF<sub>5</sub>)<sub>5</sub> undergoes rapid intramolecular exchange even at -50 °C. Similar behavior is known for the related As(OTeF<sub>5</sub>)<sub>5</sub> compound.<sup>32</sup> The <sup>19</sup>F NMR spectrum of the Bi(OTeF<sub>5</sub>)<sub>5</sub> sample also displays some weaker overlapping AB<sub>4</sub> patterns in the region δ = -36 to -41 ppm. These are thought to arise from incompletely substituted species BiF<sub>n</sub>(OTeF<sub>5</sub>)<sub>5-n</sub>, where n = 1 or 2, and indicate that a longer reaction time is required for complete conversion of BiF<sub>3</sub> into Bi(OTeF<sub>5</sub>)<sub>5</sub>.

In attempting to prepare Bi(OTeF<sub>5</sub>)<sub>5</sub><sup>-</sup>, problems were encountered

Figure 11 :  $\text{Bi}(\text{OTeF}_5)_5$  in  $\text{CClF}_2\text{CClF}_2$   
 $^{19}\text{F}$  NMR Spectrum (11.744T)  
 at  $-49^\circ\text{C}$



with regard to solvent basicity. The reactions were carried out according to equation (20).

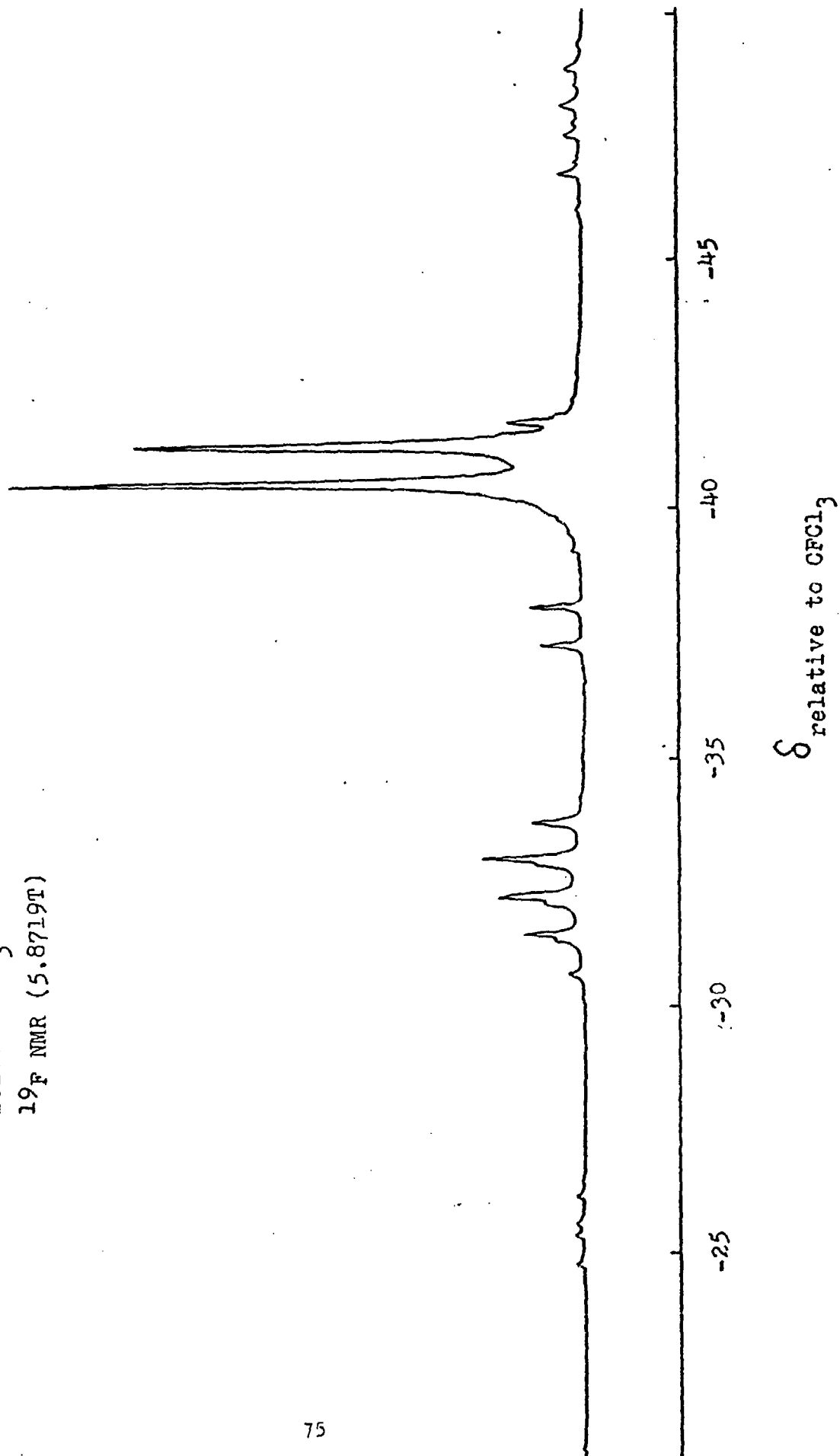


For the initial attempt, the solvent chosen was acetonitrile. When a solution of  $\text{Bi}(\text{OTeF}_5)_5$  in  $\text{CH}_3\text{CN}$  was allowed to warm room temperature, the solution turned dark yellow indicating that a reaction had occurred with the solvent. When the  $\text{Et}_4\text{N}^+\text{OTeF}_5^-$  was added, the yellow colour decreased in intensity, suggesting that the previous deep yellow colour was the result of adduct formation between the Lewis acid,  $\text{Bi}(\text{OTeF}_5)_5$ , and the Lewis base  $\text{CH}_3\text{CN}$ . The  $^{209}\text{Bi}$  NMR spectrum of the product, however, yielded no  $^{209}\text{Bi}$  resonance indicating that  $\text{Bi}(\text{OTeF}_5)_4^-$  was not present in the product. The  $^{19}\text{F}$  NMR spectrum exhibited AB<sub>4</sub> patterns which resembled those observed in the product of the first attempt to prepare  $\text{Bi}(\text{OTeF}_5)_4^-$ , with a quintet at -32 ppm and a doublet at -41 ppm, suggesting that reduction to Bi(III) may have also occurred in this instance (Fig. 12).

The reaction was attempted once more in  $\text{CH}_3\text{CN}$  but it was not allowed to warm above 0 °C. It was assumed that  $\text{Bi}(\text{OTeF}_5)_5$  reacted with the acetonitrile and that if the hexakis-anion could be formed without allowing the pentakis-compound to react, then the hexakis-anion product ought to be stable in the solvent. However, the NMR data that were obtained gave the same results as in the previous attempt.

The third attempt was carried out in an  $\text{SO}_2\text{ClF}$  solvent. The product obtained yielded a light yellow solution in  $\text{SO}_2\text{ClF}$ , which

FIGURE 12:  $\text{Bi}(\text{OTeF}_5)_5 / \text{Et}_4\text{N}^+\text{OTeF}_5^-$   
Solvent:  $\text{Cl}_3\text{CN}$   
 $^{19}\text{F}$  NMR (5.8719T)



exhibited a  $^{209}\text{Bi}$  resonance (Fig. 13). Again, as in the  $^{121}\text{Sb}$  spectrum of  $\text{Sb}(\text{OTeF}_6)_4^-$ , a single peak with satellites resulting from  $^2J(^{209}\text{Bi}-^{125}\text{Te})$  coupling was obtained (Table 2). The compound was also dissolved in the lower viscosity  $\text{CH}_3\text{CN}$  in order to obtain sharper NMR spectra, although the compound decomposed slowly in this solvent at room temperature.

The  $^{209}\text{Bi}$  NMR spectrum was run at two temperatures in  $\text{CH}_3\text{CN}$  solvent,  $-20^\circ\text{C}$  (Fig. 14) and room temperature (Fig. 15), and exhibited slightly different chemical shift values (Table 3). This temperature dependence is characteristic of heavy element nuclei. However, the  $^{209}\text{Bi}$  chemical shift value is particularly unusual in that it occurs to high frequency of that of  $\text{BiF}_4^-$ , even though the  $\text{OTeF}_6$  group is less electronegative than F. The anomaly may arise from relativistic effects associated with the heavy  $^{209}\text{Bi}$  nucleus. The  $^{209}\text{Bi}$  linewidth was also observed to increase with decreasing temperature owing to the longer correlation time of the nucleus at lower temperatures (Table 3). These effects are attributed to changes of viscosity for the solution, which increases at lower temperatures and results in slowing of the isotropic tumbling rate,  $\tau_c$ , which in turn serves to broaden the  $^{209}\text{Bi}$  spectral lines.

The  $^{19}\text{F}$  NMR spectrum of the decomposition product of  $\text{Bi}(\text{OTeF}_6)_4^-$  and  $\text{CH}_3\text{CN}$  can be seen in Figure 16. It, again, is similar to the  $^{19}\text{F}$  spectrum of  $\text{As}(\text{OTeF}_6)_3\text{Cl}^-$ ,<sup>20</sup> and suggests that this product is also reduced to a Bi(III) compound (probably  $\text{Bi}(\text{OTeF}_6)_4^-$ ) by  $\text{CH}_3\text{CN}$ .

The  $^{19}\text{F}$  NMR spectrum of  $\text{Bi}(\text{OTeF}_6)_4^-$  in  $\text{CH}_3\text{CN}$  (Fig. 17) consists of a well-resolved  $\text{AB}_4$  pattern;  $\delta_A = -30.6$  ppm, and  $\delta_B = -40.3$  ppm. The spectrum was found to essentially first order ( $J_{AB}/\delta\nu_0 = 0.037$ ), with

FIGURE 13:  $\text{Et}_4\text{N}^+\text{Bi}(\text{OTeF}_5)_3^-$   
0.1M  $\text{SO}_2\text{ClF}$   
 $^{209}\text{Bi}$  NMR (5.8719T)  
 $23^\circ\text{C}$

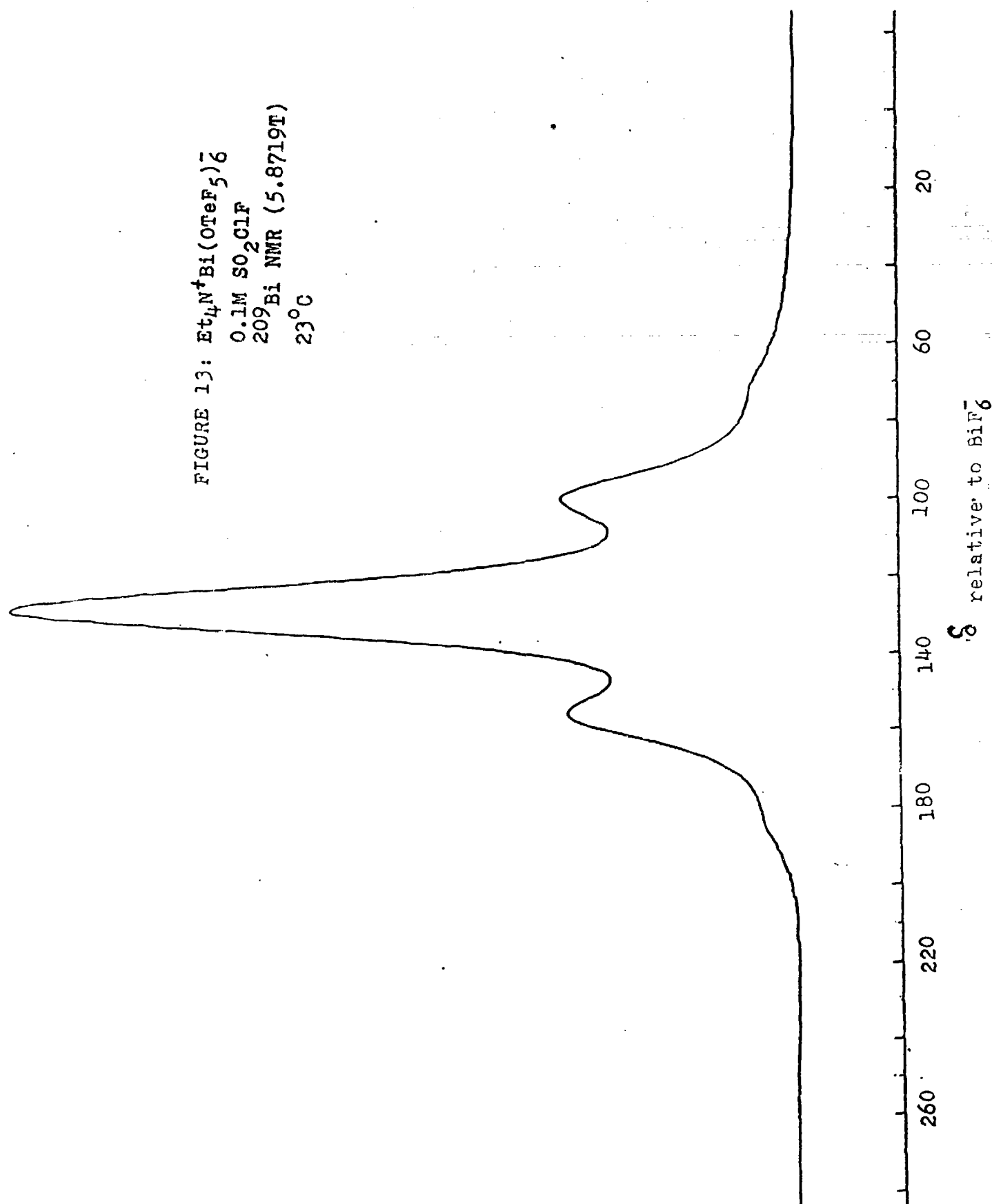




Figure 14:  $\text{Et}_4\text{N}^+\text{Bi}(\text{OTeF}_5)_6^-$  in  $\text{CH}_3\text{CN}$   
 $^{209}\text{Bi}$  NMR Spectrum (11.744T)  
 at  $-20^\circ\text{C}$

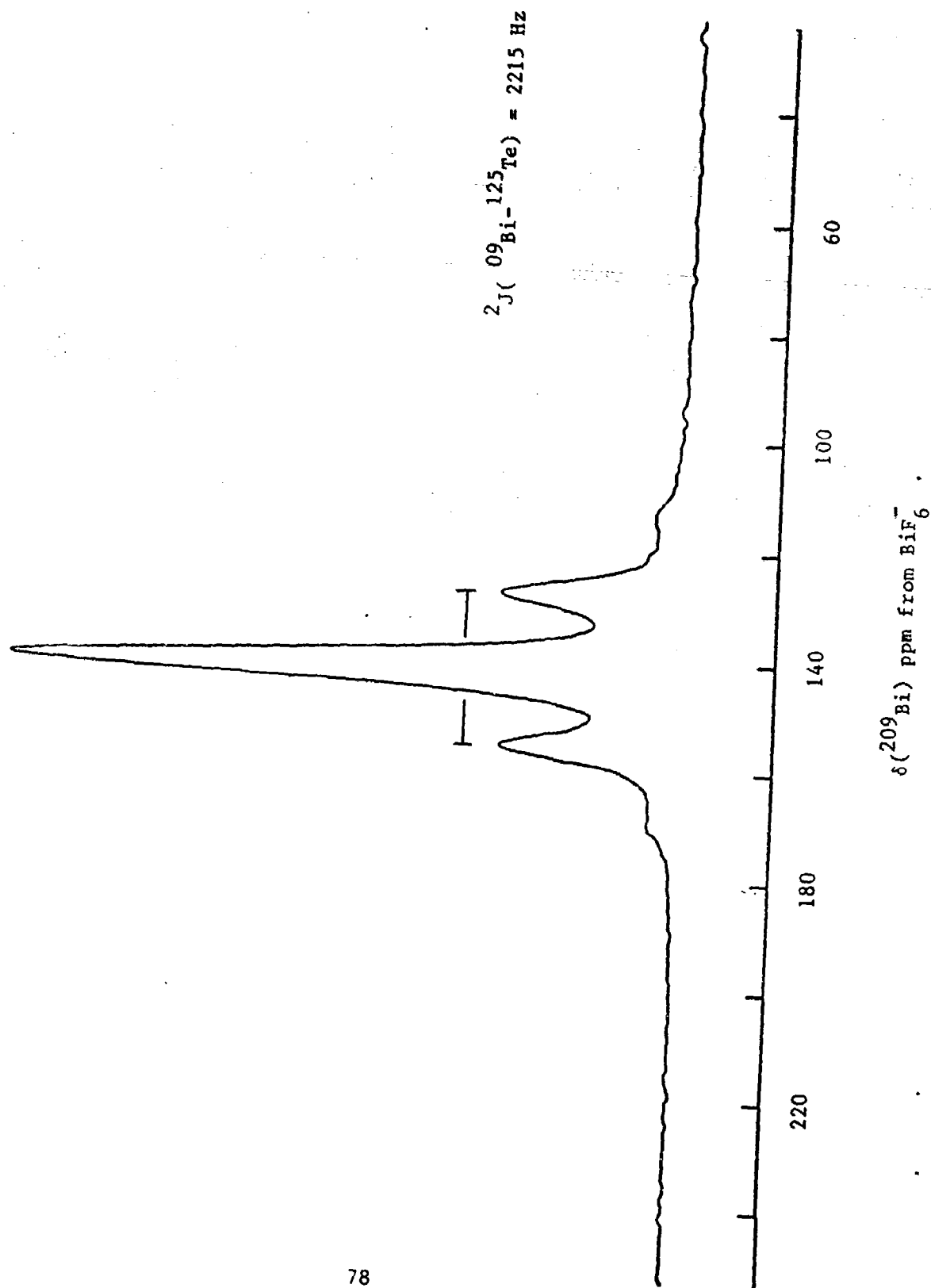


FIGURE 15:  $\text{Et}_4\text{N}^+\text{Bi}(\text{OTeF}_5)_6^-$   
0.1M  $\text{CH}_3\text{CN}$   
 $^{209}\text{Bi}$  NMR (5.8719T)  
 $23^\circ\text{C}$

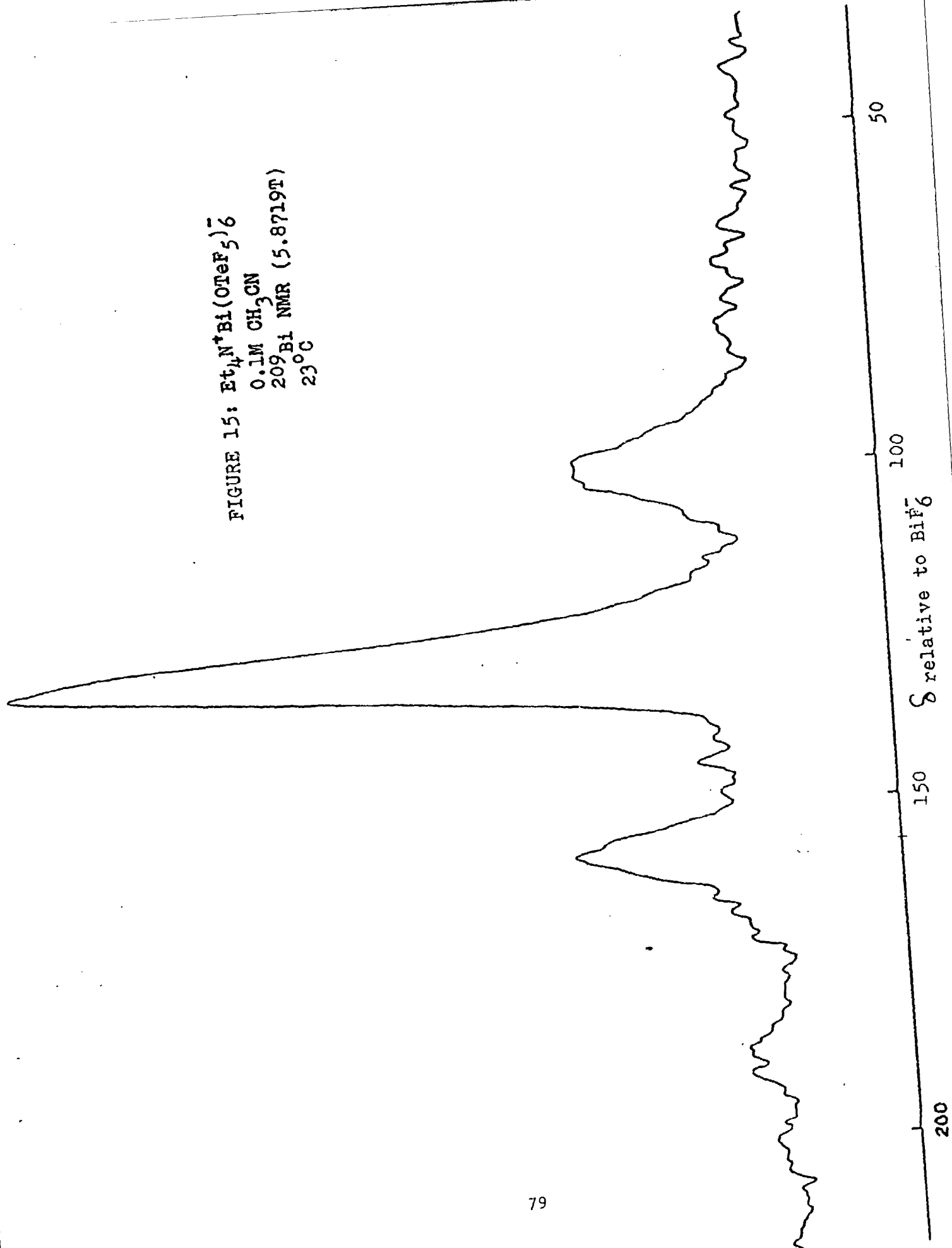


Table 3.  $^{209}\text{Bi}$  NMR Parameters for the  $\text{Bi}(\text{OTeF}_5)_4^-$  Anion

<u>Temperature (<math>^{\circ}\text{C}</math>)</u>	<u><math>^2J(^{209}\text{Bi}-^{125}\text{Te})</math> (Hz)</u>	<u><math>\delta(^{209}\text{Bi})</math> (ppm)</u>	<u>Linewidth (Hz)</u>
-20	2215	141.7	546
23	2267	128.4	321

\*Relative to  $\text{Me}_4\text{N}^+\text{BiF}_6^-$  in  $\text{CH}_3\text{CN}$ .

FIGURE 16:  $\text{Et}_4\text{N}^+\text{Bi}(\text{OTeF}_5)_6^-$   
after decomposition in  $\text{CH}_3\text{CN}$   
 $^{19}\text{F}$  NMR (5.8719T)

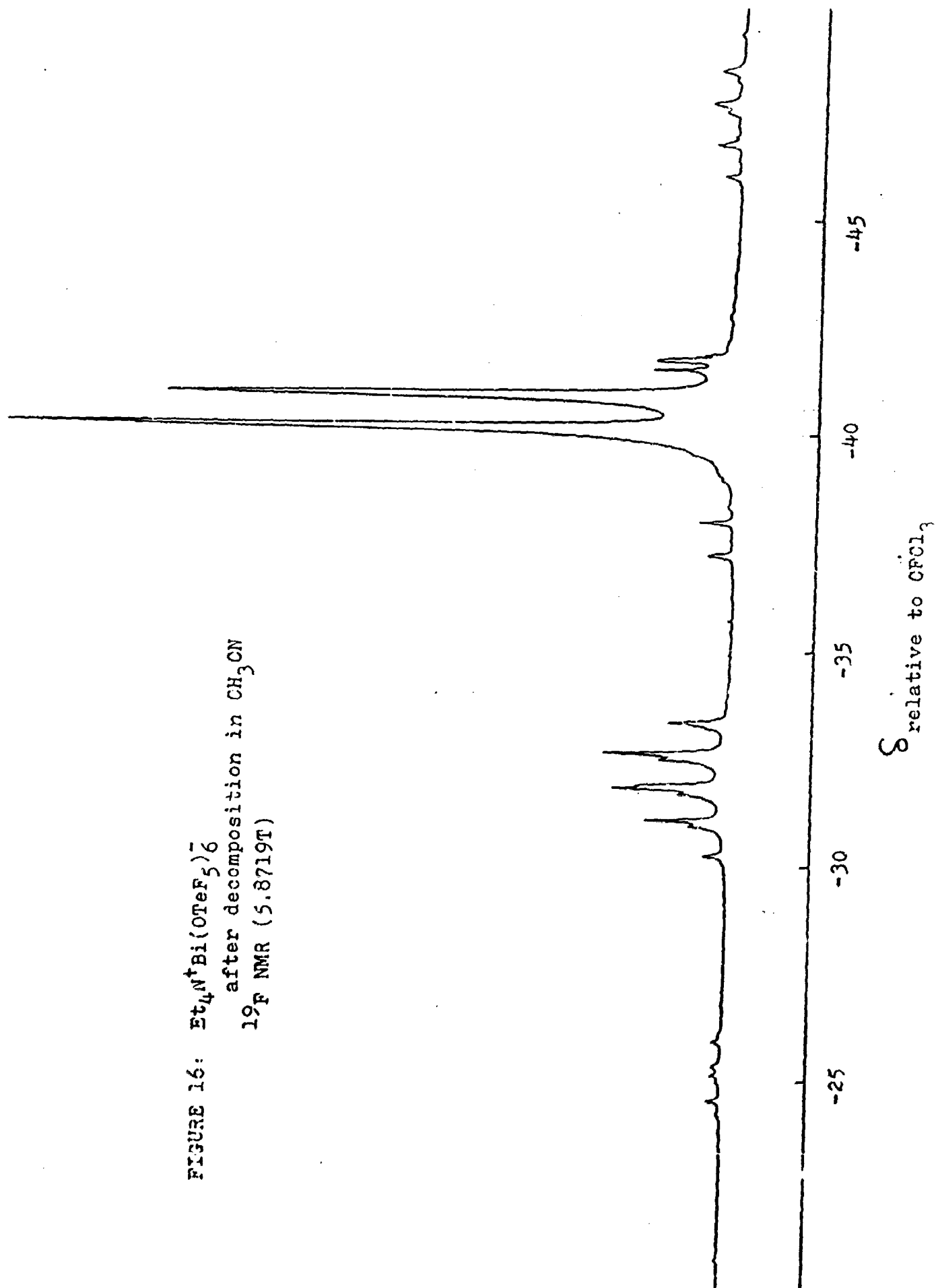
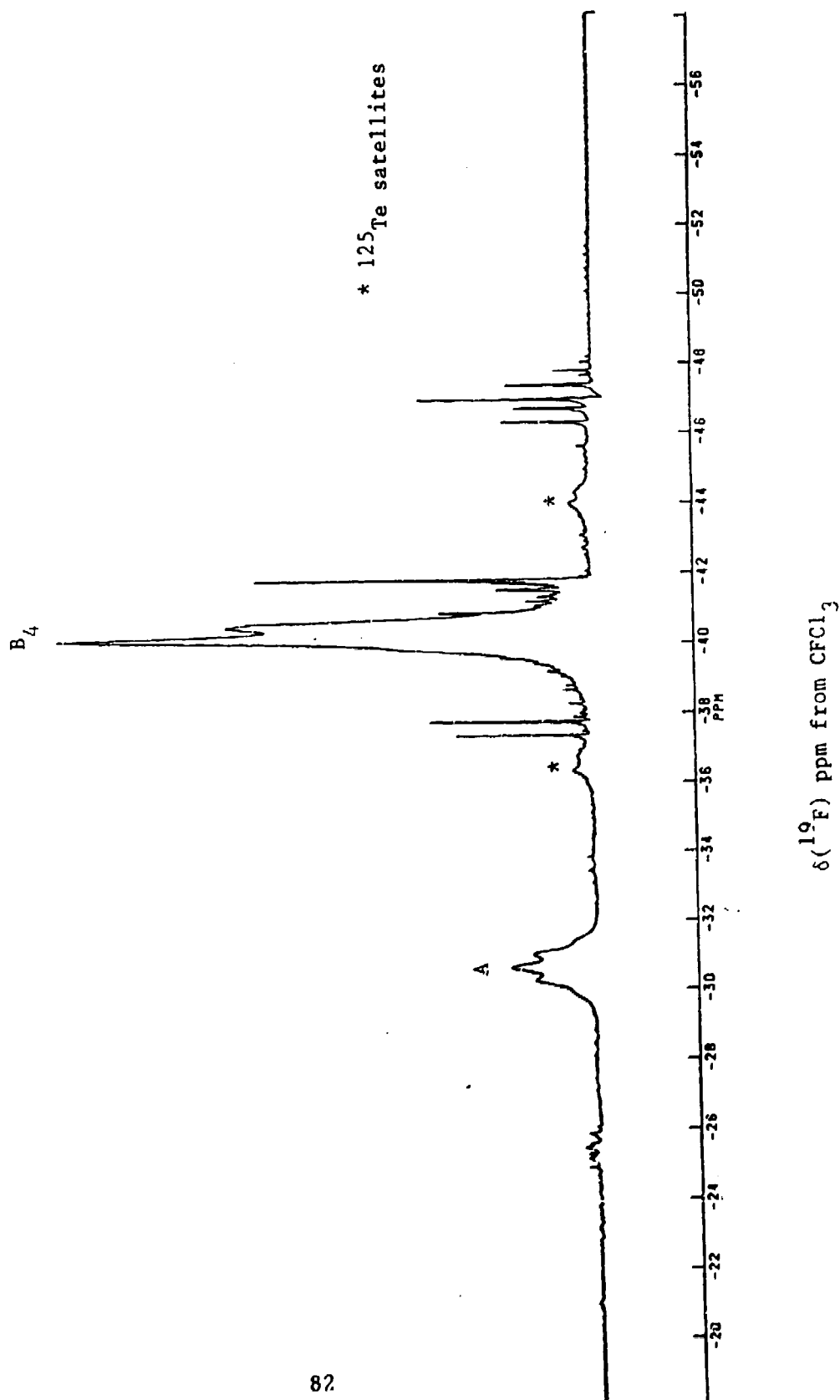


Figure 17:  $\text{Et}_4\text{N}^+ \text{Bi}(\text{OTeF}_5)_6^-$  in  $\text{CH}_3\text{CN}$   
 $^{19}\text{F}$  NMR Spectrum (11.744T)



a  $^{19}\text{F}$ - $^{19}\text{F}$  coupling constant of 171 Hz. The quintet and doublet are broadened by the partially quadrupole-collapsed coupling to the  $^{209}\text{Bi}$  nucleus. Peaks marked with asterisks are  $^{19}\text{F}$ - $^{125}\text{Te}$  coupling, with a coupling constant of 3760 Hz.

The isolation of a salt containing the  $\text{Bi}(\text{OTeF}_5)_4^-$  anion is of great interest since the anion is only the second octahedral  $\text{Bi}(\text{V})$  species known. Its  $^{209}\text{Bi}$  NMR resonance is only the second  $^{209}\text{Bi}$  resonance to be observed; the other being for  $\text{BiF}_6^-$ .

Comparison of NMR Parameters for Known  $\text{M}(\text{OTeF}_5)_4^-$  Anions (M = As, Sb, and Bi)

Several interesting comparisons of the NMR data for the three known group (V) pentafluorooxotellurate(VI) derivatives can be made based on the data summarized in Table 4.

The chemical shifts of the central metal nuclei, M, relative to those of  $\text{MF}_6^-$  tend to move to higher frequency on passing down the group, however, the  $^{209}\text{Bi}$  value is anomalous, and, as noted earlier, would have been expected to have a value less than 0 ppm based on simple electronegativity considerations alone.

The linewidths are interesting as they increase as the group is descended. This is somewhat surprising since the I values increase in size which, according to equation (10), should serve to decrease the linewidth value as the group is descended. However, the increase in size of the anion will increase the isotropic tumbling time,  $\tau_c$ , which, in turn, has a linear effect on  $w_2$ . It should also be noted that a comparison between  $\text{Cs}^+\text{As}(\text{OTeF}_5)_4^-$  and the other two salts is not completely appropriate since the counterions are different. The  $\text{Cs}^+$  counterion would be expected to exhibit a stronger ion-pairing effect than  $\text{Et}_4\text{N}^+$ , increasing  $\tau_c$  serving to broaden the  $^{75}\text{As}$

Table 4. NMR Parameters for  $M(\text{OTeF}_5)_6^-$  ( $M = {}^{75}\text{As}$ ,  ${}^{121}\text{Sb}$ , and  ${}^{209}\text{Bi}$ )

<u>Compound</u>	<u>Solvent</u>	<u><math>2J(M-{}^{125}\text{Te})</math></u> <u>(Hz)</u>	<u><math>\delta_M</math> (ppm)</u>	<u><math>w_{1/2}</math> (Hz)</u>
$\text{Cs}^+\text{As}(\text{OTeF}_5)_6^-$	$\text{CH}_3\text{CN}$	430	-28.9	165
$\text{Et}_4\text{N}^+\text{Sb}(\text{OTeF}_5)_6^-$	$\text{CH}_3\text{CN}$	773	-13.5	275
$\text{Et}_4\text{N}^+\text{Bi}(\text{OTeF}_5)_6^-$	$\text{CH}_3\text{CN}$	2267	128	321

linewidth.

The coupling constants increase on going down the period. The reduced coupling constants,  $K_{AB}$ , can be calculated from equation (21)

$$K_{AB} = \frac{4\pi^2}{h} \frac{J_{AB}}{\gamma_A \gamma_B} \quad (21)$$

where  $J_{AB}$  is the experimentally measured coupling constant, and  $\gamma_A$  and  $\gamma_B$  are the magnetogyric ratios of the spin-spin coupled nuclei. The values obtained (Table 5) increase as the group is descended, however, the increase between Bi and Sb is larger than the trend would suggest. This sharp increase is not unexpected, as this trend is seen for other elements from row six of the Periodic Table, and more relevantly is observed in the compounds  $MF_4^-$  for As, Sb, and Bi.<sup>28</sup> The trend is attributed to relativistic effects in the heavy nucleus, which results in s-orbital contractions. This, in turn, increases the s-electron density and the Fermi-contact terms in the spin-spin coupling expression.<sup>29</sup>

The relativistic effects can be factored out, as shown in equation (22), by dividing  $K_{AB}$  by the relativistically corrected s-orbital

$$K_{AB}^{RC} = \frac{K_{AB}}{|\psi(0)|_A^2 |\psi(0)|_B^2} \quad (22)$$

spin density,<sup>29</sup>  $|\psi(0)|^2$ . The values for As, Sb, Bi, and Te are  $9.708 \times 10^{31}$ ,  $1.552 \times 10^{32}$ ,  $5.652 \times 10^{32}$ , and  $1.852 \times 10^{33} \text{ m}^{-3}$  respectively.<sup>30</sup>

The  $K_{AB}^{RC}$  values obtained from these calculations (Table 5) yield



Table 5. Two-Bond Te-M Scalar Coupling Values for  $M(\text{OTeF}_5)_4^-$  ( $M = \text{As}, \text{Sb}, \text{Bi}$ )

Molecule	$^2J(M-^{125}\text{Te})$ (Hz)	$^2K_{AB}$ ( $\text{NA}^{-2}\text{m}^{-3}$ )	$^2K_{RC}$ ( $\text{NA}^{-2}\text{m}^{-3}$ )
		$\times 10^{-21}$	$\times 10^{-23}$
$\text{Cs}^+\text{As}(\text{OTeF}_5)_4^-$	430	6.59	3.67
$\text{Et}_4\text{N}^+\text{Sb}(\text{OTeF}_5)_4^-$	773	8.42	2.93
$\text{Et}_4\text{N}^+\text{Bi}(\text{OTeF}_5)_4^-$	2267	36.6	3.50

much better comparisons. As can be seen the values for  $K^{RC}$  are very close. However, the value for  $K^{RC}(^{121}\text{Sb}-^{125}\text{Te})$  appears to be significantly lower than the corresponding  $^{75}\text{As}$  and  $^{209}\text{Bi}$  couplings. The exact reasons behind this anomaly are uncertain but may be related to the post-transition element contractions which affect the high oxidation state chemistry of As and Bi.

#### DIRECTIONS FOR FUTURE RESEARCH

This work involved the synthesis of two novel compounds,  $\text{Bi}(\text{OTeF}_5)_5$  and  $\text{Bi}(\text{OTeF}_5)_6^-$ , and the further characterization of  $\text{Sb}(\text{OTeF}_5)_6^-$ , which has been studied by Bartlett and Tötsch, although the work was not published. This work enabled a comparison of the As(V), Sb(V), and Bi(V) hexakis(pentafluorooxotellurate(VI)) anions, and thus yielded a better understanding of the chemistry of the Group(V) atoms in their highest oxidation states.

There are many directions that this work can take in the future. The most obvious is to isolate and characterize  $\text{Sb}(\text{OTeF}_5)_5$ , and to more fully characterize  $\text{Bi}(\text{OTeF}_5)_5$  in the solid state by Raman spectroscopy and X-ray crystallography. Also the class of molecules could be extended to include the P analogs, which would provide a more complete group comparison study.

Once a further characterization is complete, the chemistry of the compounds can be studied. The acceptor properties of the compounds

can be explored and compared with their fluorine analogs. Also, since  $\text{Sb}(\text{OTeF}_5)_4^-$  is a large anion with high symmetry, it should be useful in stabilizing cationic species having high electron affinities, for example,  $\text{Xe}(\text{OTeF}_5)_3^+ \text{M}(\text{OTeF}_5)_4^-$  and  $\text{O}=\text{Xe}(\text{OTeF}_5)^+ \text{M}(\text{OTeF}_5)_4^-$  where the neutral precursors,  $\text{Xe}(\text{OTeF}_5)_4$  and  $\text{O}=\text{Xe}(\text{OTeF}_5)_4$  are already known.

#### REFERENCES

1. K. Seppelt, Angew. Chem. Int. Ed. Engl. 21 (1982) 877.
2. K. Seppelt, Accts. Chem. Res., 12 (1979) 211.
3. T. Birchall, R.D. Myers, H. de Waard, G.J. Schrobilgen, Inorg. Chem. 21 (1982), 1068.
4. D. Lentz, H. Pritzkow, K. Seppelt, Angew. Chem. 89 (1977) 741; Angew. Chem. Int. Ed. Engl. 16 (1977) 729.
5. D. Lentz, H. Pritzkow, K. Seppelt, Inorg. Chem. 17 (1978) 1926.
6. K. Seppelt, Chem. Ber. 109 (1976) 1046.
7. L.K. Templeton, D.H. Templeton, N. Bartlett, K. Seppelt, Inorg. Chem. 15 (1976) 2720.

8. D. Lentz, K. Seppelt, Angew. Chem. Int. Ed. Engl. 18 (1976) 66.
9. E. Jacob, D. Lentz, K. Seppelt, A. Simon, Z. Anorg. Allg. Chem. 472 (1981) 66.
10. A. Engelbrecht, F. Sladky, Angew. Chem. 76 (1964) 379; Angew. Chem. Int. Ed. Engl. 3 (1964) 383.
11. E. Mayer, F. Sladky, Inorg. Chem., 14 (1975) 589.
12. D. Lentz, K. Seppelt, Z. Anorg. Allg. Chem. 460 (1986) 5.
13. H. Pritzkow, K. Seppelt, Z. Anorg. Allg. Chem. 460 (1986) 5.
14. S.H. Strauss, K.D. Abney, O.P. Anderson, Inorg. Chem. 25 (1986) 2806.
15. K. Seppelt, Chem. Ber. 108 (1975) 1823.
16. K. Schröder, F. Sladky, Chem. Ber. 113 (1980) 1414.
17. P. Huppmann, J. Labischinski, D. Lentz, H. Pritzkow, K. Seppelt, Z. Anorg. Allg. Chem. 487 (1982) 7.
18. A. Engelbrecht, F. Sladky, Inorg. Nucl. Chem. Let. 1 (1965) 15.

19. F. Sladky, H. Kropshofer, O. Leitzke, P. Peringer, J. Inorg. Nucl. Chem., H.H.Hyman Memorial Issue (1976) 69.
20. F. Sladky, H. Kropshofer, O. Leitzke, J. Chem. Soc. Chem. Commun. (1973) 134.
21. H. Kropshofer, O. Leitzke, P. Peringer, F. Sladky, Chem. Ber. 114 (1981) 2644.
22. F. Sladky, Angew. Chem., Int. Ed. Engl. 8 (1969) 373.
23. F. Sladky, Angew. Chem., Int. Ed. Engl. 8 (1969) 523.
24. F. Sladky, H. Kropshofer, J. Chem. Soc. Chem. Commun. 1973, 600.
25. E. Jacob, D. Lentz, K. Seppelt, A. Simon, Z. Anorg. Allg. Chem. 172 (1981) 7.
26. D. Lentz, K. Seppelt, Angew. Chem. 90 (1978) 391; Angew. Chem. Int. Ed. Engl. 17 (1978) 356.
27. J.W. Emsley, J. Feeney, L.H. Sutcliffe, High Resolution Nuclear Magnetic Resonance Spectroscopy, Volume 1, Pergamon Press, London, 1965.

28. K. Morgan, B.G. Sayer, G.J. Schrobilgen, J. Mag. Reson. 52 (1983) 139.
29. (a) C. Brevard, P. Granger, "Handbook of High Resolution Multinuclear NMR", pp. 210-211, Wiley-Interscience, New York, 1981; (b) W.G. Proctor, F.G. Yu, Phys. Rev. 78 (1950) 471; (c) Y. Ng, D. Williams, Phys. Rev. 89 (1953) 596; (d) C.P. Flynn and E.F.W. Seymens, Proc. Phys. Soc 73 (1959) 945.
30. R.K. Harris, B.E. Mann, NMR and the Periodic Table, Academic Press, London, 1978, p5.
31. J.C.P. Sanders, Ph.D. Thesis, Nottingham University (1986).
32. M.J. Collins, G.J. Schrobilgen, Inorg. Chem. 24 (1985) 2608.
33. O. Leitzke, F. Sladky, Z. Naturforsch B86 (1981) 268.
34. R.G. Syvret, Ph.D. Thesis, McMaster University, 1986.
35. J.H. Holloway, G.J. Schrobilgen. Inorg. Chem. 20 (1981) 3363.
36. U. Müller, K. Dehnicke, K.S. Vorres, J. Inorg.Nucl. Chem. 30 (1968) 1719.
37.  $\text{BiF}_3$  is a very powerful fluorinating agent which reacts explosively with  $\text{H}_2\text{O}$  to form  $\text{O}_3$ ,  $\text{OF}_2$ , and several other

compounds; N.N.Greenwood, A.Earnshaw, Chemistry of the Elements, Pergamon Press, London (1984) p. 656.

38. S.H. Strauss, K.D. Abney, Inorg. Chem. 23 (1984) 516.

39. R.C. Burns, L.A. Devereux, P. Granger, G.J. Schrobilgen, Inorg. Chem. 24 (1985) 2615.

40. P. Pyykkö, L. Wiesenfeld, Mol. Phys. 43 (1981) 557.

## INTRODUCTION

### Stability of Lead(IV) Compounds

On passing down Group 14 (C, Si, Ge, Sn, Pb), there is a steady trend towards increasing stability of the M(II) rather than the M(IV) oxidation state. The preference for an oxidation state which is 2 less than the group valency is quite common among the heavier p-block elements, and is known as the "inert-pair effect". In 1958, Drago performed a thermodynamic evaluation of the inert-pair effect for the Group 14 chlorides.<sup>1</sup> The data indicated that the instability of lead(IV) compounds could be attributed to a decrease in the covalent bond forming ability of lead. The decrease in covalent bond forming ability of p-block elements as the atomic number increases can be attributed to the following two effects: (1) the radial part of the bond orbitals is changing such as to indicate a spread of the valence electrons over a larger area, resulting in less overlap and weaker covalent bonding, (2) as the number of inner shell electrons increases, the coulombic repulsion between these electrons and the inner electrons of the other bonded atoms increases. When weak covalent bonds are formed, as in the case of lead(IV) chlorides, a lower energy state for the system can be attained by utilizing only the p electrons in compound formation. Two fewer electrons will be involved in bond formation, and the stability relationship attributed to the inert pair is observed. Recent opinion indicates that the inert-pair effect is partially attri-



butable to relativistic effects which result in the radial contraction of the 6s orbital. Thus, the 6s-6p energy gap increases and the oxidation of Pb(II) becomes more difficult.<sup>2</sup>

An exception to this trend is the organometallic chemistry of Sn and Pb which is almost exclusively confined to the M(IV) state, and an extensive range of organo-lead(IV) compounds is known.

The inorganic chemistry of the highly reactive and powerfully oxidizing Pb(IV) is presently limited to the ill-characterized fluorospecies  $\text{PbF}_4$  and  $(\text{PbF}_6)^{2-}$ , and to  $\text{PbO}_2$ ,  $\text{PbCl}_4$ ,  $\text{H}_2\text{PbCl}_6$ ,  $(\text{PbCl}_6)^{2-}$ ,  $\text{Pb}(\text{SO}_4)_2$ ,  $\text{Pb}(\text{CH}_3\text{COO})_4$  and  $\text{Pb}(\text{CF}_3\text{COO})_4$  and is virtually unexplored. Owing to their hydrolytic instability, handling of all the above compounds requires vacuum line and dry box techniques.

#### Lead Tetrahalides

Lead forms two series of halides:  $\text{PbX}_2$  and  $\text{PbX}_4$ . The  $\text{PbX}_2$  halides are more stable, both thermally and chemically, than  $\text{PbX}_4$ . The only stable tetrahalide is  $\text{PbF}_4$ , a white, crystalline, highly moisture sensitive solid with a melting point of approximately 600°C, and a density of 6.7 g/cm<sup>3</sup>. X-ray diffraction studies have shown that  $\text{PbF}_4$  forms tetragonal, body-centered crystals with dimensions,  $a = 4.24 \text{ \AA}$ ,  $c = 8.03 \text{ \AA}$ .<sup>4</sup> Lead tetrachloride,  $\text{PbCl}_4$ , is a yellow oil (m.p. -15°C,  $d(0^\circ\text{C}) 3.18 \text{ g/cm}^3$ ) that is experimentally difficult to obtain in a pure state.<sup>5</sup> The compound has a tetrahedral structure<sup>6</sup> and is stable below 0°C

when stored in the dark under concentrated  $\text{H}_2\text{SO}_4$ ,<sup>5</sup> but rapid decomposition to  $\text{PbCl}_2$  and  $\text{Cl}_2$  occurs above  $50^\circ\text{C}$ .<sup>7</sup> Lead tetrabromide is even less stable, and the existence of  $\text{PbI}_4$  is uncertain.<sup>7</sup>

#### The Hexachloroplumbate(IV) Anion, $[\text{PbCl}_6]^{2-}$

All elements of Group 14, except carbon, form hexahalide complex anions of the type  $[\text{MX}_6]^{2-}$ , for  $\text{M} = \text{Si}$ :  $\text{X} = \text{F}$ ;  $\text{M} = \text{Ge}$  or  $\text{Pb}$ :  $\text{X} = \text{F}$ , or  $\text{Cl}$ ;  $\text{M} = \text{Sn}$ :  $\text{X} = \text{F}$ ,  $\text{Cl}$ ,  $\text{Br}$ , or  $\text{I}$ . In the case of  $\text{Pb}$ , increasing the coordination number from 4 to 6 leads to a marked stabilization of the +4 oxidation state. Direct chlorination of  $\text{PbCl}_2$  in aqueous  $\text{HCl}$  yields a solution of the free acid,  $\text{H}_2\text{PbCl}_6$ . Although  $\text{H}_2\text{PbCl}_6$  is unstable above  $-5^\circ\text{C}$ , the octahedral  $[\text{PbCl}_6]^{2-}$  anion attains maximum stability with large, poorly polarizing cations (e.g.,  $\text{NH}_4^+$ ,  $\text{K}^+$ , and  $\text{py}^+$ ). The stability of these salts is such that, on exposure to air, neither hydrolysis nor loss of chlorine occurs. The  $[\text{PbCl}_6]^{2-}$  salts can then serve as a stable source for other lead(IV) compounds; for example, the unstable  $\text{PbCl}_4$  can be prepared by treatment of these salts with cold concentrated  $\text{H}_2\text{SO}_4$ .<sup>4</sup>

#### The Hexafluoroplumbate(IV) Anion, $[\text{PbF}_6]^{2-}$

Very early work in the study of lead(IV) compounds centered around the potassium and sodium double salts of lead tetrafluoride. In 1919, the only strictly chemical method for the preparation of free fluorine involved the thermal decomposition

of the double salt tripotassium lead hydrogen octafluoride,  $K_3HPbF_8$ .<sup>9</sup> The term "chemical method" for the preparation of free fluorine implies that  $F_2$  is generated by purely chemical means that excludes techniques such as electrolysis, photolysis, discharge, etc. or the use of elemental fluorine for the synthesis of any of the starting materials. The compound,  $K_3HPbF_8$ , was first prepared in pure form and studied by Brauner.<sup>9</sup> He prepared  $K_3HPbF_8$  by fusing  $PbO_2$  and  $KOH$ , dissolving the product in aqueous  $HF$ , and evaporating off the excess acid to obtain pure  $K_3HPbF_8$ . Brauner showed that  $HF$  could be completely removed at temperatures below  $250^\circ C$ , and that at temperatures above  $250^\circ C$ ,  $F_2$  was evolved. This method was believed to hold satisfactory possibilities as a source for free fluorine since both  $BrF_3$  and  $IF_5$  could be prepared by passing the  $F_2$  evolved from the decomposition of the double salt over  $Br_2$  and  $I_2$ , respectively.<sup>9</sup> Recently, Christie,<sup>10</sup> developed a more feasible method for the chemical synthesis of elemental fluorine according to equation (4).



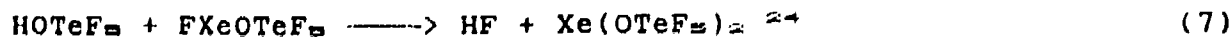
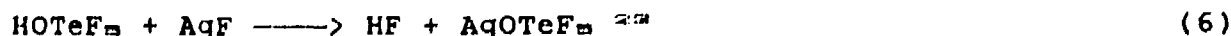
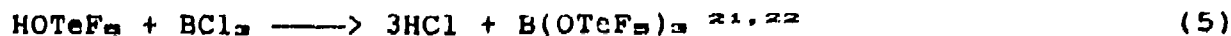
The salt,  $K_3HPbF_8$ , has been studied by X-ray powder photography, infrared spectroscopy,<sup>11</sup> and Raman spectroscopy.<sup>12</sup> The solid was found to contain the octahedral  $[PbF_6]^{2-}$  anion and the  $HF_2^-$  anion. In order to determine whether these anions persisted in solution, the  $^{19}F$  NMR spectrum of a solution of  $K_3HPbF_8$  in 20%

HF was obtained. The spectrum consisted of a single broad line, indicating that rapid fluorine exchange was occurring, and consequently no conclusions about the structure of the  $[\text{PbF}_6]^{2-}$  anion in solution could be drawn.<sup>12</sup>

### Pentafluoroorthotellurate(VI) Derivatives

The highly electronegative,  $\text{OTeF}_5$  group is capable of stabilizing high positive oxidation states of the atom to which it is bonded.<sup>13</sup> In addition, the ligand is capable of forming stable derivatives whose only analogues are fluorine compounds, e.g.,  $\text{TeF}_6$ ,  $\text{Te}(\text{OTeF}_5)_4$ ; <sup>14, 15, 16</sup> and  $\text{O}=\text{XeF}_4$ ,  $\text{O}=\text{Xe}(\text{OTeF}_5)_4$ .<sup>14, 17, 18</sup> Unlike fluorine, the  $\text{OTeF}_5$  ligand rarely forms bridges, owing to its size and internal bonding. Consequently, compounds containing the  $\text{OTeF}_5$  ligand invariably have molecular monomeric structures whereas the corresponding fluoride may be polymeric. Examples include  $\text{TiF}_4$ ,  $\text{Ti}(\text{OTeF}_5)_4$ ; <sup>19</sup> and  $\text{XeF}_6$ ,  $\text{Xe}(\text{OTeF}_5)_4$ .<sup>20</sup>

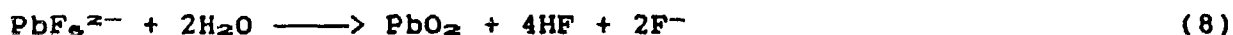
The starting material for  $\text{OTeF}_5$  derivatization is the pseudo-octahedral, moderately strong, monoprotic acid  $\text{HOTeF}_5$ . The most direct method for the preparation of  $\text{OTeF}_5$  derivatives involves reactions of a halide with  $\text{HOTeF}_5$  leading to the elimination of volatile hydrogen halides; for example



The products of equations (5) and (6) can be used for substitution reactions of F by  $\text{OTeF}_5$ , whereas,  $\text{Xe}(\text{OTeF}_5)_2$  can be used to introduce  $\text{OTeF}_5$  oxidatively.

#### Purpose of Present Research

The research described in this thesis is aimed at expanding our knowledge of the high-oxidation-state chemistry of lead. The work involved the preparation of fluoro, mixed chlorofluoro and  $\text{OTeF}_5$  derivatives of lead(IV). The purpose was three-fold: 1) the synthesis of the previously unknown salt,  $(\text{Et}_4\text{N}^+)_2\text{PbF}_6^{2-}$ , the first  $[\text{PbF}_6]^{2-}$  salt containing an organic cation. It was thought that an organic cation would provide good solubility in non-aqueous solvents, (e.g., acetonitrile). This was important since the  $[\text{PbF}_6]^{2-}$  anion decomposes in water according to equation (8).



Consequently, the  $[\text{PbF}_6]^{2-}$  anion can be characterized in solution by  $^{19}\text{F}$  and  $^{207}\text{Pb}$  for the first time;

2) the synthesis and characterization, by  $^{19}\text{F}$  and  $^{207}\text{Pb}$  NMR spectroscopy, of the unknown  $[\text{PbCl}_n\text{F}_{6-n}]^{2-}$  anions; and

3) the synthesis and characterization of the new anion,  $[\text{Pb}(\text{OTeF}_5)_6]^{2-}$ .

This would be the first example of a lead(IV) compound containing the highly electronegative  $\text{OTeF}_5$  ligand. The

$[\text{Pb}(\text{OTeF}_6)_6]^{2-}$  anion is expected to be a large oxidatively resistant anion which could be used as a precursor for other work. It is thought that this anion could stabilize highly oxidizing cations, such as the noble-gas cations (e.g.,  $\text{XeOTeF}_6^+$ ,  $\text{Xe}(\text{OTeF}_6)_3^+$ ,  $\text{O}=\text{Xe}(\text{OTeF}_6)_3^+$ ). The  $\text{OIF}_4=\text{O}$  group, which is of greater electronegativity than  $\text{OTeF}_6$ , can be introduced by the reaction of the acid  $\text{HOIF}_4=\text{O}$  with an  $\text{OTeF}_6$  derivative according to equation (9).



## EXPERIMENTAL

### Apparatus and Materials

Almost all of the compounds used in the course of this research were air and moisture sensitive requiring the use of dry box and vacuum line techniques. Non-volatile reagents were transferred and manipulated directly either in a glove bag or in a dry box with an atmosphere of less than 0.1 ppm of  $O_2$  and 0.01 ppm of  $H_2O$ , (Vacuum Atmospheres Model DLX). Volatile reactants were transferred on either a metal, (316 stainless steel, nickel, Teflon and FEP) or glass vacuum line (see Figure 1).

### Preparation and Purification of Starting Materials

Solid Reagents The following commercial materials were used:  $PbF_2$  (99+%, Aldrich),  $PbCl_2$  (99+%, Baker Chemicals),  $AgF$  (Canadian Scientific Ltd.),  $AgF$  (99.9%, Aldrich),  $Pb(OCOCH_3)_4$  (Aldrich), and  $Te(OH)_6$  (Analar grade, BDH Chemicals).

$Et_4NCl \cdot xH_2O$  (Aldrich) was dried under vacuum at  $100^\circ C$  overnight and used without further purification.

$[(n-Bu)_4N^+]_2PbCl_6^{2-}$  was prepared in an analogous manner to the preparation of pyridinium hexachloroplumbate(IV)<sup>4</sup> and was recrystallized from dry acetonitrile.

$XeF_2$ ,  $Xe(OTeF_5)_2$ ,  $B(OTeF_5)_3$  and were prepared by literature methods.<sup>20, 26, 21</sup>

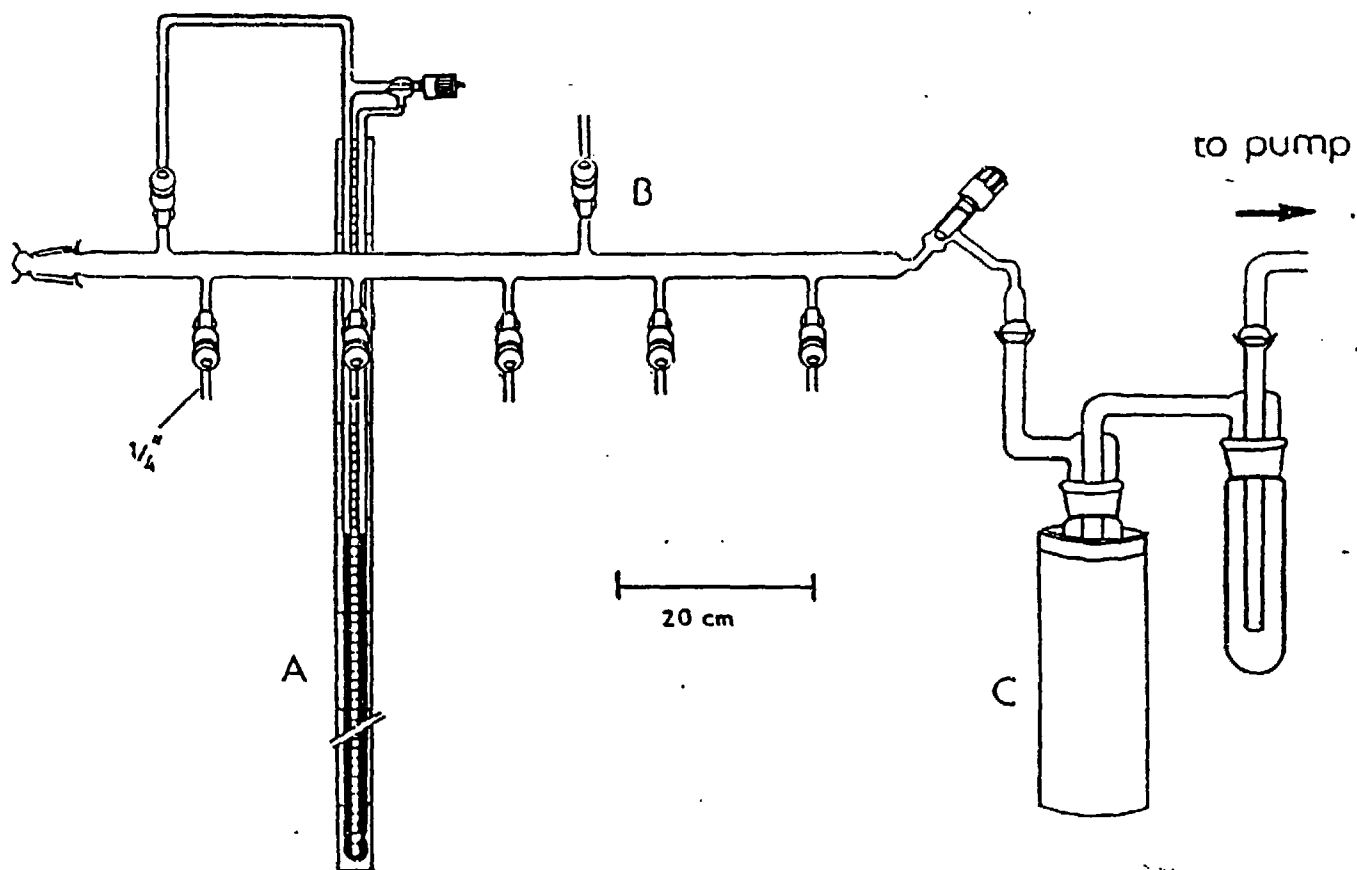


Figure 1. Glass Vacuum Line

A Manometer. B Dry Nitrogen Inlet. C Liquid Nitrogen Trap



$\text{AgOTeF}_6$  was prepared in  $\text{CH}_2\text{Cl}_2$  according to literature methods,<sup>23</sup> and pumped down, to constant weight, yielding  $\text{AgOTeF}_6$  and not  $\text{AgOTeF}_6 \cdot \text{CH}_2\text{Cl}_2$  as reported.

### Solvents

All solvents were dried rigorously before use.

$\text{CH}_3\text{CN}$  (Baker Chemicals) was dried using the method described by Winfield,<sup>27</sup> excluding the reflux step involving  $\text{KHSO}_4$ .

$\text{CH}_2\text{Cl}_2$  (BDH Chemicals) and  $d_3\text{-CH}_3\text{CN}$  were dried over  $\text{CaH}_2$ .

$\text{CFCl}_3$ , and Freon 114 (Aldrich), were dried over  $\text{P}_2\text{O}_5$ .

Anhydrous HF (Harshaw), which was used as both a solvent and a reactant, was purified by storing it under 5 atm. of  $\text{F}_2$  for at least one month as previously described.<sup>28</sup>

$\text{HSO}_3\text{F}$  (Allied) was purified by the standard literature method.<sup>29</sup>

### Preparations

#### A) Reagents for the preparation of $(\text{Et}_4\text{N}^+)_2[\text{PbF}_6]^{2-}$

##### Preparation of $\text{Et}_4\text{NF}(\text{HF})_n$

In a typical preparation,  $\text{Et}_4\text{NCl}$  (4.2458 g, 25.622 mmol) was transferred into a dry 10 mm FEP tube equipped with a Kel-F valve in the dry box. On a metal vacuum line, anhydrous HF was distilled onto the solid at  $-196^\circ\text{C}$ . The sample was allowed to

warm to room temperature with vigorous agitation to effect even distribution of the liquid throughout the solid. Reaction was generally complete within 30 min., resulting in the formation of HCl and a clear, light beige, viscous liquid. The tube was opened to an isolated section of the vacuum line with a pressure of ca. 0.7 atm. of dry N<sub>2</sub>, and the HCl pumped away. The tube was then pressurized with ca. 1 atm. of dry N<sub>2</sub> at -78°, and stored at -78°C until used.

#### Preparation of PbF<sub>4</sub>

Lead tetrafluoride was prepared by a high temperature fluorination of PbF<sub>2</sub>.<sup>30</sup> The PbF<sub>2</sub> (5.0 g, 20 mmol) was transferred, in the dry box, into a nickel boat and the boat placed in a clean, dry, prehydrogenated and prefluorinated nickel bomb (O.D. = 3.5 cm, I.D. 3.0 cm, L = 20 cm). Fluorine (0.1020 mol) was condensed into the bomb at -196°C. The bomb was placed in a furnace at 300°C and left to react for 1.5 days. After cooling, the bomb was returned to the dry box, and the boat removed. The product, a white fused solid, was crushed with mortar and pestle and stored in the dry box in a fluoroplastic container. A sample for Raman spectroscopy was loaded into a glass tube (1/4 inch o.d.) and flame sealed under vacuum. Raman spectrum (cm<sup>-1</sup>, values in parentheses denote intensities) at -196°C: 563(93), 545(100), 532(21), 500(7), 479(4), 238(4), 202(8), 185(9), 134(4).

#### Preparation of $(\text{Et}_4\text{N}^+)_2[\text{PbCl}_6]^{2-}$

The title compound was prepared according to equations (10) and (11).



An aqueous solution of  $(\text{Et}_4\text{N})\text{Cl}$  (106.5 mL, 0.1438 mol) was prepared by neutralizing aqueous  $(\text{Et}_4\text{N})\text{OH}$  with concentrated  $\text{HCl}$ . The  $(\text{Et}_4\text{N})\text{Cl}$  solution was added to an ice-cold solution containing the stoichiometric amount of  $\text{H}_2[\text{PbCl}_6]$ , prepared according to literature methods.<sup>4</sup> The crude product was filtered using a Büchner funnel, washed with ice-cold absolute ethanol then vacuum dried. The  $(\text{Et}_4\text{N}^+)_2[\text{PbCl}_6]^{2-}$ , a bright yellow, dry powder (44.1% yield, 21.5972 g, 0.0317 mol) was stored in the dry box.

#### Recrystallization of $\text{AgF}$

Commercial  $\text{AgF}$ , a brown solid, was transferred in the dry box into an FEP tube equipped with a Kel-F valve. The tube was attached to a metal vacuum line and anhydrous  $\text{HF}$  distilled into the tube at  $-196^\circ\text{C}$ . The tube was covered with aluminum foil to prevent photodecomposition of the  $\text{AgF}$ . The  $\text{AgF}$  dissolved as the solution warmed to room temperature forming a clear colourless solution. The  $\text{HF}$  was pumped off slowly for a day, then fresh  $\text{HF}$  distilled in. The  $\text{HF}$  solvent was again removed, initially yielding a light gray solid, but when pumping was continued for a

day, a light orange solid was obtained. The solid was dried in vacuum for a further two days to ensure the complete removal of HF.

#### B) Preparation of $(Et_4N^+)_2[PbF_6]^{2-}$

##### Reaction of $Et_4NF(HF)_n$ with $Pb(OCOCH_3)_4$ in Anhydrous HF

The first attempt to prepare tetraethylammonium hexafluoroplumbate(IV) was performed according to equation (12).



Lead tetraacetate was transferred into a preweighed 1/2 inch FEP tube, equipped with a Kel-F valve, in the glove bag. The sample was then dried on a metal vacuum line for 2 hours, then reweighed. On a metal vacuum line, anhydrous HF was distilled onto  $Pb(OCOCH_3)_4$  (4.2458 g, 9.5760 mmol) at  $-196^\circ C$ . The sample was allowed to dissolve at room temperature. A second 1/2 inch FEP tube containing  $Et_4NF(HF)_n$  dissolved in HF was connected as shown in Figure 2. The two reactants were mixed at liquid  $N_2$  temperature by pouring  $Et_4NF(HF)_n$  in HF onto the  $Pb(OAc)_4$  dissolved in HF. The mixture was allowed to warm to room temperature. A white precipitate formed and the solution turned a dark red-brown colour. On pumping in dynamic vacuum, the solution became colourless. The HF solvent was pumped off,

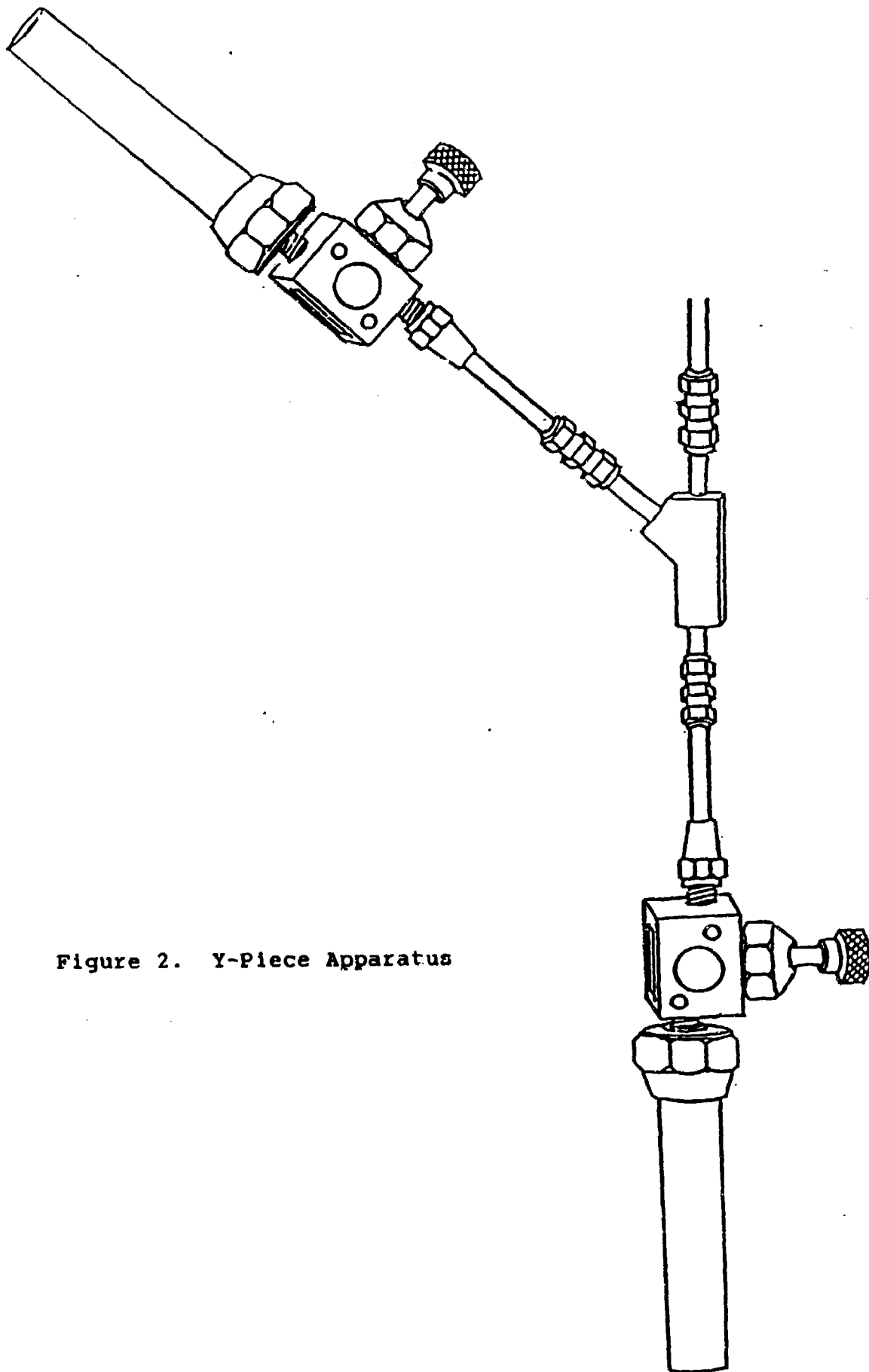


Figure 2. Y-Piece Apparatus

leaving a white solid suspended in a light beige viscous liquid. The non-volatile liquid, believed to be protonated acetic acid, was decanted into a separate FEP tube and the remaining solid was washed several times with HF and again decanted. Both FEP tubes were pumped to dryness, each producing a white solid. The HF soluble product, thought to be  $(Et_4N^+)_2[PbF_6]^{2-}$ , was tested for solubility in  $CH_3CN$ , but proved to be insoluble. Raman samples of both solids were made up in 1/4 inch glass tubes and stored at  $-196^\circ C$ .

#### Reaction of $PbF_4$ with $Et_4NF(HF)_n$

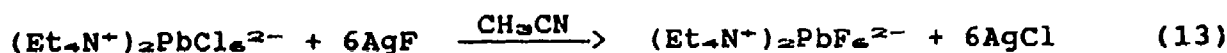
The  $PbF_4$  (0.9917 g, 3.5018 mmol) was transferred into a 10 mm FEP tube, equipped with a Kel-F valve, in the dry box. Anhydrous HF was vacuum distilled into the tube at  $-196^\circ C$  and the sample allowed to warm to room temperature. A white solid suspension was obtained since  $PbF_4$  is essentially insoluble in HF. An FEP tube containing  $Et_4NF(HF)_n$  dissolved in HF was attached as shown in Figure 2, and the solution poured into the sample tube at  $-196^\circ C$ . The reaction was allowed to warm to room temperature with vigorous agitation to distribute the two reactants throughout the solvent. After 3 hours of mixing, it was observed that the amount of solid present in solution did not decrease. The HF solvent was removed under vacuum, and the reaction mixture consisted of a white solid suspended in a light beige viscous liquid. The product was believed to comprise only unreacted  $PbF_4$  and  $Et_4NF(HF)_n$ , and was not characterized further.

#### Reaction of $(\text{Et}_4\text{N}^+)_2\text{PbCl}_4^{2-}$ with $\text{XeF}_2$ in Anhydrous HF

In another attempt to prepare  $(\text{Et}_4\text{N}^+)_2(\text{PbF}_6)^{2-}$ , the reaction of  $(\text{Et}_4\text{N}^+)_2\text{PbCl}_4^{2-}$  with excess (1:5 mole ratio) of  $\text{XeF}_2$  in anhydrous HF was performed.  $\text{XeF}_2$  (1.2741 g, 7.5263 mmol) was transferred in the dry box into a 10 mm FEP tube equipped with a Kel-F valve. The tube was removed from the dry box, attached to a metal vacuum line and anhydrous HF distilled into the sample at  $-196^\circ\text{C}$ . The  $\text{XeF}_2$  was allowed to dissolve at room temperature. The tube was returned to the dry box, cooled to  $-196^\circ\text{C}$ , and  $(\text{Et}_4\text{N}^+)_2\text{PbCl}_4^{2-}$  (1.0239 g, 1.5048 mmol) added. The sample was removed from the dry box and maintained at  $-196^\circ\text{C}$ . The tube was attached to a metal vacuum line. The sample was evacuated and allowed to warm to room temperature. The reaction proceeded rapidly, with the formation of a white precipitate and the evolution of Xe and  $\text{Cl}_2$ . The tube was opened to the vacuum line and the gases pumped off at  $-196^\circ\text{C}$ . When the reaction had subsided, the tube was placed in a warm water bath to drive the reaction to completion. When the evolution of gas had ceased, the HF was removed in vacuum, leaving a white solid suspended in a light beige viscous liquid. The nature of the product indicated it was a mixture of  $\text{PbF}_4$  or  $\text{PbF}_2$  and  $\text{Et}_4\text{NF}(\text{HF})_n$  and was not characterized further.

#### Reaction of $(\text{Et}_4\text{N}^+)_2\text{PbCl}_4^{2-}$ with $\text{AgF}$

The preparation of  $(\text{Et}_4\text{N}^+)_2\text{PbF}_6^{2-}$  was carried out according to equation (13).



The first four attempts at this reaction using commercial AgF, without prior purification, yielded a brown solid product, possibly due to hydrolysis reactions. The reaction was then repeated using AgF recrystallized from HF. In a typical preparation, AgF (1.9622 g, 15.467 mmol), recrystallized from anhydrous HF, and  $(\text{Et}_4\text{N}^+)_2\text{PbCl}_6^{2-}$  (1.7538 g, 2.5775 mmol) were transferred in the dry box into a glass H-vessel equipped with J. Young valves, (see Figure 3). The reagents were placed in the arm of the H-vessel containing a magnetic stir bar. The H-vessel was attached to a metal vacuum line as shown in Figure 3, and dry  $\text{CH}_3\text{CN}$  distilled onto the reagents at  $-196^\circ\text{C}$ . The vessel was covered with aluminum foil to prevent ingress of light. The reaction mixture was allowed to warm to room temperature with stirring. The solution turned a pale yellow, probably due to dissolved  $(\text{Et}_4\text{N}^+)_2\text{PbCl}_6^{2-}$ , with concomitant precipitation of off-white AgCl. The reaction proceeded quickly, and after three hours, stirring was halted and the precipitate allowed to settle. The tube was placed on the vacuum line and evacuated at  $-196^\circ\text{C}$ . The clear, colourless solution was then carefully decanted, through the medium sintered frit into the opposite arm of the H-vessel at  $-78^\circ\text{C}$ . Further extraction of the product from the AgCl solid layer was achieved by distilling  $\text{CH}_3\text{CN}$  back through the frit onto the AgCl solid at  $-78^\circ\text{C}$ , allow-



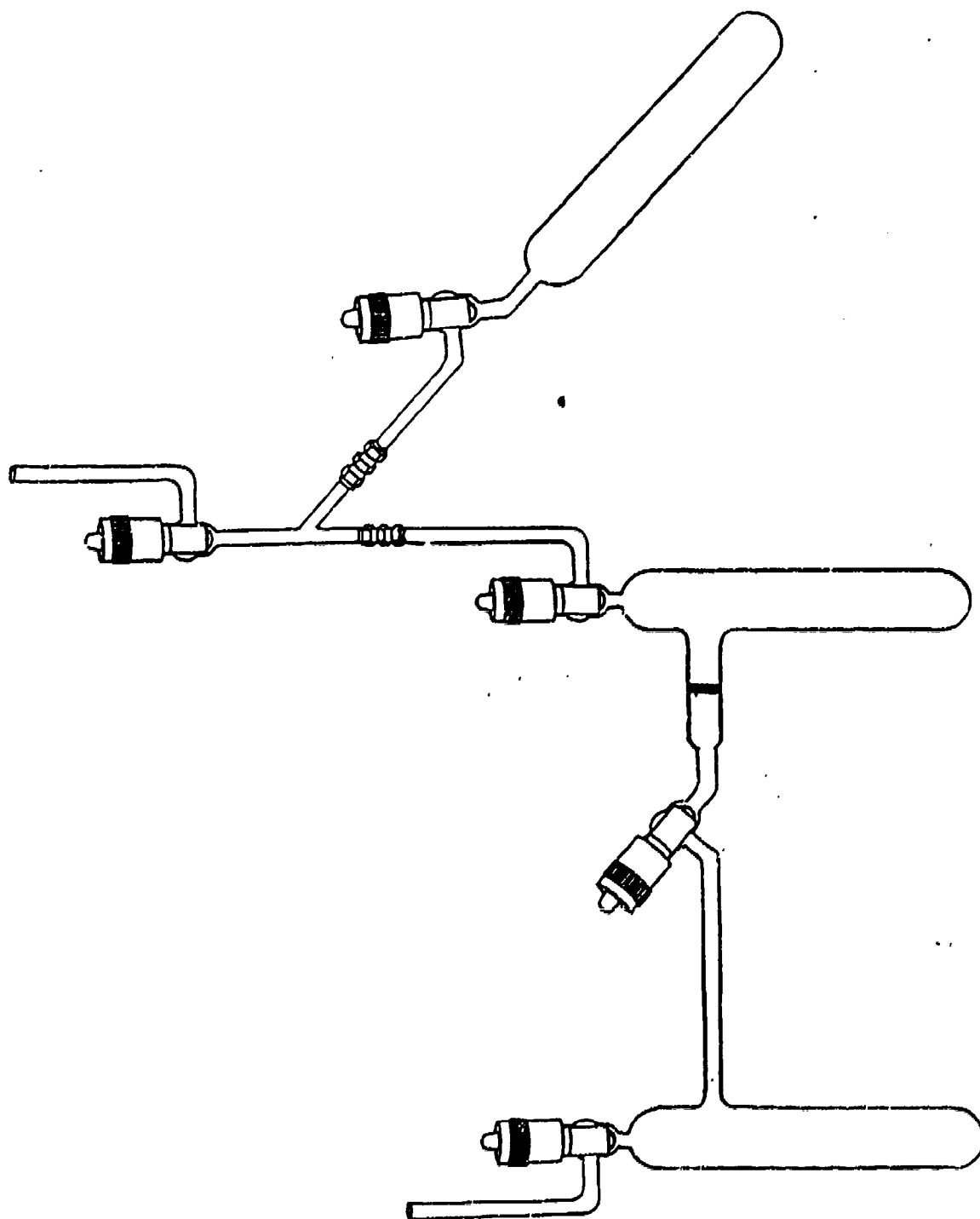


Figure 3. Glass Distillation Apparatus and H-Vessel

ing the solid to settle and decanting the solution back through the frit to the opposite arm of the H-vessel. The vessel was placed in a glove bag, and the solution pipetted into another H-vessel. The solvent was removed under vacuum yielding a white crystalline solid. Two samples for  $^{207}\text{Pb}$  and  $^{19}\text{F}$  NMR spectroscopy were prepared in 10 mm and 5 mm glass NMR tubes, respectively, using  $\text{CH}_3\text{CN}$  as solvent. In the dry box, the white solid was loaded into a glass NMR tube. The tube was removed from the dry box, placed on a metal vacuum line, and  $\text{CH}_3\text{CN}$  distilled into the tube at  $-196^\circ\text{C}$ . The sample was allowed to reach room temperature, evacuated, and the tubes flame sealed, in vacuum at  $-196^\circ\text{C}$  and stored in the dark in the refrigerator.

### C) Synthesis of the $[\text{PbCl}_n\text{F}_{6-n}]^{2-}$ Anions

#### 1) Synthesis of $[(n\text{-Bu})_4\text{N}^+]_2[\text{PbCl}_n\text{F}_{6-n}]^{2-}$ Salts

Solutions of  $[(n\text{-Bu})_4\text{N}^+]_2[\text{PbCl}_n\text{F}_{6-n}]^{2-}$  in  $\text{CH}_3\text{CN}$  were prepared in situ in 10 mm glass NMR tubes by allowing  $\text{XeF}_2$  and  $[(n\text{-Bu})_4\text{N}^+]_2[\text{PbCl}_6]^{2-}$  to react in dry  $\text{CH}_3\text{CN}$ . Two samples with different stoichiometries were prepared in  $\text{CH}_3\text{CN}$ :

- 1)  $[(n\text{-Bu})_4\text{N}^+]_2[\text{PbCl}_6]^{2-}$  (1.3542 g, 1.4966 mmol) with  $\text{XeF}_2$  (0.7623 g, 4.5030 mmol); mole ratio 1:3.
- 2)  $[(n\text{-Bu})_4\text{N}^+]_2[\text{PbCl}_6]^{2-}$  (1.3479 g, 1.4836 mmol) with  $\text{XeF}_2$  (0.3773 g, 2.2288 mmol); mole ratio 1:1.5.

In a typical preparation,  $\text{XeF}_2$  and  $[(n\text{-Bu})_4\text{N}^+]_2[\text{PbCl}_6]^{2-}$  were loaded into a 10 mm glass tube in the dry box. The sample was removed from the dry box, evacuated and dry  $\text{CH}_3\text{CN}$  distilled onto the reagents at  $-196^\circ\text{C}$ . The reaction was then allowed to warm to room temperature. Initially, the reaction mixture produced a clear yellow solution with the evolution of both Xe and  $\text{Cl}_2$  gas. As the reaction progressed, the solution became cloudy and white precipitate formed. The gas evolution ceased after four hours and the tube was evacuated at  $-196^\circ\text{C}$ . The tube was removed from the vacuum line, placed in a glove bag, and a portion of the sample from the 10 mm glass tube, was pipetted into a 5 mm glass NMR tube. The glass tubes were flame sealed under vacuum and stored in the dark in the refrigerator.

#### 11) Synthesis of $(\text{Et}_4\text{N}^+)_2[\text{PbCl}_n\text{F}_{6-n}]^{2-}$ Salts

##### a) Reaction of $(\text{Et}_4\text{N}^+)_2\text{PbCl}_6^{2-}$ with $\text{XeF}_2$

Solutions of the salts were prepared in an analogous manner to the preparation of  $[(n\text{-Bu})_4\text{N}^+]_2[\text{PbCl}_6]^{2-}$  anions. Two NMR samples of different stoichiometries were prepared in situ in 10 mm glass NMR tubes in dry  $\text{CH}_3\text{CN}$  using the following quantities of reagents:

- 1)  $(\text{Et}_4\text{N}^+)_2\text{PbCl}_6^{2-}$  (1.0220 g, 1.5020 mmol),  $\text{XeF}_2$  (0.7643 g, 4.5148 mmol) giving a 1:3 mole ratio.
- 2)  $(\text{Et}_4\text{N}^+)_2\text{PbCl}_6^{2-}$  (1.0213 g, 1.5010 mmol),  $\text{XeF}_2$  (0.3894 g, 2.3002 mmol) giving a 1:1.5 mole ratio.

In a typical preparation,  $\text{XeF}_2$  and  $(\text{Et}_4\text{N}^+)_2[\text{PbCl}_6]^{2-}$  were loaded into a 10 mm glass tube in the dry box. The sample was removed from the dry box, evacuated and dry  $\text{CH}_3\text{CN}$  distilled onto the reagents at  $-196^\circ\text{C}$ . The reaction was then allowed to warm to room temperature. The reaction progressed slowly, with the majority of  $(\text{Et}_4\text{N}^+)_2[\text{PbCl}_6]^{2-}$  remaining undissolved. The reaction rate was increased by warming the mixture in a warm water bath at ca.  $40^\circ\text{C}$ . After 7 hours, gas evolution had ceased and the solution was a clear light green colour with some undissolved yellow solids. The  $\text{CH}_3\text{CN}$  solvent and any remaining  $\text{XeF}_2$  were pumped off at  $-196^\circ\text{C}$  and the solid dried in vacuum for 3 hours.  $\text{CH}_3\text{CN}$  was distilled into the tube at  $-196^\circ\text{C}$ , the mixture allowed to warm to room temperature, and the solid allowed to dissolve. The reaction mixture was a clear light green colour with yellow precipitates. The tube was evacuated at  $-196^\circ\text{C}$ . The tube was removed from the vacuum line, placed in a glove bag, and a portion of the sample from the 10 mm glass tube, was pipetted into a 5 mm glass NMR tube. The glass tubes were flame sealed under vacuum and stored in the dark in the refrigerator.

b) Reaction of  $(\text{Et}_4\text{N}^+)_2[\text{PbCl}_6]^{2-}$  and  $(\text{Et}_4\text{N}^+)_2[\text{PbF}_6]^{2-}$

Solutions containing the  $(\text{Et}_4\text{N}^+)_2[\text{PbCl}_n\text{F}_{6-n}]^{2-}$  salts were prepared in situ in 10 mm glass NMR tubes by allowing  $(\text{Et}_4\text{N}^+)_2[\text{PbCl}_6]^{2-}$  and  $(\text{Et}_4\text{N}^+)_2[\text{PbF}_6]^{2-}$  to undergo ligand redistribution in dry  $\text{CH}_3\text{CN}$ . Three NMR samples with different stoichiometries were prepared in  $\text{CH}_3\text{CN}$ :

- 1)  $(\text{Et}_4\text{N}^+)_2\text{PbCl}_6^{2-}$  (0.1956 g, 0.2875 mmol) and  $(\text{Et}_4\text{N}^+)_2\text{PbF}_6^{2-}$  (1.0028 g, 1.7239 mmol); mole ratio = 1:6.
- 2)  $(\text{Et}_4\text{N}^+)_2\text{PbCl}_6^{2-}$  (0.2153 g, 0.3164 mmol) and  $(\text{Et}_4\text{N}^+)_2\text{PbF}_6^{2-}$  (0.9235 g, 1.6384 mmol); mole ratio = 1:5.
- 3)  $(\text{Et}_4\text{N}^+)_2\text{PbCl}_6^{2-}$  (1.0072 g, 1.4803 mmol) and  $(\text{Et}_4\text{N}^+)_2\text{PbF}_6^{2-}$  (0.4306 g, 0.7402 mmol); mole ratio = 2:1.

In a typical preparation,  $(\text{Et}_4\text{N}^+)_2\text{PbCl}_6^{2-}$  and  $(\text{Et}_4\text{N}^+)_2\text{PbF}_6^{2-}$  were loaded into a 10 mm glass tube in the dry box. The sample was removed from the dry box, evacuated and dry  $\text{CH}_3\text{CN}$  distilled onto the reagents at  $-196^\circ\text{C}$ . The reaction was then allowed to warm to room temperature. The reaction proceeded very quickly and after 20 min., a clear light brown solution was obtained. The tube was evacuated at  $-196^\circ\text{C}$ . The tube was removed from the vacuum line, placed in a glove bag, and a portion of the sample from the 10 mm glass tube, was pipetted into a 5 mm glass NMR tube. The glass tubes were flame sealed under vacuum and stored in the dark in the refrigerator.

#### D) Reagents for preparation of $\text{OTeF}_5$ derivatives

##### Preparation of $\text{HOTeF}_5$

The  $\text{HOTeF}_5$  was prepared according to equation (14).



Several attempts were made to prepare pure  $\text{HOTeF}_3$  in good yield. The general method used is described by Sladky.<sup>31</sup> The initial preparations utilized pure, distilled  $\text{HSO}_3\text{F}$  and  $(\text{HO})_6\text{Te}$ , vacuum dried at  $120^\circ\text{C}$ , but these only lead to very poor yields of  $\text{HOTeF}_3$ . The preparation was then repeated using commercial crude  $\text{HSO}_3\text{F}$ . Finely ground  $(\text{HO})_6\text{Te}$  (70.1307 g, 0.3054 mol) was loaded into the reaction bulb through port E (see Figure 4). The glass cap was sealed onto port E with Halocarbon wax, and the vessel attached to a glass vacuum line by a Telfon union and tubing connected to the valve at port D. The reaction vessel was evacuated overnight; then pressurized with 1 atm dry  $\text{N}_2$ . The receiving vessel was attached to the end of the condenser at port C and a dry  $\text{N}_2$  flush was passed through port D and out through port B. The  $\text{HSO}_3\text{F}$  (122.58 mL, 2.1377 mol) was added to a dropping buret in a glove bag. The glass cap on E was removed and the buret installed. The 500 mL reaction bulb was immersed in a dry ice/acetone bath, and when cold, the  $\text{HSO}_3\text{F}$  was added at a moderately fast rate with constant stirring. After addition was complete, the buret was removed and the cap replaced on port E. The dry ice/acetone bath removed and stirring continued while the reaction vessel was allowed to reach room temperature. Simultaneously, the  $\text{N}_2$  flush was moved to port A from port D. At this point, the reaction mixture was a thick white solution. The upper glass cup was filled with a dry ice/acetone slush to prevent escape of volatile  $\text{Te(VI)}$  compounds. The reaction flask was then heated with a heating mantle and a J-cloth was wrapped

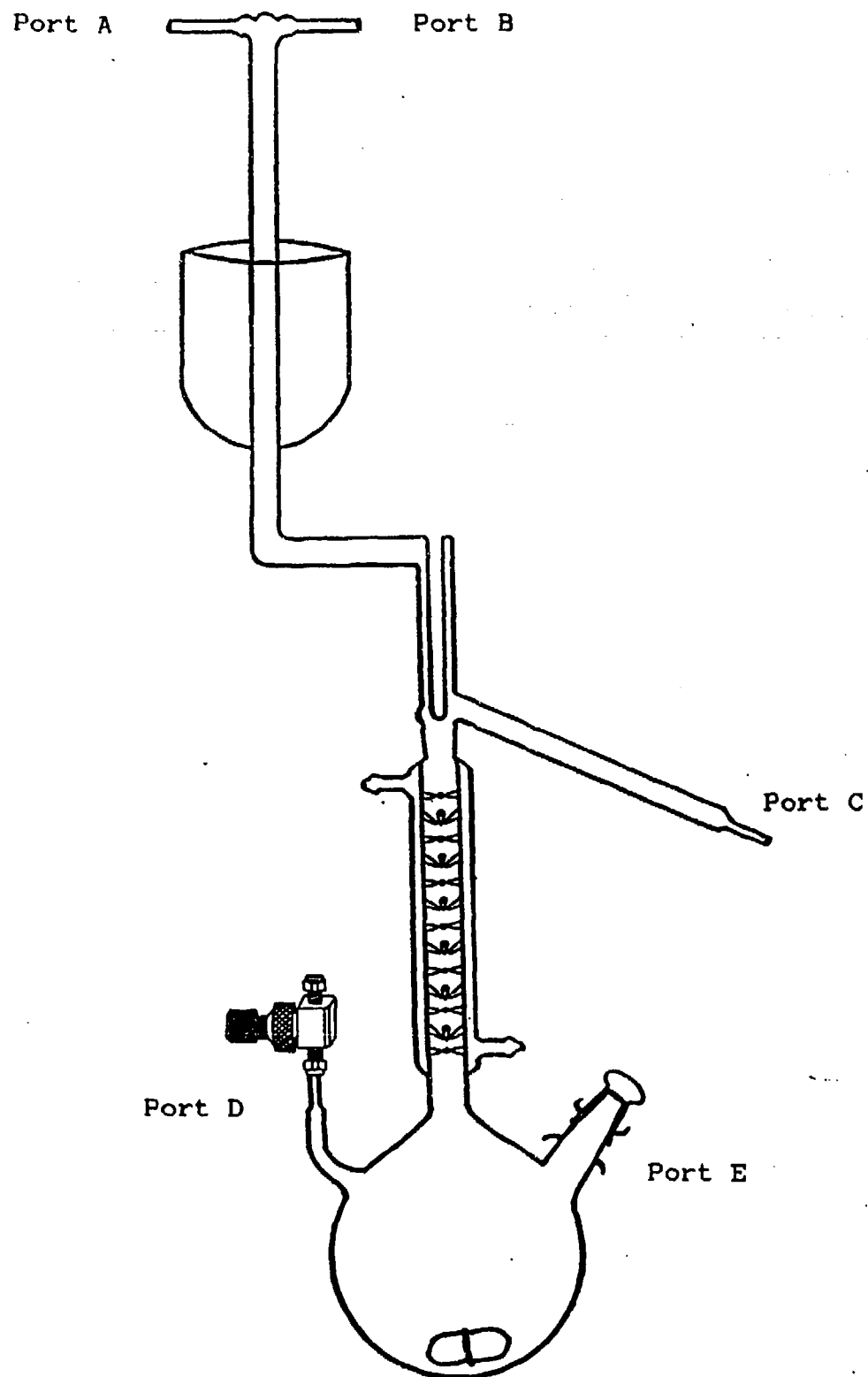


Figure 4. Apparatus for HOTEfs Preparation

around the condenser and secured with two pieces of wire. When reflux started, the solution became clear. The reaction flask was wrapped with glass wool, and the J-cloth soaked with liquid  $N_2$ . The first distillation fraction began at  $30^\circ C$  and at  $40^\circ C$  the reaction mixture became cloudy. The crude  $HO\text{TeF}_6$  collected in the cold condenser arm. When sufficient solid had collected, the J-cloth was removed, the valve to the receiving vessel opened, and the solid melted with a heat gun. After the clear, viscous liquid had run into the receiving vessel, the valve was closed and the J-cloth replaced on the condenser and soaked with liquid  $N_2$ . This process was repeated for 1 hour, until the temperature reached  $100^\circ C$  and the distillation halted. The crude  $HO\text{TeF}_6$  was distilled in vacuo from the receiving vessel into a sublim器, (see Figure 5), containing a three-fold excess by weight of concentrated  $H_2SO_4$  (96%, 125 mL) at  $-196^\circ C$ . The sublim器 was removed from the vacuum line and immersed in a hot oil bath in the fume hood. The cold finger was cooled by passing a rapid flow of cold water through it. The sublimation was performed at  $100-145^\circ C$  overnight. The  $HO\text{TeF}_6$  was distilled from the sublim器 on a metal vacuum line into a dry, preweighed, FEP tube equipped with a Kel-F valve. The yield of pure  $HO\text{TeF}_6$  was 81% (58.5378 g).



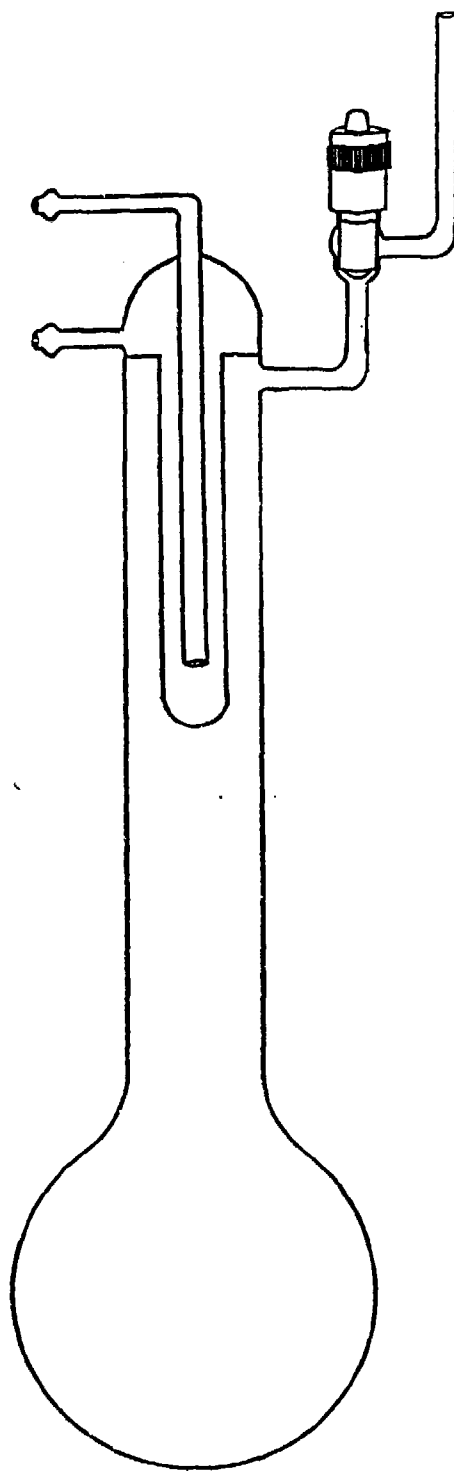


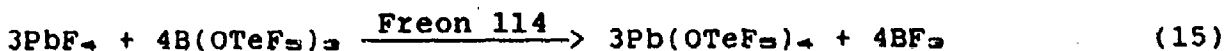
Figure 5. Sublimier for  $\text{HOTeF}_5$  Purification

## E) Preparation of OTeF<sub>3</sub> derivatives

### 1) Preparation of Pb(OTeF<sub>3</sub>)<sub>4</sub>

#### Reaction of PbF<sub>4</sub> with B(OTeF<sub>3</sub>)<sub>3</sub>

The reaction was performed according to equation (15).



The PbF<sub>4</sub> (0.5055 g, 1.7850 mmol) was loaded in the dry box into the arm of a dry H-vessel that contained a magnetic stirring bar. The B(OTeF<sub>3</sub>)<sub>3</sub> (1.7850 g, 2.4567 mmol) was weighed into a glass funnel and, with the use of a hair dryer, transferred into the opposite arm of the H-vessel. The vessel was evacuated on a metal vacuum line and Freon 114 distilled onto B(OTeF<sub>3</sub>)<sub>3</sub>. The mixture was allowed to warm to room temperature. When the B(OTeF<sub>3</sub>)<sub>3</sub> had dissolved, the solution was decanted onto the PbF<sub>4</sub> at -78°C. The reaction mixture was cooled in an ice bath and stirred. The reaction progressed slowly, with the formation of a light yellow solid in a clear liquid, and after 4 hours, the vessel was evacuated. The reaction appeared to be incomplete as judged from the amount of gas released. The reaction was continued for two weeks with intermittent evacuation of the vessel. The reaction was then halted and the solvent pumped off under vacuum. The light yellow solid was pumped to dryness, and transferred into an FEP storage vessel in the dry box. A Raman sample was made in a 1/4 inch glass tube and stored at -196°C.

#### Reaction of PbF<sub>4</sub> with HOTeF<sub>5</sub>

The reaction was performed according to equation (16).

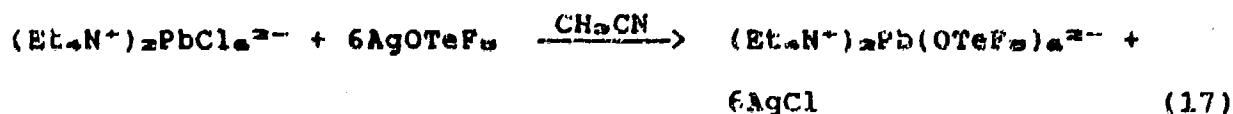


The PbF<sub>4</sub> (0.2424 g, 0.8560 mmol) was loaded into a dry 1/4 inch FEP tube in the dry box. The HOTeF<sub>5</sub> (0.8203 g, 3.4238 mmol) was vacuum distilled onto the PbF<sub>4</sub> at -196°C and the tube warmed to reach room temperature. There was no apparent reaction at room temperature: the PbF<sub>4</sub> remained at the bottom of the tube, with the HOTeF<sub>5</sub> as a vitrified solid on top. When warmed with a hot water bath, the HOTeF<sub>5</sub> melted but no interaction between the two reagents occurred. The experiment was halted and the product was not characterized further.

#### 11) Preparation of (Et<sub>4</sub>N<sup>+</sup>)<sub>2</sub>Pb(OTeF<sub>5</sub>)<sub>4</sub><sup>2-</sup>

##### Reaction of (Et<sub>4</sub>N<sup>+</sup>)<sub>2</sub>PbCl<sub>4</sub><sup>2-</sup> with AgOTeF<sub>5</sub>

The (Et<sub>4</sub>N<sup>+</sup>)<sub>2</sub>Pb(OTeF<sub>5</sub>)<sub>4</sub><sup>2-</sup> salt was prepared according to equation (17).

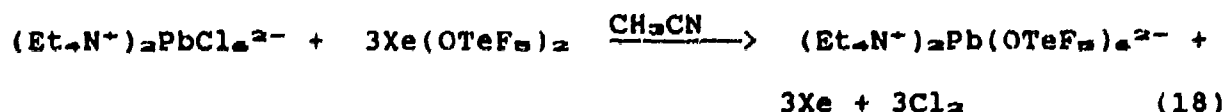


In a typical preparation, (Et<sub>4</sub>N<sup>+</sup>)<sub>2</sub>PbCl<sub>4</sub><sup>2-</sup> (1.7541 g, 2.5779 mmol) and AgOTeF<sub>5</sub> (5.1983 g, 1.5004 mmol) were placed in

the arm of the H-vessel containing a magnetic stir bar (see Figure 3). The H-vessel was attached to a metal vacuum line and evacuated. Dry  $\text{CH}_3\text{CN}$  was distilled onto the reagents at  $-196^\circ\text{C}$ . The reaction mixture was allowed to warm slowly to room temperature with stirring and periodic immersion in a  $-78^\circ\text{C}$  bath. During warming, the reaction turned a series of different colours: yellow, brown, brown-purple, red then finally, to light green. The vessel was covered to prevent ingress of light. At room temperature, the solution turned a pale green and off-white  $\text{AgCl}$  was formed. The reaction was allowed to proceed overnight. The stirring was halted and the precipitate allowed to settle. The tube was placed on the vacuum line and evacuated at  $-196^\circ\text{C}$ . The clear, pale green solution was then carefully decanted, through the medium sintered frit into the opposite arm of the H-vessel at  $-78^\circ\text{C}$ . Further extraction of the product from the  $\text{AgCl}$  solid layer was achieved by distilling  $\text{CH}_3\text{CN}$  back through the frit onto the  $\text{AgCl}$  solid at  $-78^\circ\text{C}$ , allowing the solid to settle and decanting the solution back through the frit to the opposite arm of the H-vessel. The vessel was placed in a glove bag, and the solution pipetted into 10 mm and 5 mm glass NMR tubes. The tubes were flame sealed in vacuum at  $-196^\circ\text{C}$  and stored in the refrigerator in the dark.

#### Reaction of $(\text{Et}_4\text{N}^+)_2\text{PbCl}_4^{2-}$ with $\text{Xe}(\text{OTeF}_5)_2$

A solution of the  $(\text{Et}_4\text{N}^+)_2\text{Pb}(\text{OTeF}_5)_4^{2-}$  salt in  $\text{CH}_3\text{CN}$  was prepared according to equation (18).



Sample solutions were prepared in situ in both 10 mm and 5 mm glass NMR tubes, equipped with Kel-F valves. In a typical preparation,  $(\text{Et}_4\text{N}^+)_2\text{PbCl}_6^{2-}$  (0.1809 g, 0.2659 mmol) was loaded into a 10 mm glass NMR tube in the dry box, cooled to  $-196^\circ\text{C}$ , and  $\text{Xe}(\text{OTeF}_5)_2$  (0.4853 g, 0.7976 mmol) added. The sample was removed from the dry box and maintained at  $-196^\circ\text{C}$ . The tube was attached to a metal vacuum line, evacuated, and dry  $\text{CH}_3\text{CN}$  was distilled onto the reagents at  $-196^\circ\text{C}$ . The tube was opened to an isolated section of the vacuum line at a pressure of ca. 1 atm. of dry  $\text{N}_2$ . The reaction was allowed to warm to  $-10^\circ\text{C}$ . Vigorous bubbling occurred and the solid,  $(\text{Et}_4\text{N}^+)_2\text{PbCl}_6^{2-}$ , dissolved to give a pale green solution. When gas evolution had ceased, the sample was cooled to  $-78^\circ\text{C}$  and the Xe gas pumped away. The sample was flame sealed in vacuum at  $-196^\circ\text{C}$  and stored at  $-196^\circ\text{C}$ .

### Instrumentation

#### Nuclear Magnetic Resonance Spectroscopy

Two different tubes were used for the NMR samples depending on the nucleus under investigation:

<u>Nucleus</u>	<u>Sample Tube Type and Dimensions</u>
$^{19}\text{F}$	Wilmad 5 mm o.d. medium wall glass tube
$^{207}\text{Pb}$	Wilmad 10 mm o.d. thin wall precision glass tube

Spectra were recorded unlocked (field drift  $<0.1$  Hz/hr) on Bruker WM-250 and AM-500 instruments equipped with superconducting magnets operating at 5.8719 T and 11.744 T, respectively. Fluorine-19 spectra were recorded on 5 mm dual  $^1\text{H}/^{19}\text{F}$  probes. Lead-207 spectra were recorded on 10 mm VSP probes broad-banded over the frequency ranges 23-103 MHz and 46-206 MHz, respectively. Typical acquisition parameters are summarized in Table 1. NMR spectra were referenced externally at 24°C using the following neat reference substances:  $\text{CFCl}_3$  ( $^{19}\text{F}$ ), and  $\text{Pb}(\text{CH}_3)_4$  ( $^{207}\text{Pb}$ ). The number of scans obtained varied with each sample, with  $^{19}\text{F}$  spectra generally requiring 500-2000 scans and  $^{207}\text{Pb}$  spectra requiring between 75,000 and 200,000 scans for a sufficiently good signal/noise ratio.

#### Laser Raman Spectroscopy

All Raman spectra were obtained from solid samples in sealed glass tubes (1/4 inch o.d.). A Coherent Nova 90-5 argon ion laser, providing up to 5W at 514.5 nm was used as the excitation source in combination with a Spex Industrial Model 14018 double monochromator equipped with 1800-grooves/mm holographic grating. The spectra were accumulated using a RCA C 31034 phototube detector in conjunction with a pulse count system (Hamner NA11)

Table 1: Typical NMR acquisition parameters

	<sup>19</sup> F		<sup>207</sup> Pb	
	WM 250	AM 500	WM 250	AM 500
Magnetic Flux Density (T)	5.8719	11.744	5.8719	11.744
Resonance Frequency (MHz)	235.361	470.599	52.330	104.632
Memory Size (K)	32	64	32	64
Spectral Width (KHz)	38	83	29	36
Data Point Resolution (Hz)	2.3	2.5	1.8	1.1
Acquisition time (s)	0.426	0.393	0.557	0.918
Pulse Width (≈90°, μs)	1	1	1	1
Relaxation Delay	0.0	0.0	0.0	0.0

consisting of a pulse amplifier analyzer (Hamner NC-11), and a rate meter (Hamner N-708 A). Spectra were recorded using a Texas Instruments Model FSOZWBA strip chart recorder. Slit widths were set to 150, 200, 200, 150 mμ and all spectra were recorded at a chart speed of 0.5 cm<sup>-1</sup>/s. The gains ranged between 10K and 100K with a time constant of 1.0 s and the approximate power of the beam at the sample ranged from 0.50 to 1.00W.

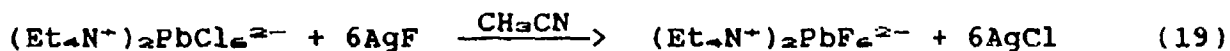
Sample tubes were mounted vertically in an unsilvered Pyrex glass Dewar such that the angle between the incident beam and the sample was 45°. All spectra were run at -196°C.



## Results and Discussion

### Synthesis and Characterization of the $[\text{PbF}_6]^{2-}$ Anion

The successful synthesis of a  $\text{PbF}_6^{2-}$  salt with an organic cation was achieved by the reaction of  $(\text{Et}_4\text{N}^+)_2\text{PbCl}_6^{2-}$  with  $\text{AgF}$  according to equation (19).



The colourless, highly moisture sensitive, crystalline solid obtained was characterized from its  $^{19}\text{F}$  and  $^{207}\text{Pb}$  NMR spectra in  $\text{CH}_3\text{CN}$  solution. The  $^{19}\text{F}$  NMR spectrum (Figure 6) consisted of a sharp singlet ( $\delta(^{19}\text{F}) = -103.8$ ) flanked by satellites due to  $^{207}\text{Pb}$  ( $I = 1/2$ , natural abundance = 22.6%) with a coupling constant,  $^1J(^{207}\text{Pb}-^{19}\text{F}) = 3331 \text{ Hz}$ . The  $^{207}\text{Pb}$  NMR spectrum (Figure 7) displayed the expected 1:6:15:20:15:6:1 binomial septet at  $\delta(^{207}\text{Pb}) = -1978.9 \text{ ppm}$ . The coupling constant,  $^1J(^{207}\text{Pb}-^{19}\text{F}) = 3331 \text{ Hz}$ , was in excellent agreement with that measured from the  $^{19}\text{F}$  NMR spectrum.

Prior studies of the potassium salt of the  $[\text{PbF}_6]^{2-}$  anion by X-ray powder diffraction, infrared spectroscopy,<sup>11</sup> and Raman spectroscopy,<sup>12</sup> demonstrated that the anion had an octahedral structure in the solid state. The  $^{19}\text{F}$  NMR spectrum of a solution of  $\text{K}_2\text{HPbF}_6$  in 20% HF consisted of a single broad line, indicating that rapid fluorine exchange was occurring, and consequently no conclusions about the structure of the  $[\text{PbF}_6]^{2-}$  anion in

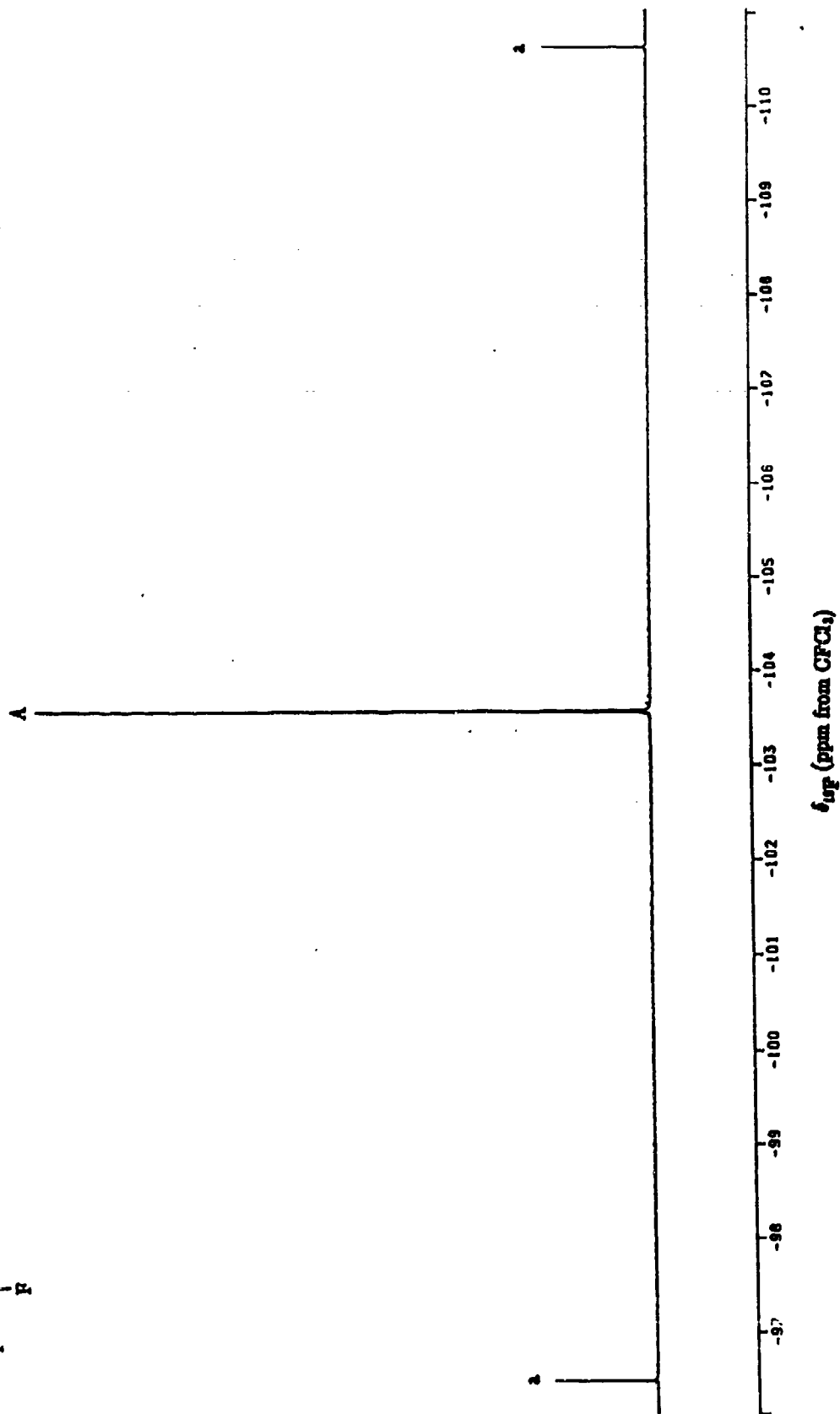
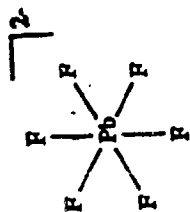


Figure 6.  $^{19}\text{F}$  NMR Spectrum (470.599 MHz) of  $0.7\text{M } (\text{Et}_4\text{N})_2\text{PbF}_2$  in dry  $\text{CH}_3\text{CN}$  at room temperature. (a) denotes  $^{207}\text{Pb}$  satellites.

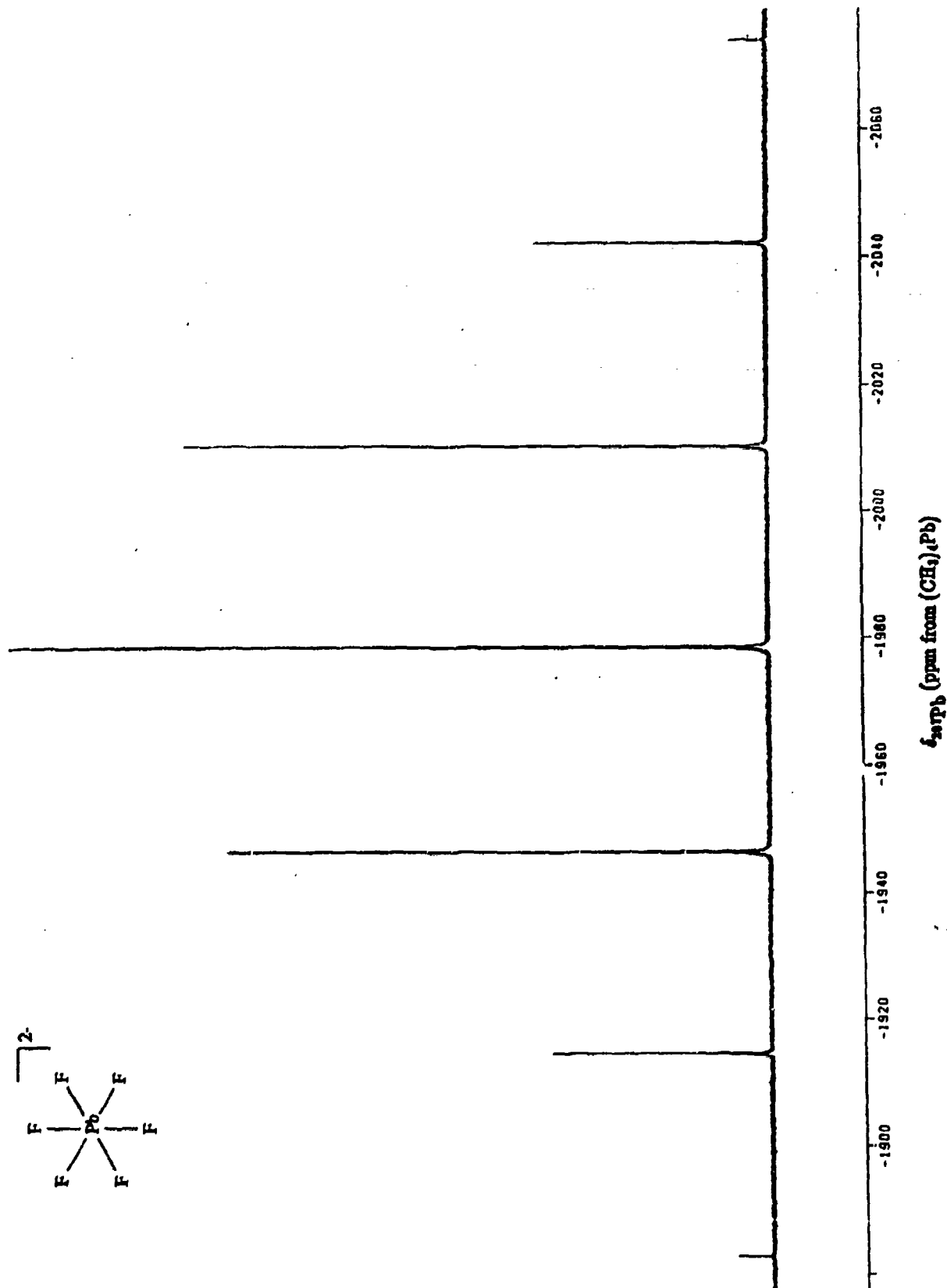
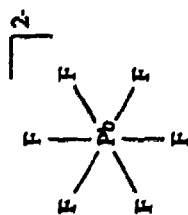
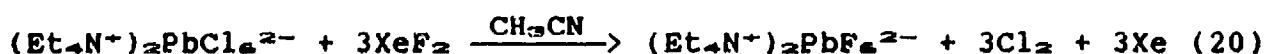


Figure 7.  $^{207}\text{Pb}$  NMR Spectrum (104.632 MHz) of 0.1M  $(\text{Et}_4\text{N})_2\text{PbF}_6$  in dry  $\text{CH}_3\text{CN}$  at room temperature.

solution could be drawn.<sup>12</sup> The observed singlet in the  $^{19}\text{F}$  NMR spectrum and the binomial septet in the  $^{207}\text{Pb}$  NMR spectrum of  $(\text{Et}_4\text{N}^+)_2\text{PbF}_6^{2-}$  in  $\text{CH}_3\text{CN}$  confirms the presence of the octahedral  $[\text{PbF}_6]^{2-}$  anion in solution.

Several other approaches to the synthesis of  $[\text{PbF}_6]^{2-}$  salts with organic ( $\text{R}_4\text{N}^+$ ,  $\text{R} = \text{C}_2\text{H}_5$  or  $n\text{-C}_4\text{H}_9$ ) cations were also investigated, however none of them was successful in producing a pure salt.

The reaction of  $(\text{Et}_4\text{N}^+)_2\text{PbCl}_6^{2-}$  with  $\text{XeF}_2$  in  $\text{CH}_3\text{CN}$  was performed according to equation (20).

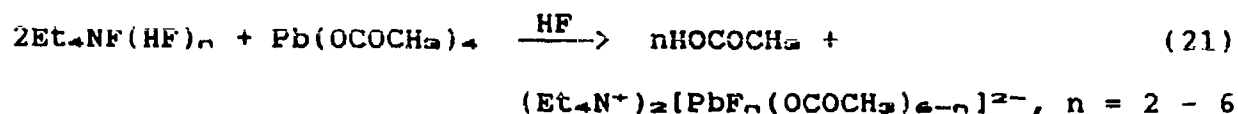


The reaction of  $(\text{Et}_4\text{N}^+)_2\text{PbCl}_6^{2-}$  with  $\text{XeF}_2$  in a 1:3 mole ratio produced a clear light green solution with some yellow insoluble material after a 7 hour reaction time. The reaction of  $(\text{Et}_4\text{N}^+)_2\text{PbCl}_6^{2-}$  with a 1:1.5 mole ratio of  $\text{XeF}_2$  produced, after 9 hours, a pale green clear solution with some yellow insoluble material. The  $^{207}\text{Pb}$  and  $^{19}\text{F}$  NMR spectra revealed that the reaction did not go to completion within 7-9 hours, and that a mixture of  $[\text{PbCl}_n\text{F}_{6-n}]^{2-}$ ,  $n = 0 - 5$ , was produced (see later discussion). The presence of some  $[\text{PbF}_6]^{2-}$  was revealed by the observation of a sharp singlet, flanked by  $^{207}\text{Pb}$  satellites, at  $\delta = -104.3$  ppm in the  $^{19}\text{F}$  NMR spectrum and a corresponding septet ( $^1J(^{207}\text{Pb}-^{19}\text{F}) = 3346$  Hz) at  $\delta = -1980.8$  ppm in the  $^{207}\text{Pb}$  spectrum.

Initial attempts to prepare a salt of the  $[\text{PbF}_n]^{2-}$  anion containing an organic cation involved the reaction of  $\text{XeF}_2$  and  $[(n\text{-Bu})_4\text{N}^+]_2[\text{PbCl}_6]^{2-}$  in dry  $\text{CH}_3\text{CN}$ . The reaction produced a large amount of white precipitate suspended in a cloudy solution. The white precipitate was thought to be the result of attack by  $\text{XeF}_2$  on the cation,  $n\text{-C}_4\text{H}_9$ , or on  $\text{CH}_3\text{CN}$ . The  $^{207}\text{Pb}$  NMR spectrum of the solution revealed that the reaction did not go to completion and that a mixture of  $[\text{PbCl}_{6-n}\text{F}_n]^{2-}$ ,  $n = 0 - 2$ , was produced.

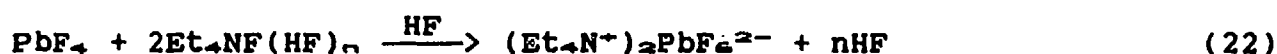
The reaction of an excess of  $\text{XeF}_2$  (1:5 mole ratio) with  $(\text{Et}_4\text{N}^+)_2\text{PbCl}_6^{2-}$  in anhydrous HF was attempted in the hope that the reaction would be driven to completion in this medium. However, the resulting product was an intractable suspension of a white solid in a light beige viscous liquid. The nature of the product indicated it was a mixture of  $\text{PbF}_4$  or  $\text{PbF}_2$  and  $\text{Et}_4\text{N}^+\text{F}(\text{HF})_n$  and was not characterized further. Lead(II) fluoride could possibly arise from the oxidation of HCl by Pb(IV) yielding Pb(II).

The reaction of  $\text{Pb}(\text{OCOCH}_3)_4$  with HF has been reported to give the partially substituted product  $\text{PbF}_2(\text{OCOCH}_3)_2$ .<sup>33</sup> In view of this, the solvolysis of  $\text{Pb}(\text{OCOCH}_3)_4$  in HF in the presence of  $\text{Et}_4\text{N}^+\text{F}(\text{HF})_n$  was carried out in hope that the reaction would proceed according to equation (21).



The product obtained from the reaction was a suspension of a white solid in a light beige viscous liquid. Separation of the liquid fraction and subsequent pumping in vacuo resulted in the formation of a white solid. The two solid products, (HF soluble and HF insoluble) were analysed by Raman spectroscopy. The Raman spectrum of the HF insoluble solid displayed one weak peak at  $532\text{ cm}^{-1}$  in the Pb-F stretching region. The Raman spectrum of the HF soluble solid did not give any discernable peaks.

The reaction of  $\text{BiF}_3$  with  $\text{Et}_4\text{NF}(\text{HF})_n$  in HF gives  $\text{Et}_4\text{NBiF}_6$  in quantitative yield.<sup>34</sup> It therefore seemed reasonable to attempt the preparation of  $(\text{Et}_4\text{N}^+)_2\text{PbF}_6^{2-}$  by the corresponding reaction with  $\text{PbF}_4$  according to equation (22).



However, the product obtained was not the expected dry white crystalline solid, but an involatile viscous white suspension, which was not amenable to further characterization. The reason for failure of this reaction may be due to the inertness of  $\text{PbF}_4$ . This inertness may be a consequence of the  $\text{PbF}_4$  being prepared by high temperature fluorination of  $\text{PbF}_2$ . Similar chemical unreactivity has been observed for other fluorides prepared by high temperature methods.<sup>32</sup> For example, it has been noted that a high temperature fluorination preparation of  $\text{FeF}_3$ , produced a compound that proved to be very unreactive. The preparation of the same compound using a low temperature reaction

with  $\text{KrF}_2$  yielded  $\text{FeF}_3$  in a chemically reactive form.

#### The Mixed Chlorofluoroplumbate(IV) Anions, $[\text{PbCl}_n\text{F}_{4-n}]^{2-}$

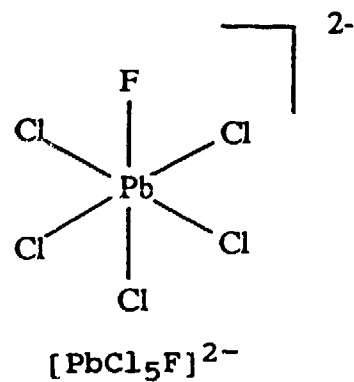
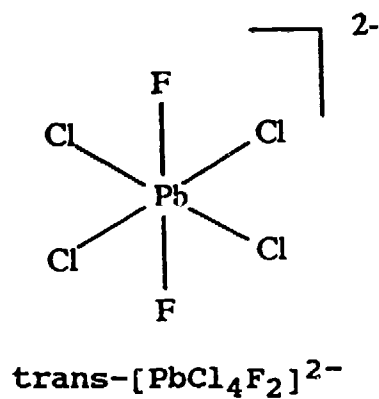
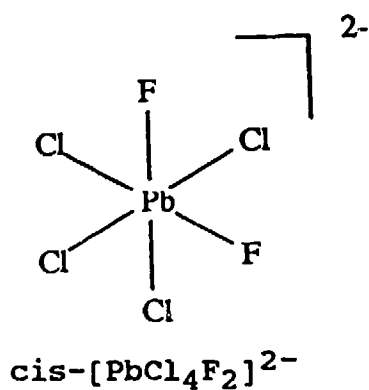
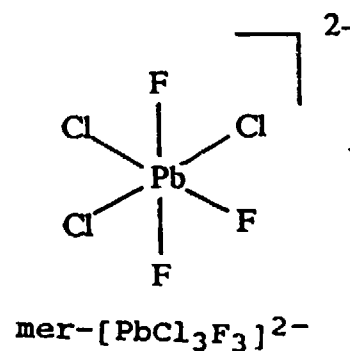
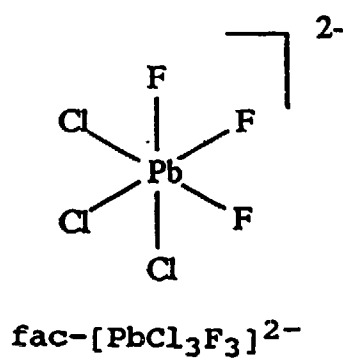
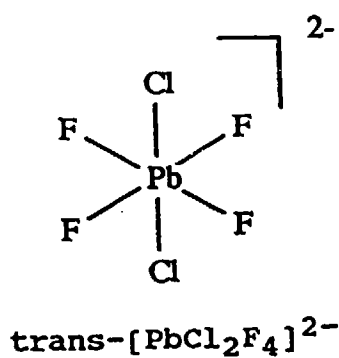
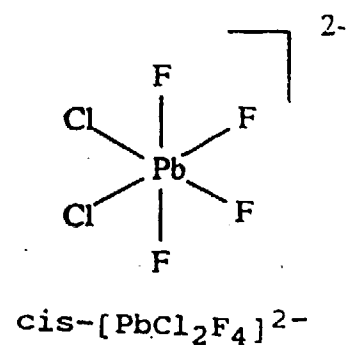
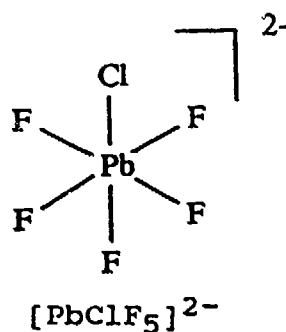
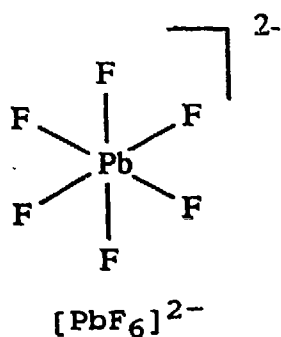
All ten possible species, including isomers, in the previously unknown  $[\text{PbCl}_n\text{F}_{4-n}]^{2-}$  series have been identified by  $^{19}\text{F}$  and  $^{207}\text{Pb}$  NMR spectroscopy as the products of the reaction of  $(\text{Et}_4\text{N}^+)_2\text{PbCl}_4^{2-}$  with  $\text{XeF}_2$  in  $\text{CH}_3\text{CN}$ . The idealized structures of these anions are depicted in Figure 8.

The same species were also readily generated by facile Cl/F ligand redistribution reactions between  $(\text{Et}_4\text{N}^+)_2\text{PbF}_6^{2-}$  and  $(\text{Et}_4\text{N}^+)_2\text{PbCl}_4^{2-}$  in  $\text{CH}_3\text{CN}$  at ca 40°C. All ten possible anions were again identified by  $^{19}\text{F}$  and  $^{207}\text{Pb}$  NMR spectroscopy (Figures 9 - 15). The distribution of the products could be weighted to give mainly fluorine-rich or chlorine-rich anions, depending on the ratio of  $\text{PbCl}_4^{2-}$  to  $\text{XeF}_2$  or  $\text{PbF}_6^{2-}$ . The solubility of the chlorine-rich  $\text{Et}_4\text{N}^+$  salts was markedly less than the fluorine-rich salts and consequently resulted in the observation of relatively low intensities for these species in the  $^{19}\text{F}$  and  $^{207}\text{Pb}$  NMR spectra.

The  $^{19}\text{F}$  and  $^{207}\text{Pb}$  NMR data for the  $[\text{PbCl}_n\text{F}_{4-n}]^{2-}$  anions are collected in Tables 2 and 3, respectively.

Mixed chlorofluoro species of the type  $[\text{MCl}_n\text{F}_{4-n}]^{m-}$ , where M = a p-block or transition element, are known for several p-block and transition elements. In many cases, structural characterization and insight into the bonding in such species has been obtained from  $^{19}\text{F}$  NMR studies, as well as from

Figure 8. Geometric Isomers for the  $[\text{PbCl}_n\text{F}_{6-n}]^{2-}$  Anions





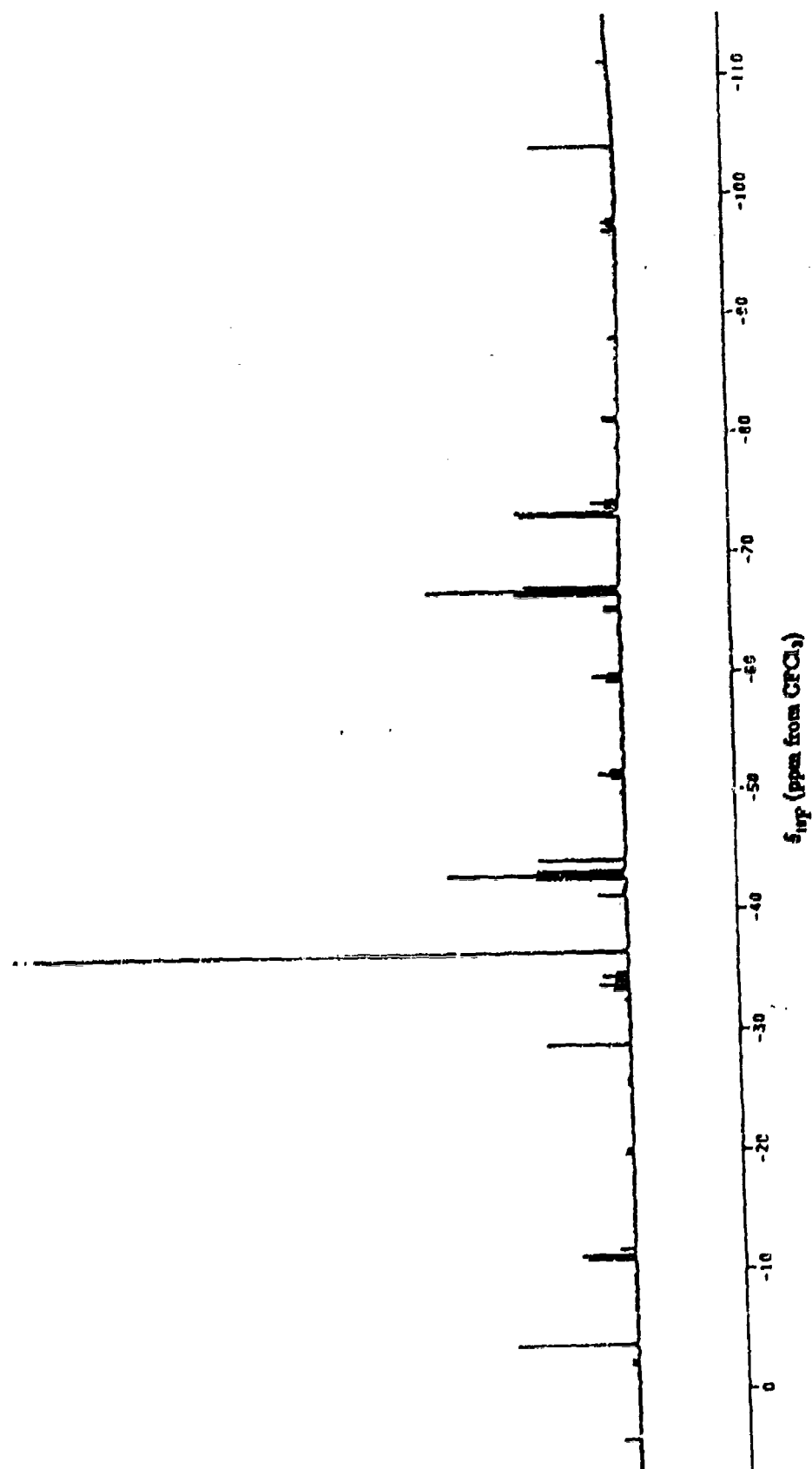


Figure 9.  $^{19}\text{F}$  NMR Spectrum (235.361 MHz) of  $1(\text{Et}_4\text{N})_2\text{PbF}_6 : 1(\text{Et}_4\text{N})_2\text{PbF}_6$  in dry  $\text{CH}_3\text{CN}$  at room temperature.

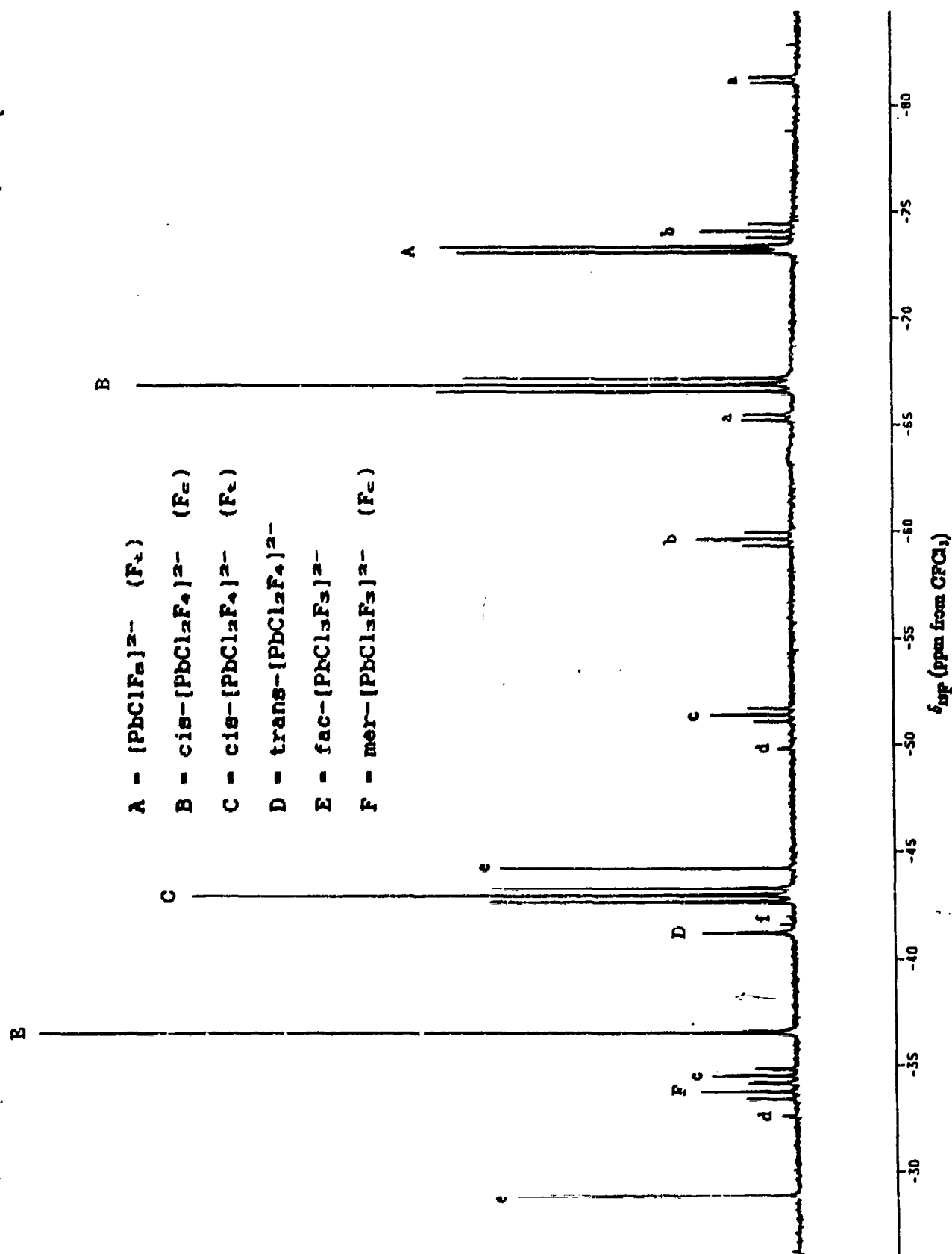


Figure 10.  $^{19}\text{F}$  NMR spectrum (235.361 MHz) of  $6(\text{Et}_4\text{N})_2\text{PbF}_6$  in dry  $\text{CH}_3\text{CN}$  at room temperature. Lower case letters denote  $^{207}\text{Pb}$  satellites.

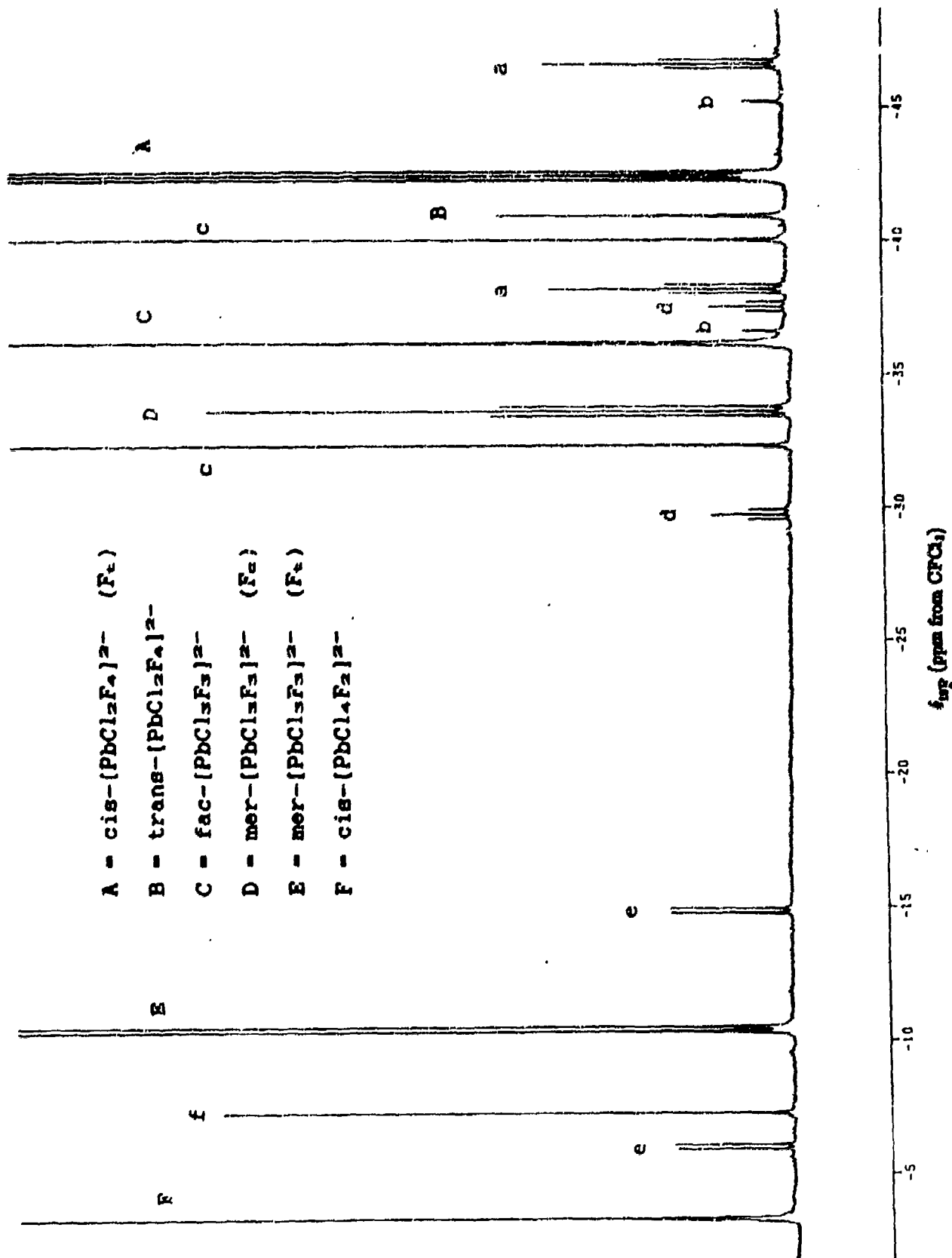


Figure 11.  $^{19}\text{F}$  NMR Spectrum (470.599 MHz) of  $1(\text{Et}_4\text{N})_2\text{PbF}_6 : 2(\text{Et}_4\text{N})_2\text{PbF}_6$  in dry  $\text{CH}_3\text{CN}$  at room temperature. Lower case letters denote  $^{207}\text{Pb}$  satellites.

- A - mer-[PbCl<sub>3</sub>F<sub>3</sub>]<sup>2-</sup> (F<sub>2</sub>)  
 B - cis-[PbCl<sub>4</sub>F<sub>2</sub>]<sup>2-</sup>  
 C - trans-[PbCl<sub>4</sub>F<sub>2</sub>]<sup>2-</sup>  
 D - [PbCl<sub>6</sub>F]<sup>2-</sup>

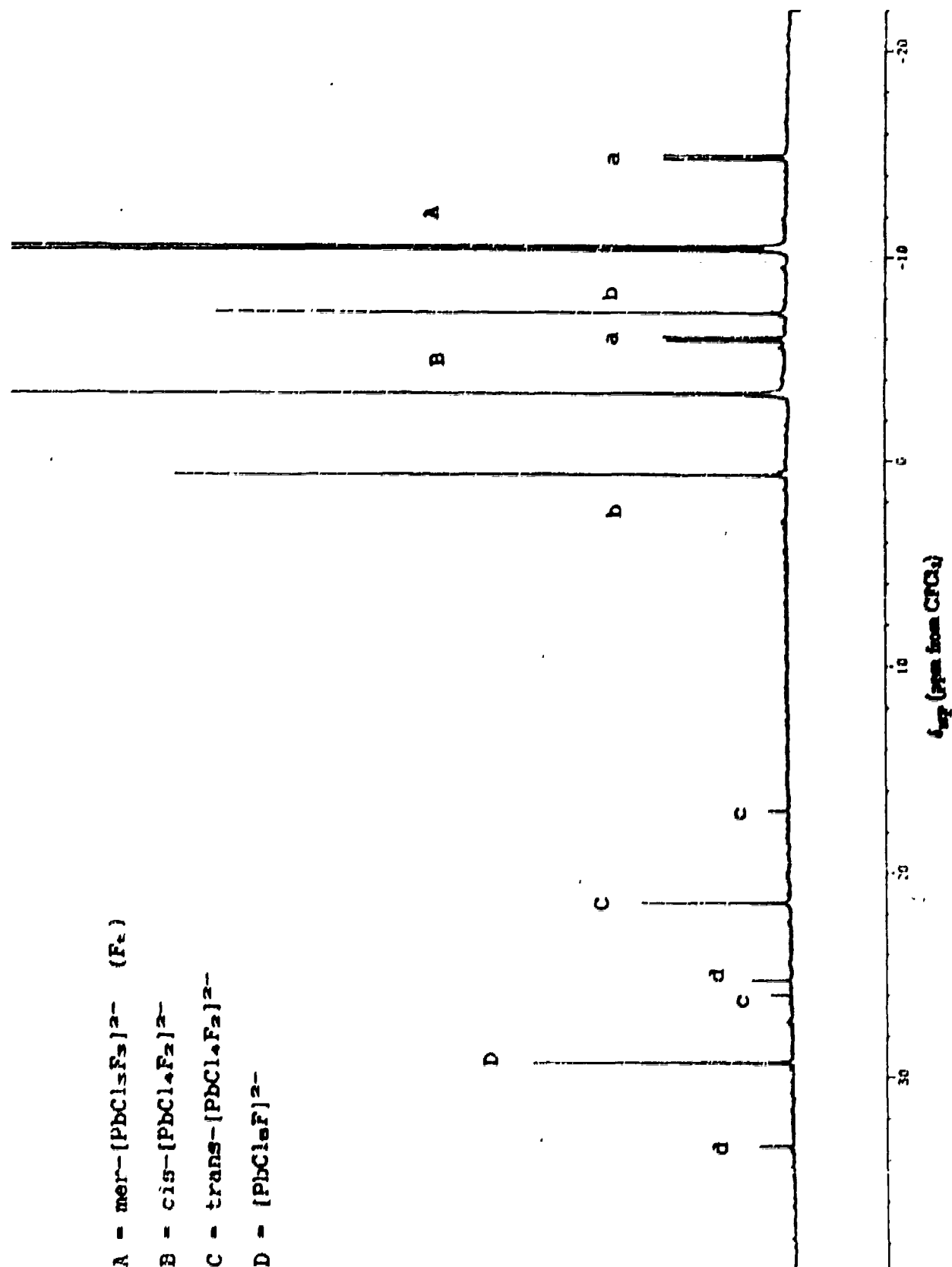


Figure 12. <sup>19</sup>F NMR Spectrum (470.599 MHz) of 1(Et<sub>4</sub>N)<sub>2</sub>PbF<sub>6</sub> : 2(Et<sub>4</sub>N)<sub>2</sub>PbF<sub>6</sub> in dry CH<sub>3</sub>CN at room temperature. Lower case letters denote <sup>207</sup>Pb satellites.

A -  $[\text{PbF}_4]^{2-}$   
 B -  $[\text{PbClF}_3]^{2-} \text{ (F}_c\text{)}$   
 C -  $[\text{PbClF}_3]^{2-} \text{ (F}_e\text{)}$   
 D -  $\text{cis-}[\text{PbCl}_2\text{F}_2]^{2-} \text{ (F}_c\text{)}$   
 E -  $\text{cis-}[\text{PbCl}_2\text{F}_2]^{2-} \text{ (F}_e\text{)}$

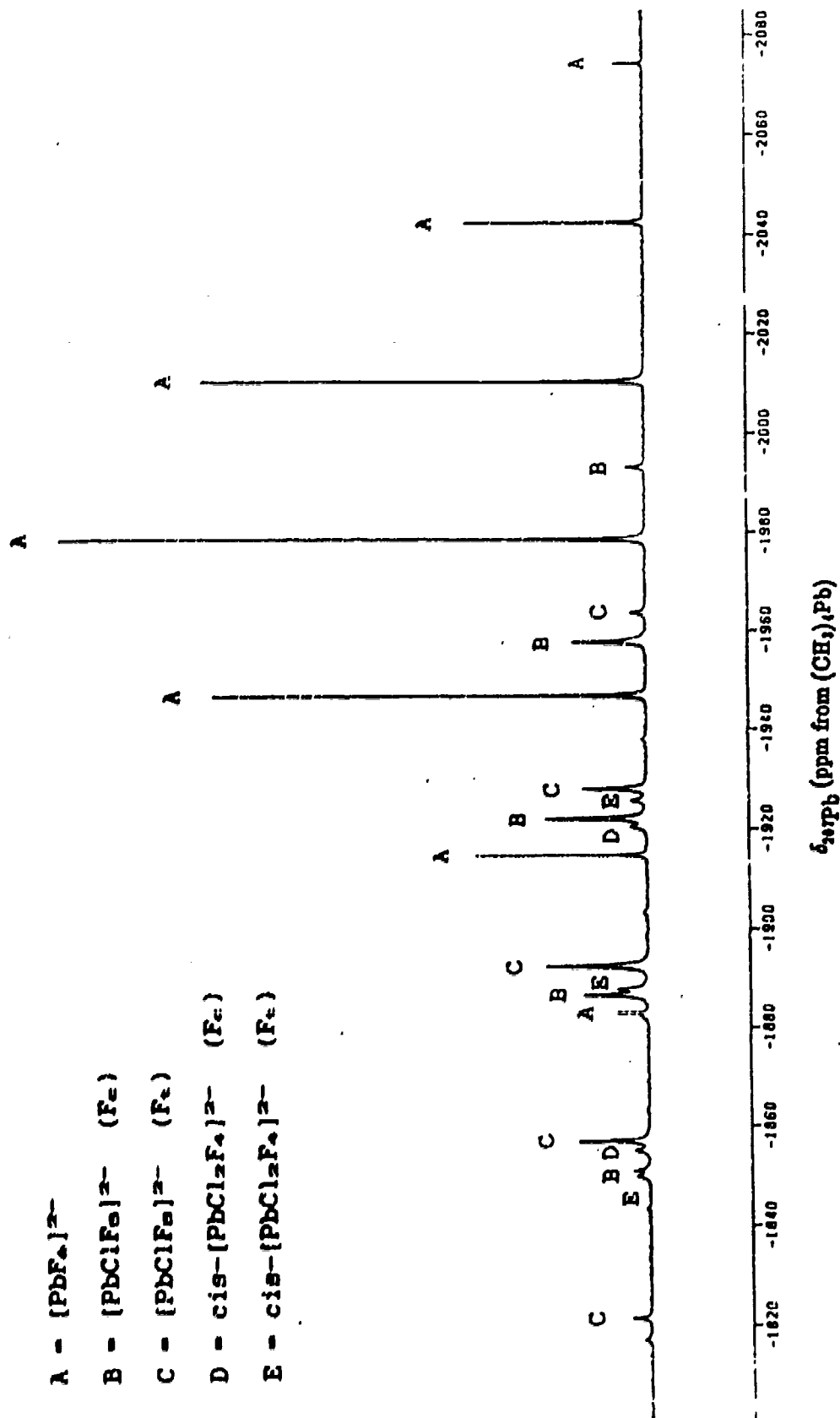


Figure 13.  $^{207}\text{Pb}$  NMR spectrum (104.599 MHz) of  $1(\text{Et}_4\text{N})_2\text{PbF}_6$  in dry  $\text{CH}_3\text{CN}$  at room temperature.

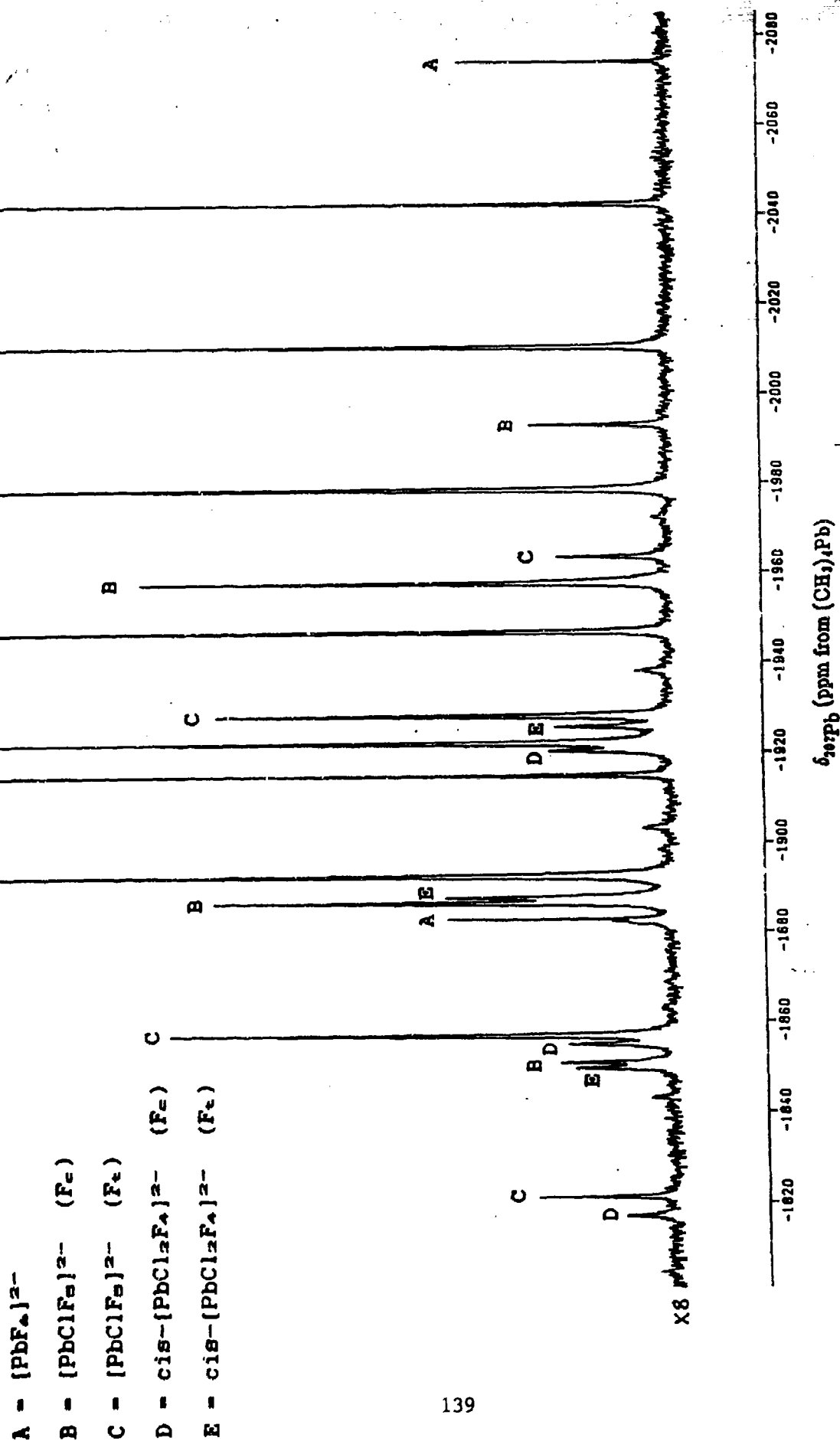


Figure 14.  $^{207}\text{Pb}$  NMR Spectrum (104.599 MHz) of  $6(\text{Et}_4\text{N})_2\text{PbF}_6 : 1(\text{Et}_4\text{N})_2\text{PbF}_6$  in dry  $\text{CH}_3\text{CN}$  at room temperature.

A -  $(\text{PbCl}_5\text{F})^{2-}$

B -  $\text{cis}-(\text{PbCl}_4\text{F}_2)^{2-}$

C -  $\text{trans}-(\text{PbCl}_4\text{F}_2)^{2-}$

D -  $\text{fac}-(\text{PbCl}_3\text{F}_3)^{2-}$

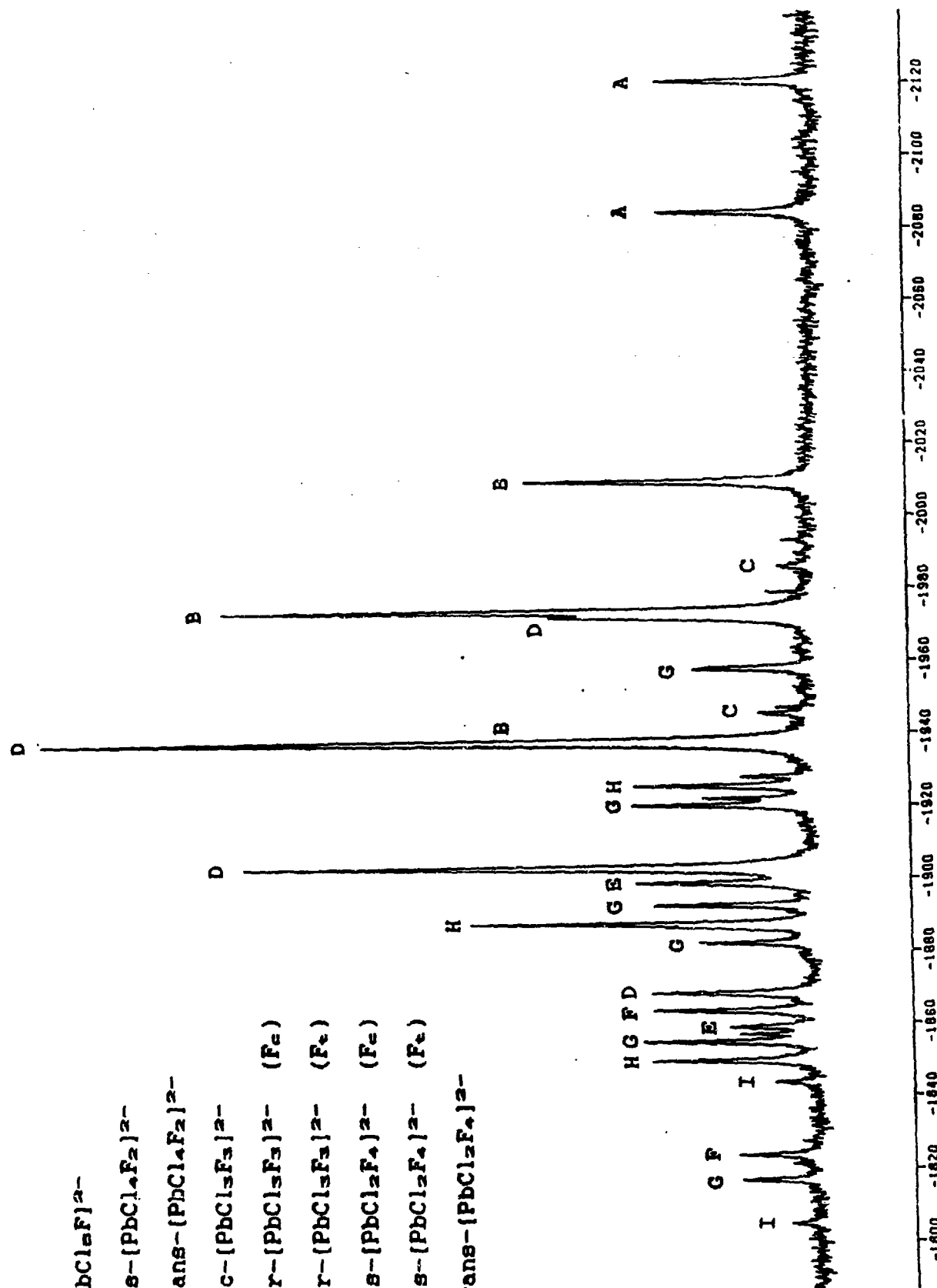
E -  $\text{mer}-(\text{PbCl}_3\text{F}_3)^{2-} (\text{F}_e)$

F -  $\text{mer}-(\text{PbCl}_3\text{F}_3)^{2-} (\text{F}_e)$

G -  $\text{cis}-(\text{PbCl}_2\text{F}_4)^{2-} (\text{F}_e)$

H -  $\text{cis}-(\text{PbCl}_2\text{F}_4)^{2-} (\text{F}_e)$

I -  $\text{trans}-(\text{PbCl}_2\text{F}_4)^{2-}$



$\delta_{\text{Pb}}$  (ppm from  $(\text{CH}_3)_4\text{Pb}$ )

Figure 15.  $^{207}\text{Pb}$  NMR spectrum (104.599 MHz) of  $1(\text{Et}_4\text{N})_2\text{PbF}_6 : 2(\text{Et}_4\text{N})_2\text{PbF}_6$  in dry  $\text{CH}_3\text{CN}$  at room temperature.

Table 2:  $^{19}\text{F}$  NMR data for the  $\text{PbCl}_n\text{F}_{6-n}^{2-}$ ,  $n = 0 - 5$ , anions

Anion <sup>b</sup>	$\delta(^{19}\text{F})^a$ ppm		Multiplicity	$J(\text{M}-^{19}\text{F})$ Hz	
	Obs.	[Calc.] <sup>c</sup>		$^{207}\text{Pb}$	$^{19}\text{F}$
$[\text{PbF}_6]^{2-}$	-103.8	[-104.0]	singlet	3331	—
$[\text{PbClF}_5]^{2-}$	$\text{F}_c^d$	-97.7	[-98.2]	quintet	3086
	$\text{F}_t$	-72.9	[-72.8]	doublet	3722
$c\text{-}[\text{PbCl}_2\text{F}_4]^{2-}$	$\text{F}_c$	-66.8	[-66.5]	triplet	3416
	$\text{F}_t$	-42.4	[-41.5]	triplet	3970
$t\text{-}[\text{PbCl}_2\text{F}_4]^{2-}$	$\text{F}_t$	-40.9	[-41.5]	singlet	4041
$f\text{-}[\text{PbCl}_3\text{F}_3]^{2-}$	$\text{F}_c$	-36.2	[-34.7]	singlet	3613
$m\text{-}[\text{PbCl}_3\text{F}_3]^{2-}$	$\text{F}_c$	-33.7	[-34.7]	triplet	3682
	$\text{F}_t$	-10.4	[-10.2]	doublet	4162
$c\text{-}[\text{PbCl}_4\text{F}_2]^{2-}$	$\text{F}_c$	-3.3	[-3.0]	singlet	3759
$t\text{-}[\text{PbCl}_4\text{F}_2]^{2-}$	$\text{F}_t$	21.5	[21.0]	singlet	4236
$[\text{PbCl}_5\text{F}]^{2-}$	$\text{F}_c$	29.3	[28.8]	singlet	3790

<sup>a</sup> ppm from  $\text{CFCl}_3$ . <sup>b</sup> Values for:  $[\text{PbF}_6]^{2-}$  and  $[\text{PbClF}_5]^{2-}$  from 0.1M  $6(\text{Et}_4\text{N}^+)\text{PbF}_6^{2-}$ ;  $1(\text{Et}_4\text{N}^+)\text{PbCl}_2^{2-}$  in  $\text{CH}_3\text{CN}$ ; remaining anions from 0.1M  $1(\text{Et}_4\text{N}^+)\text{PbF}_6^{2-}$ ;  $2(\text{Et}_4\text{N}^+)\text{PbCl}_2^{2-}$  in  $\text{CH}_3\text{CN}$ . <sup>c</sup> Calculated values from linear equation. <sup>d</sup>  $\text{F}_c$  = fluorine trans to chlorine,  $\text{F}_t$  = fluorine trans to fluorine



Table 3:  $^{207}\text{Pb}$  NMR data for the  $\text{PbCl}_n\text{F}_{6-n}^{2-}$ ,  $n = 0 - 6$ , anions

Anion <sup>a</sup>	$\delta(^{207}\text{Pb})^b$ ppm		Multiplicity	$^1J(^{207}\text{Pb}-^{19}\text{F})$ Hz
	Obs.	[Calc.] <sup>c</sup>		
$[\text{PbF}_6]^{2-}$	-1978.9	[-1978.9]	septet	3337
$[\text{PbClF}_5]^{2-}$	$\text{F}_\text{tr}$ <sup>d</sup>		doublet	3087
	$\text{F}_\text{tr}$	-1908.1 [-1889.7]	of quintets	3720
$\text{c-}[\text{PbCl}_2\text{F}_4]^{2-}$	$\text{F}_\text{tr}$		triplet	3414
	$\text{F}_\text{tr}$	-1887.6 [-1874.0]	of triplets	3975
$\text{t-}[\text{PbCl}_2\text{F}_4]^{2-}$	$\text{F}_\text{tr}$	-1843.6 [-1800.4]	quintet	4042
$\text{f-}[\text{PbCl}_2\text{F}_4]^{2-}$	$\text{F}_\text{tr}$	-1920.3 [-1931.8]	quartet	3614
$\text{m-}[\text{PbCl}_2\text{F}_4]^{2-}$	$\text{F}_\text{tr}$		doublet	3685
	$\text{F}_\text{tr}$	-1881.2 [-1858.3]	of triplets	4165
$\text{c-}[\text{PbCl}_4\text{F}_2]^{2-}$	$\text{F}_\text{tr}$	-1973.7 [-1989.6]	triplet	3754
$\text{t-}[\text{PbCl}_4\text{F}_2]^{2-}$	$\text{F}_\text{tr}$	-1945.6 [-1916.1]	triplet	4230
$[\text{PbCl}_5\text{F}]^{2-}$	$\text{F}_\text{tr}$	-2102.6 [-2121.0]	doublet	3774
$[\text{PbCl}_6]^{2-}$		-2326.0 [-2326.0]	singlet	—

<sup>a</sup> ppm from  $\text{Pb}(\text{CH}_3)_4$ . <sup>b</sup> Values for:  $[\text{PbCl}_6]^{2-}$  from 0.3M  $[(n\text{-Bu})_4\text{N}^+]_2[\text{PbCl}_6]^{2-}$  in  $\text{CH}_3\text{CN}$ ;  $[\text{PbF}_6]^{2-}$  and  $[\text{PbClF}_5]^{2-}$  from 0.1M  $6(\text{Et}_4\text{N}^+)_2\text{PbF}_6^{2-}$  :  $1(\text{Et}_4\text{N}^+)_2\text{PbCl}_6^{2-}$  in  $\text{CH}_3\text{CN}$ ; remaining anions from 0.1M  $1(\text{Et}_4\text{N}^+)_2\text{PbF}_6^{2-}$  :  $2(\text{Et}_4\text{N}^+)_2\text{PbCl}_6^{2-}$  in  $\text{CH}_3\text{CN}$ . <sup>c</sup> Calculated using the pairwise additivity model. <sup>d</sup>  $\text{F}_\text{tr}$  = fluorine trans to chlorine,  $\text{F}_\text{tr}$  = fluorine trans to fluorine.

NMR studies involving the central element nucleus (M). Examples of p-block metal complexes studied by NMR spectroscopy include:  $[\text{SnCl}_n\text{F}_{6-n}]^{2-}$  ( $^{19}\text{F}$ ,  $^{117}\text{Sn}$ ),<sup>35,36</sup>  $[\text{PCl}_n\text{F}_{6-n}]^-$  ( $^{19}\text{F}$ ,  $^{31}\text{P}$ ),<sup>37</sup>  $[\text{AsCl}_n\text{F}_{6-n}]^-$  ( $^{19}\text{F}$ ,  $^{75}\text{As}$ ),<sup>38</sup> and  $[\text{SbCl}_n\text{F}_{6-n}]^-$  ( $^{19}\text{F}$ ,  $^{121}\text{Sb}$ ).<sup>39</sup> Analogous studies of transition metal series include:  $[\text{TiCl}_n\text{F}_{6-n}]^{2-}$  ( $^{19}\text{F}$ ),<sup>39</sup>  $[\text{NbCl}_n\text{F}_{6-n}]^-$  ( $^{19}\text{F}$ ,  $^{93}\text{Nb}$ ),<sup>40,41</sup> and  $[\text{TaCl}_n\text{F}_{6-n}]^-$ , ( $^{19}\text{F}$ ).<sup>40</sup> The  $[\text{PbCl}_n\text{F}_{6-n}]^{2-}$  anions represent the first example of an octahedral mixed-ligand series to be synthesized and characterized for a 6p element.

### Geometric Preferences

A preference for the cis and fac configurations (Figure 8) in mixed chlorofluoro species of the type  $[\text{MCl}_n\text{F}_{6-n}]^{m-}$  has been noted in many of the previously studied systems, (e.g.,  $[\text{SnCl}_n\text{F}_{6-n}]^{2-}$ ,  $[\text{AsCl}_n\text{F}_{6-n}]^-$  and  $[\text{SbCl}_n\text{F}_{6-n}]^-$ ),<sup>35,36,38</sup> and the  $[\text{PbCl}_n\text{F}_{6-n}]^{2-}$  series is consistent with this pattern. The relative abundance distributions of these isomers were found to be: for  $[\text{PbCl}_4\text{F}_2]^{2-}$ , cis/trans = 12.5; for  $[\text{PbCl}_3\text{F}_3]^{2-}$ , fac/mer = 2.5; and for  $[\text{PbCl}_2\text{F}_4]^{2-}$ , cis/trans = 15.2. The expected ratios for statistical distribution of these isomers are: cis/trans = 4, fac/mer = 2/3.

The traditional view towards configurational preference has been that cis interactions between bulky ligands give rise to steric repulsions that are greater than those arising from trans interactions and, other factors being equal, the trans isomers will predominate. Where cis isomers predominate, the other

factors are not equal. A number of workers,<sup>42,43,44</sup> have argued that the preference for cis-isomers is due to the existence of ligand  $\rightarrow$  metal  $\pi$ -bonding. Clark, et al<sup>42</sup> suggest that the  $\pi$ -donor ability of the halogens to the  $t_{2g}$  orbitals of the metal is the major factor favoring the cis configuration over the sterically more favorable trans isomer. In the trans configuration, the stronger electron donors would be competing for the same  $t_{2g}$  orbital, whereas, in the cis configuration, the ligands could  $\pi$ -donate into different  $t_{2g}$  orbitals resulting in a more stable complex.

An alternative view presented by Zahrobsky<sup>45</sup> argues on geometric grounds that steric factors alone favour the formation of cis-isomers by octahedral mixed halide complexes, regardless of the size of the ligands, and thereby undercutting the argument that  $\pi$ -bonding is the major factor for the predominance of cis-isomers.

It is not presently possible to state which of the two different views is the correct one.

#### NMR Parameters for the $[PbCl_nF_{6-n}]^{2-}$ Anions, $n = 0 - 6$

##### Fluorine-19 Chemical Shifts

Nuclear shielding is usually discussed according to the formalism developed by Ramsey.<sup>46</sup> The shielding constant ( $\sigma$ ) is expressed as the sum of diamagnetic ( $\sigma^d$ ) and paramagnetic ( $\sigma^p$ ) shielding contributions as shown in equation (23).

$$\sigma = \sigma^d + \sigma^p \quad (23)$$

The  $\sigma^d$  component involves free rotation of electrons about the nucleus whereas the  $\sigma^p$  component involves the restriction to this rotation due to other electrons and nuclei in the molecule. It is generally found that for nuclei other than  $^1\text{H}$ , the paramagnetic term, ( $\sigma^p$ ), provides the dominant changes in the shielding constant ( $\sigma$ ). The  $^{19}\text{F}$  chemical shifts for  $[\text{PbCl}_n\text{F}_{4-n}]^{2-}$  anions are summarized in Table 2. The data show two clear trends: 1) the  $^{19}\text{F}$  chemical shifts move to higher frequency (i.e., become less shielded) with progressive substitution of F ligands by Cl ligands; 2) in those anions where two fluorine environments are present, the chemical shift of the F-trans-F environment always occurs at higher frequency than that for the F-trans-Cl environment. In addition, a plot of the  $^{19}\text{F}$  chemical shift as a function of the number of Cl ligands in the  $[\text{PbCl}_n\text{F}_{4-n}]^{2-}$  anions reveals two straight lines (Figure 16). The two lines arise from the  $\text{F}_e$  and  $\text{F}_a$  ligand environments and are described by the following equations:

$$\delta(^{19}\text{F}_e) = 31.3n - 104.03, \quad R = 0.9999 \quad (24)$$

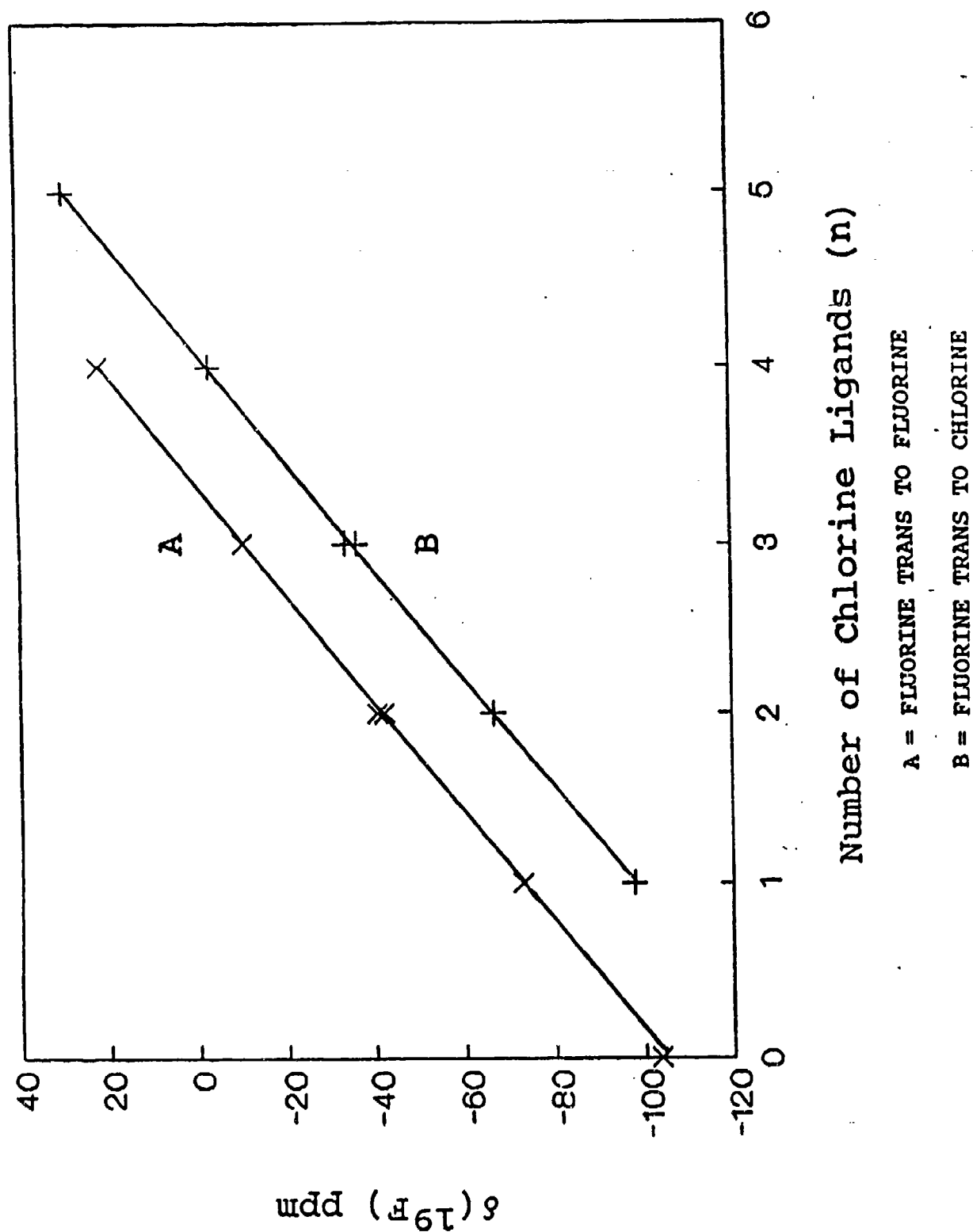
$$\delta(^{19}\text{F}_a) = 31.7n - 129.97, \quad R = 0.9998 \quad (25)$$

where R is the correlation coefficient.

The linear relationships clearly demonstrate the additivity of the  $^{19}\text{F}$  chemical shifts in the  $[\text{PbCl}_n\text{F}_{4-n}]^{2-}$

$\delta(^{19}\text{F})$  VERSUS NUMBER OF CHLORINE LIGANDS (n)  
FOR  $\text{PbCl}_n\text{F}_{6-n}^{2-}$

Figure 16.



series. Similar additivity relationships have also been observed in the  $^{19}\text{F}$  chemical shifts of other  $[\text{MCl}_n\text{F}_{6-n}]^{m-}$  series, (e.g.,  $[\text{SnCl}_n\text{F}_{6-n}]^{2-}$ ,  $[\text{AsCl}_n\text{F}_{6-n}]^{-}$  and  $[\text{SbCl}_n\text{F}_{6-n}]^{-}$ ),<sup>33,34,35</sup> as well as in  $^1\text{H}$  chemical shifts,<sup>47</sup>  $^{13}\text{C}$  chemical shifts<sup>48</sup> in acyclic hydrocarbons,  $\text{RCOR}'$ , and  $^{31}\text{P}$  chemical shifts<sup>49</sup> in phosphonium ions.

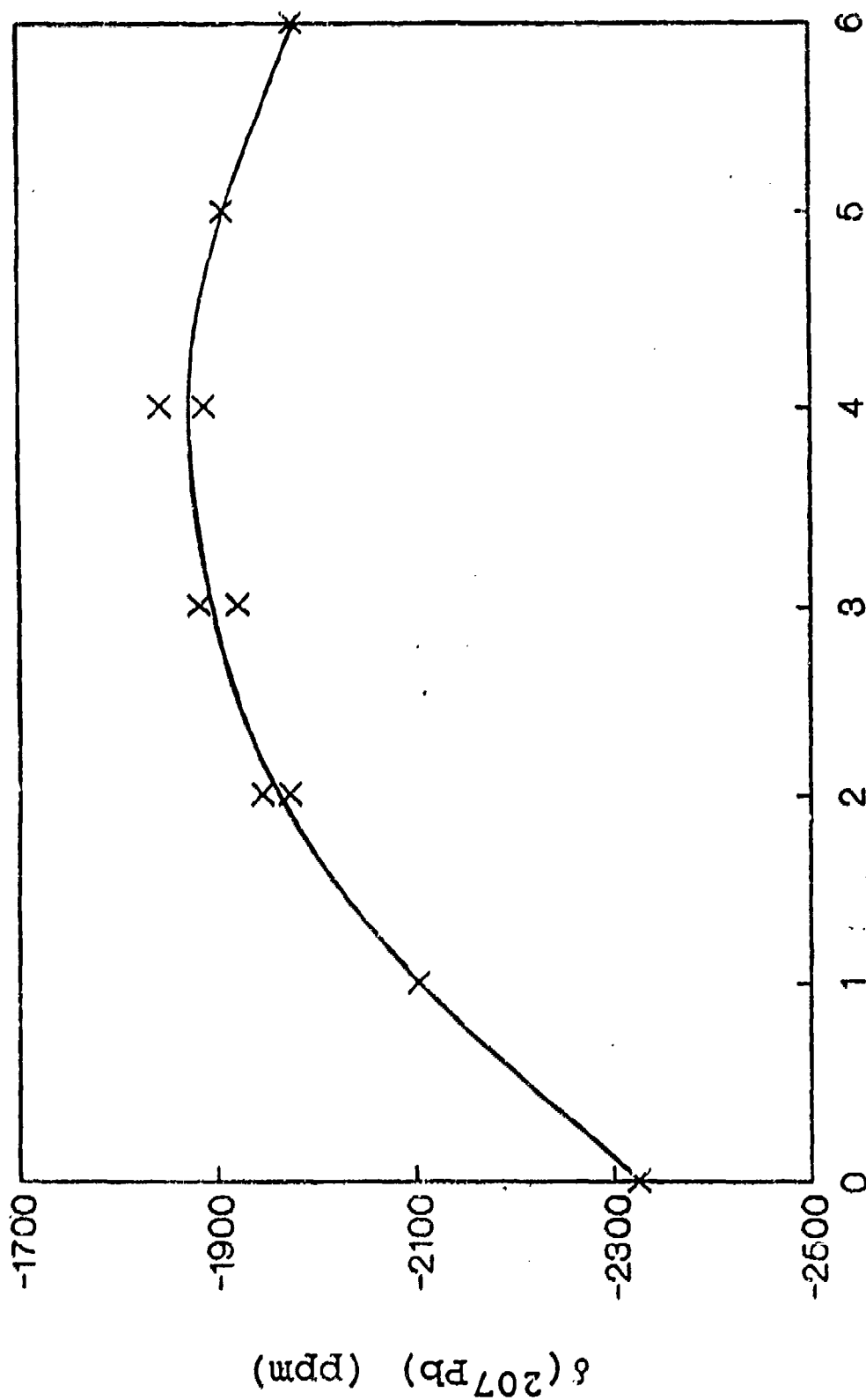
The observed increase in the  $^{19}\text{F}$  chemical shifts as the number of Cl ligands in the anion increases is thought to reflect the dominant influence of changes in the paramagnetic contribution to  $\sigma(^{19}\text{F})$ .<sup>50</sup> The changes in  $\sigma^p$  most likely arise from time-dependent electric dipoles which are mutually induced between the Pb-F and Pb-Cl bonds in the  $[\text{PbCl}_n\text{F}_{6-n}]^{2-}$  anions.<sup>50</sup> Consequently, as the number of Pb-Cl bonds in the anion increases,  $\sigma^p$  increases and so does  $\delta(^{19}\text{F})$ . The effect is expected to be additive, thereby accounting for the observed linear relationships.

#### Lead-207 Chemical Shifts

The  $^{207}\text{Pb}$  NMR chemical shifts for the  $[\text{PbCl}_n\text{F}_{6-n}]^{2-}$  anions are presented in Table 3. A plot of the  $^{207}\text{Pb}$  chemical shift versus the number of F ligands in the anion reveals non-linear relationship with a maximum at the  $^{207}\text{Pb}$  chemical shift for the trans- $[\text{PbCl}_2\text{F}_4]^{2-}$  anion (Figure 17). Furthermore, the shifts cannot be satisfactorily calculated by the pairwise additivity (PWA) model. The PWA model has been very successful in reproducing the shielding pattern of the central nucleus in several

$\delta(^{207}\text{Pb})$  VERSUS NUMBER OF FLUORINE LIGANDS (n)  
FOR  $\text{PbCl}_6\text{-nF}_n^{2-}$

Figure 17.



Number of Fluorine Ligands (n)

octahedral mixed halide systems, (e.g.,  $[\text{SnCl}_n\text{F}_{6-n}]^{2-}$ ,  $[\text{SnBr}_n\text{Cl}_{6-n}]^{2-}$  and  $[\text{SbBr}_n\text{Cl}_{6-n}]^{-}$ ).<sup>30,31</sup> The pairwise additivity model, introduced by Vladimiroff and Malinowski,<sup>40</sup> recognizes the change caused by one substituent in the wave function for all neighbouring substituents. In the use of the pairwise additivity model, the halides are regarded as contributing to the lead shielding in pairs, with 12 independent contributions corresponding to the 12 edges of the octahedron. The chemical shift calculated according to this model is given by the sum of three  $C_{ij}n_{ij}$  terms in which  $n_{\text{Cl-Cl}}$ ,  $n_{\text{F-Cl}}$ , and  $n_{\text{F-F}}$  are the three pairwise additivity parameters and  $C_{ij}$  are the numerical coefficients determined by the structure and summing to 12. Whereas the substituent additive model yields the same calculated shift for cis- and trans-isomers of the same complex, the pairwise additivity model gives calculated shifts that differ, thus providing a method of identifying specific isomers in a solution mixture of several. The  $n_{\text{Cl-F}}$  parameter varies in the  $[\text{PbCl}_n\text{F}_{6-n}]^{2-}$  series and as the model assumes a constant  $\text{O}_h$  geometry, deviations from this idealized structure may account in part for the observed variation in the interaction terms. Although the PWA model does not calculate the  $^{207}\text{Pb}$  chemical shifts successfully, it does predict the general trend in the shifts of the  $[\text{PbCl}_n\text{F}_{6-n}]^{2-}$  anions.

In theory, an increase in the number of more electro-negative ligands (F in this case) attached to the  $^{207}\text{Pb}$  atom should lead to a decrease in the shielding of that nucleus. This



may be correlated with a change in the electron density at the  $^{207}\text{Pb}$  nucleus which gives rise to a diamagnetic contribution ( $\sigma^d$ ) to the shielding of that nucleus. If  $\sigma^d$  provided the dominant contribution to the shielding, then a linear decrease in shielding as the number of fluorine ligands increased would be expected.<sup>50</sup> As this is not observed for the  $^{207}\text{Pb}$  nucleus, the paramagnetic contribution ( $\sigma^p$ ) must be primarily responsible for the observed  $^{207}\text{Pb}$  shifts.<sup>50</sup> According to Jameson and Gutowsky<sup>52</sup>

$$\sigma^p = \frac{-\mu_0 e^2 h^2}{6\pi m^2 \Delta E} (\langle r^{-3} \rangle_{np} P_p + \langle r^{-3} \rangle_{nd} D_d) \quad (26)$$

where  $\Delta E$  is the mean electronic excitation energy,  $\langle r^{-3} \rangle_{np}$  and  $\langle r^{-3} \rangle_{nd}$  are the mean inverse cubes of the p and d electron-nucleus distances, and  $P_p$  and  $D_d$  represent the valence electron imbalance in the p and d orbitals centered on the nucleus in question. The numerical values of  $P_p$  and  $D_d$  depend upon the coordination of the atom and the ionicity of its bonds. The maximum values for  $P_p$  and  $D_d$  are 2 and 12, respectively; both have a minimum value of zero.

The non-additive shielding variation observed for the  $[\text{PbCl}_n\text{F}_{6-n}]^{2-}$  series is a reasonably common phenomenon for octahedral species, e.g.,  $[\text{SnCl}_n\text{F}_{6-n}]^{2-}$ .<sup>35</sup> In a series of closely related tetrahedral or octahedral molecules, the terms  $\Delta E$ ,  $\langle r^{-3} \rangle_{np}$  and  $\langle r^{-3} \rangle_{nd}$  are assumed to remain constant and the observed shielding variation attributable to changes in the  $P_p$

term.<sup>22</sup> It then seems reasonable to attribute the variations in  $^{207}\text{Pb}$  shielding for the  $[\text{PbCl}_n\text{F}_{4-n}]^{2-}$  series to changes in the electron imbalance terms. However, in addition to  $P_\nu$ , the  $D_\nu$  term may also provide a significant contribution to  $\sigma^\nu$ . Such contributions could arise from the Pb 6d orbitals participating in  $\sigma$ - and  $\pi$ -bonding to the chlorine and fluorine ligands.<sup>23</sup>

#### Coupling Constants $^1J(^{207}\text{Pb}-^{19}\text{F})$

The spin-spin coupling constant originates from the interaction of nuclear spins with the surrounding electronic environment. In high-resolution NMR spectroscopy spin-spin coupling is usually dominated by the Fermi contact mechanism. Provided that the Fermi contact mechanism is dominant, one-bond coupling constants can be represented by equation (27).<sup>24</sup>

$$^1J_{AB} = \frac{16\pi^2}{9h} \left( \frac{g\beta h}{2\pi} \right)^2 \gamma_A \gamma_B |\psi_{ns,A}(0)|^2 |\psi_{ns,B}(0)|^2 \kappa_{AB} \quad (27)$$

where,  $|\psi_{ns,A}(0)|^2$  and  $|\psi_{ns,B}(0)|^2$  are the s-electron densities for the ns valance orbitals at the nuclei of atoms A and B,  $\kappa_{AB}$  is the mutual polarizability of the ns orbitals on A and B,  $\gamma_A$  and  $\gamma_B$  are the magnetogyric ratios for nuclei of atoms A and B. Equation (27) demonstrates that the coupling constant is dependent on both the electronic (i.e., s-electron density and  $\kappa_{AB}$ ) and nuclear ( $\gamma_A$  and  $\gamma_B$ ) properties of the coupled nuclei.

A plot of  $^1J(^{207}\text{Pb}-^{19}\text{F})$  coupling constants versus the number of chlorine ligands in the  $[\text{PbCl}_n\text{F}_{4-n}]^{2-}$  series reveals a

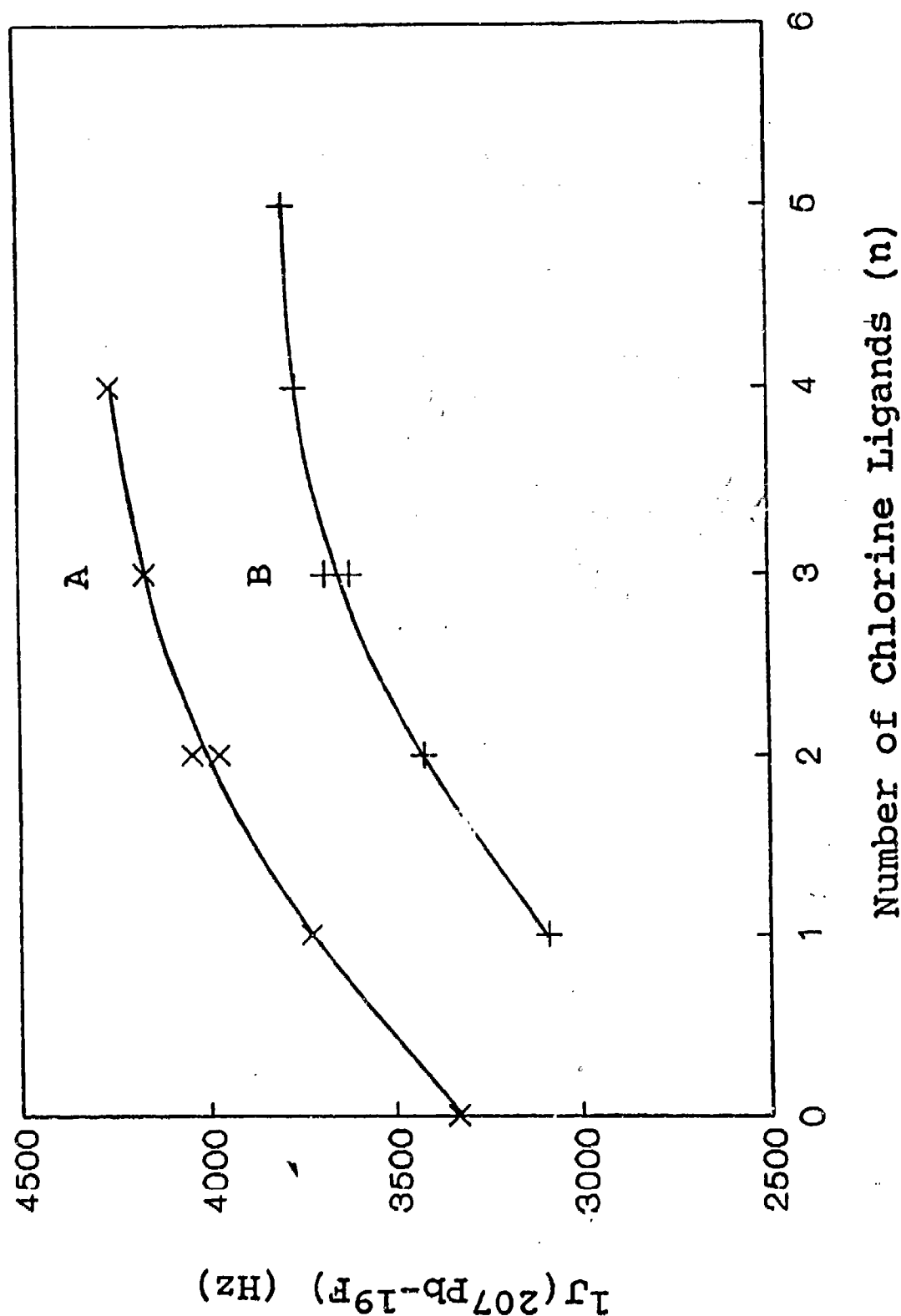
non-linear relationship for both the fluorine trans to fluorine and fluorine trans to chlorine environments (Figure 18). In each case, the coupling constant is greater for the fluorine trans to fluorine ligand environment. The smaller value obtained for the fluorine trans to chlorine ligand environment denotes the greater ionic character of this bond and a decrease in s-electron density at the Pb nucleus. A more detailed discussion would involve the comparison of the reduced coupling constants of  $\text{PbF}_n^{2-}$  with group congeners: Si, Ge and Sn and the adjacent group anion,  $\text{BiF}_n^-$ . The importance of relativistic effects on the s-electron densities for the ns valence orbitals of the  $[\text{PbCl}_n\text{F}_{4-n}]^{2-}$  series would also be compared with the  $[\text{SnCl}_n\text{F}_{4-n}]^{2-}$  series.

#### Lead-207 Linewidths

Increase in linewidth  $\Delta\nu_{1/2}$  from 3 Hz ( $\text{PbF}_4^{2-}$ ) to 63 Hz ( $\text{PbCl}_4^{2-}$ ), demonstrates that the  $^{207}\text{Pb}$  linewidth increases as the number of Cl ligands increases. The increase may be a result of  $^{207}\text{Pb}$ - $^{35,37}\text{Cl}$  induced isotopic shifts or due to a contribution from scalar relaxation of the second kind, through  $^1J(^{207}\text{Pb}-^{35,37}\text{Cl})$ , to  $T_2(^{207}\text{Pb})$ . Since  $\Delta\nu_{1/2} = (\pi T_2)^{-1}$ , the linewidth is expected to increase with the number of Pb-Cl bonds in the anion. Scalar relaxation of the second kind, through  $^1J(^{207}\text{Pb}-^{35,37}\text{Cl})$ , has found to be an important relaxation mechanism for  $^{207}\text{Pb}$  in  $\text{PbCl}_4^{2-}$ .

$1J(207\text{Pb}-19\text{F})$  VERSUS NUMBER OF CHLORINE LIGANDS (n)  
FOR  $\text{PbCl}_n\text{F}_{6-n}^{2-}$

Figure 18.



## Pentafluoroorthotellurate Derivatives of Lead(IV)

### Synthesis of $\text{Pb}(\text{OTeF}_5)_4$

The reaction of  $\text{PbF}_4$  with  $\text{B}(\text{OTeF}_5)_3$  produced a light yellow solid suspended in a clear colourless liquid. The solid did not give a Raman spectrum, and as a consequence, no conclusions could be drawn as to the nature of the product.

The second preparative attempt involved the reaction of  $\text{PbF}_4$  with  $\text{HOTeF}_5$ . The amount of solid present in the mixture did not vary throughout the reaction and was concluded to be unreacted  $\text{PbF}_4$ . As a consequence, no further characterization was performed on the reaction product.

The failure to prepare  $\text{Pb}(\text{OTeF}_5)_4$  by either of these two methods is probably due to the reasons described on page 39.

### Synthesis of $(\text{Et}_4\text{N}^+)_2\text{Pb}(\text{OTeF}_5)_6^{2-}$

The reaction of  $(\text{Et}_4\text{N}^+)_2\text{PbCl}_6^{2-}$  with  $\text{AgOTeF}_5$  produced a clear pale green solution. The  $^{19}\text{F}$  spectrum of the solution displayed an  $\text{AB}_4$  nuclear spin system,<sup>5a</sup> with  $\delta_A = -26.4$  ppm,  $\delta_B = -39.7$  ppm,  $J_{AB} = 176.9$  Hz and  $R = J_{AB}/\delta_{AB} = 0.023$ . The  $^{207}\text{Pb}$  spectrum consisted of one broad 346 Hz peak ( $\delta(^{207}\text{Pb}) = -2344.1$  ppm) exhibiting no fine structure or  $^{125}\text{Te}$  satellites. The appearance of this spectrum indicated that rapid intermolecular  $\text{OTeF}_5^-$  anion exchange was occurring at room temperature.

A pale green solution was also produced from the reaction of

$(\text{Et}_4\text{N}^+)_2\text{PbCl}_6^{2-}$  with  $\text{Xe}(\text{OTeF}_5)_2$ . The  $^{19}\text{F}$  spectrum of the solution revealed an almost first-order  $\text{AX}_4$  nuclear spin system (see Figure 19), as well as an  $\text{AB}_4$  pattern arising from the excess  $\text{Xe}(\text{OTeF}_5)_2$ . The  $^{19}\text{F}$  NMR values obtained for the  $\text{Pb}(\text{OTeF}_5)_6^{2-}$  anion were,  $\delta_A = -30.7903$  ppm,  $\delta_B = -43.0$  ppm,  $J_{AB} = 178.2$  Hz and  $R = 0.010$ . The  $^{207}\text{Pb}$  spectrum consisted of one broad 344 Hz peak at  $\delta(^{207}\text{Pb}) = -2393.7$  ppm, but no evidence of  $^{125}\text{Te}$  satellites or fine structure. This indicated that rapid intermolecular  $\text{OTeF}_5^-$  anion exchange was occurring at room temperature. A possible exchange mechanism is presented in equation (28).



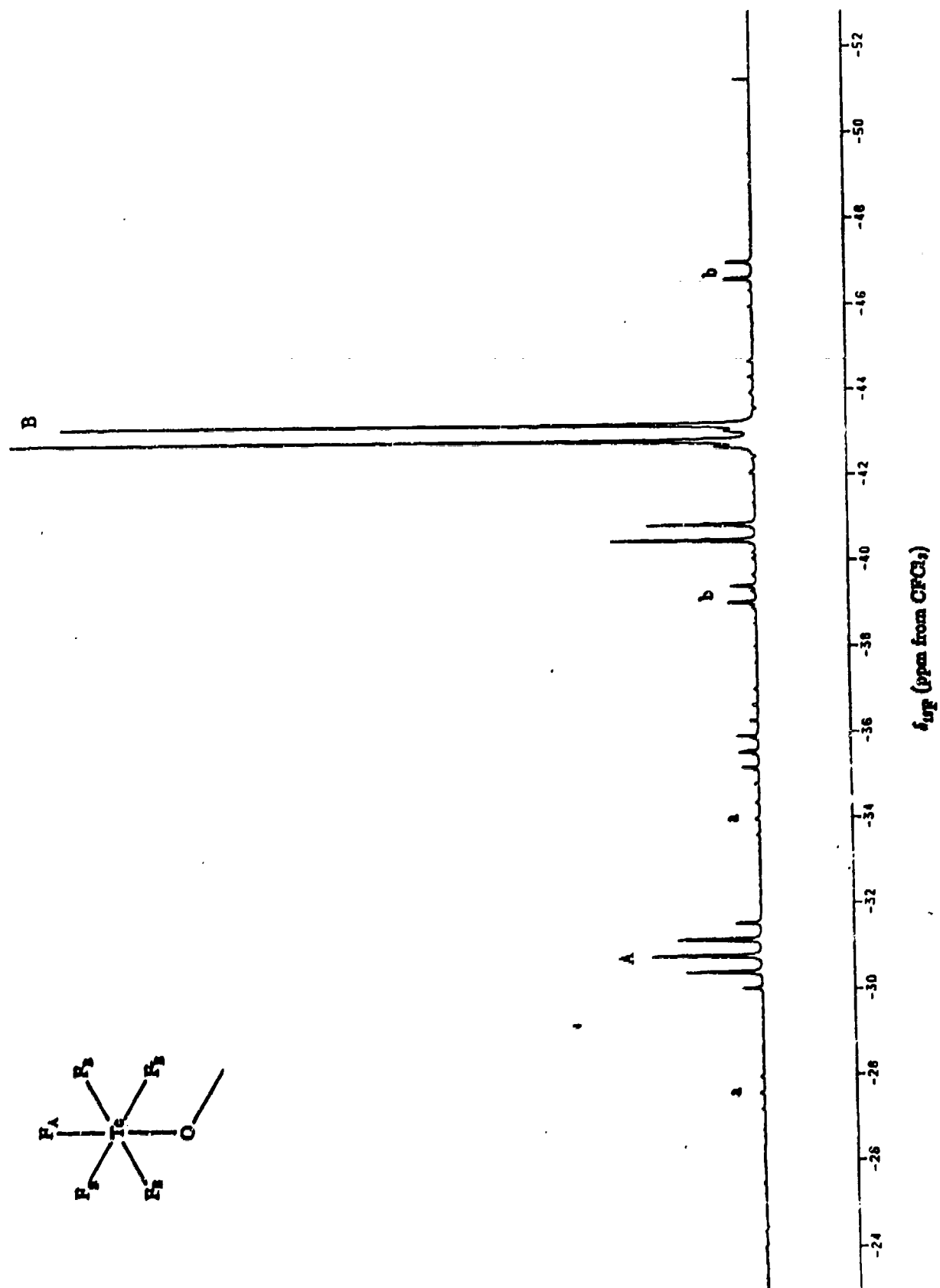
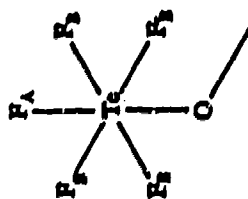


Figure 19.  $^{19}\text{F}$  NMR Spectrum (470.599 MHz) of  $(\text{Et}_4\text{N})_2\text{Pb}(\text{OTeF}_5)_2$  in dry  $\text{CH}_3\text{CN}$  at room temperature. Lower case letters denote  $^{125}\text{Te}$  satellites.

### CONCLUSIONS AND DIRECTIONS FOR FUTURE RESEARCH

The research for this thesis involved the synthesis of novel fluoro, mixed chlorofluoro and  $\text{OTeF}_5$  derivatives of lead(IV).  $(\text{Et}_4\text{N}^+)_2\text{PbF}_6^{2-}$  was the first  $[\text{PbF}_6]^{2-}$  salt containing an organic cation successfully synthesized and characterized. The  $[\text{PbF}_6]^{2-}$  anion has been shown to have an octahedral geometry in solution by  $^{19}\text{F}$  and  $^{207}\text{Pb}$  NMR spectroscopy. The synthesis and characterization of the  $(\text{Et}_4\text{N}^+)_2\text{PbCl}_n\text{F}_{6-n}^{2-}$  anions demonstrated the additivity of  $^{19}\text{F}$  chemical shifts in these octahedral fluorocomplexes, the dominance of the paramagnetic contribution to  $^{207}\text{Pb}$  shielding constants, and the preference for the cis- and fac-isomers in solution. In the characterization of the new  $[\text{Pb}(\text{OTeF}_5)_4]^{2-}$  anion it was found that rapid intermolecular  $\text{OTeF}_5^-$  anion exchange was occurring in solution at room temperature.

There are a variety of directions that this research can take in the future:

- 1) Vibrational spectra for  $(\text{Et}_4\text{N}^+)_2\text{PbF}_6^{2-}$ .
- 2) The synthesis of the  $[(n\text{-Bu})_4\text{N}^+]_2\text{PbCl}_n\text{F}_{6-n}^{2-}$  anions by ligand redistribution of  $[(n\text{-Bu})_4\text{N}^+]_2\text{PbF}_6^{2-}$  with  $[(n\text{-Bu})_4\text{N}^+]_2\text{PbCl}_6^{2-}$  would allow better characterization of the chlorine-rich  $\text{PbCl}_n\text{F}_{6-n}^{2-}$ ,  $n = 1$  and  $2$ , anions by an increasing the solubility of these species.
- 3) The synthesis of  $\text{Pb}(\text{OTeF}_5)_4$  can be reexamined using  $\text{PbF}_4$  prepared by a low temperature reaction of  $\text{KrF}_2$  and  $\text{PbF}_2$ .
- 4) Characterization of the  $[\text{Pb}(\text{OTeF}_5)_4]^{2-}$  anion in  $\text{CH}_2\text{Cl}_2$  by NMR



spectroscopy at low temperatures to determine whether the ligand exchange reaction can be slowed or stopped. The  $[\text{Pb}(\text{OTeF}_3)_4]^{2-}$  anion could then prove to be useful in stabilizing high oxidation state cations.

5) Extention of the investigation by the synthesis and characterization of the fluoro and  $\text{OTeF}_3$  derivatives of  $\text{Sn}(\text{IV})$  and  $\text{Ge}(\text{IV})$ .

### REFERENCES

1. R.S. Drago, J. Phys. Chem. 62 (1958) 353-357.
2. P. Pyykkö, Chem. Rev. 88 (1988) 563.
3. R. Hoppe, W. Dähne, Naturwissenschaften 49 (1962) 254.
4. G. Kauffman, L. Kim, D. Marino, Inorganic Synthesis 22 (1983) 149.
5. M. Baudler, "Handbook of Preparative Inorganic Chemistry". G. Brauer, Ed., Academic Press, New York, Vol. 1 (1963) p.750.
6. J.H. Hildebrand, J. Chem. Phys. 15(10) (1947) 727.
7. N. Greenwood and A. Earnshaw, "Chemistry of the Elements", Pergamon Press, Toronto, (1984) p.444
8. G.L. Clark, J. Am. Chem. Soc. 41 (1919) 1477.
9. B.Z. Brauner, J. Chem. Soc. 65 (1894) 393.
10. K.O. Christie, Inorg. Chem. 25 (1986) 3721.
11. M.F.A. Dove, J. Chem. Soc. (1959) 3722-3725.
12. P.A.W. Dean, D.F. Evans, J. Chem. Soc. (A) (1967) 698.
13. K. Seppelt, Angew. Chem. Int. Ed. Engl. 21 (1982) 877-888.
14. T. Birchall, R.D. Myers, H. deWaard, G.J. Schrobilgen, Inorg. Chem. 21 (1982) 1068.
15. D. Lentz, H. Pritzkow, K. Seppelt, Angew. Chem. Int. Ed. Engl. 16 (1977) 729.
16. D. Lentz, H. Pritzkow, K. Seppelt, Inorg. Chem. 17 (1978) 1926.
17. D. Lentz, K. Seppelt, Angew. Chem. Int. Ed. Engl. 18 (1976) 66.
18. E. Jacob, D. Lentz, K. Seppelt, A. Simon, Z. Anorg. Allg. Chem. 472 (1981) 66.
19. K. Schödel, F. Sladky, Chem. Ber. 113 (1980) 1414.
20. E. Jacob, D. Lentz, K. Seppelt, A. Simon, Z. Anorg. Allg. Chem. 472 (1981) 7.

21. F. Sladky, H. Kropshofer, O. Leitzke, J. Chem. Soc. Chem. Commun. (1973), 134.
22. H. Kropshofer, O. Leitzke, P. Peringer, F. Sladky, Chem. Ber. 114 (1981) 2644.
23. S. Strauss, M. Noirot, O. Anderson, Inorg. Chem. 24 (1985) 4308.
24. F. Sladky, Angew. Chem. Int. Ed. Engl. 8(4) (1969) 523.
25. W. Falconer and W. Sunder, J. Inorg. Nucl. Chem. 29 (1967) 1380.
26. R.G. Syrvet, Ph.D. Thesis, McMaster University, (1986) 58.
27. J.M. Winfield, J. Fluor. Chem. 25 (1984) 92.
28. R.G. Syrvet, Ph.D. Thesis, McMaster University, (1986).
29. J. Barr, R.J. Gilliespie, R.C. Thompson, Inorg. Chem. 3 (1964) 1149.
30. H.V. Wartenburg, Z. Anorg. Chem. 244 (1940) 254.
31. F. Sladky, Inorg. Synth. 24 (1983) 33.
32. Personal communication with B. Zemva.
33. T. Mitchell, J. Gmehling, and F. Huber J. Chem. Soc., Dalton Trans. (1978) 960.
34. G. Schrobilgen and B. Sayer, J. Magn. Res. 52(1) (1983) 139.
35. P.A.W. Dean, D.F. Evans, J. Chem. Soc. (A) (1968) 1154.
36. K.B. Dillon and A. Marshall, J. Chem. Soc. Dalton Trans. (1984) 1245.
37. E.G. Il'in, M.N. Shcherbakova, and Yu.A. Buslaev, Koord. Khim. 1 (1975) 1179.
38. M.F.A. Dove and J.C.P. Sanders, J. Chem. Soc. Chem. Commun. (1984) 1548.
39. P.A.W. Dean and B.J. Ferguson, Can. J. Chem. 52(4) (1974) 667.
40. Yu.A. Buslaev and E.G. Il'in, J. Fluor. Chem. 4 (1974) 271.

41. E. Il'in, V. Tarasov, M. Ershova, V. Ermakov, M. Glushova, and Yu. Buslaev, Soviet J. Coord. Chem. Int. Ed. Engl. 4(9) (1978) 1370.
42. R.J. Clark, L. Maresca and R.J. Puddephatt, Inorg. Chem. 7 (1968) 1603.
43. H.H. Jaffé, J. Phys. Chem. 58 (1954) 185.
44. D.C. Bradley and C.E. Holloway, J. Chem. Soc. Chem. Commun. (1965) 284.
45. R.F. Zahrobsky, J. Am. Chem. Soc. 93 (1971) 3313.
46. N.F. Ramsey, Phys. Rev. 91 (1953) 303.
47. J.N. Shoolery, "Technical Information Bulletin", Varian Associates, Palo Alto, California, 2(1959) No. 3.
48. E.R. Malinowski, T. Vladimiroff, and R.F. Tavares, J. Phys. Chem. 70 (1962) 2046.
49. S.O. Grim, W. McFarlane, E.F. Davidoff and T.J. Marks, J. Phys. Chem. 70 (1966) 581.
50. R.K. Harris and B.E. Mann, "NMR and the Periodic Table", Academic Press, New York, (1978) p.188.
51. R.G. Kidd, H.G. Spinney, Can. J. Chem. 59 (1981) 2940.
52. C. Jameson and H.S. Gutowsky, J. Chem. Phys. 40 (1964) 1714.
53. J.C.P. Sanders, Ph.D. Thesis, Nottingham University (1986).
54. J.A. Pople and D.P. Santry, Mol. Phys. 8 (1964) 1.
55. R.M. Hawk and R.R. Sharp, J. Chem. Phys. 60 (1974) 1109.
56. R.K. Harris and K.J. Parker, J. Chem. Soc., (1961) 4736.

PART XI

ON THE EXISTENCE OF PENTACOORDINATED NITROGEN,  $\text{NF}_5$ ;  
AN  $^{18}\text{F}$  RADIOTRACER STUDY

Contribution from Rocketdyne, A Division of Rockwell International, Canoga Park, California 91303,  
 Department of Chemistry, McMaster University, Hamilton, Ontario, Canada L8S 4M1,  
 Department of Nuclear Medicine, Chedoke-McMaster Hospitals, Hamilton, Ontario, Canada L8N 3Z5,  
 and Loker Hydrocarbon Research Institute and Department of Chemistry,  
 University of Southern California, Los Angeles, California 90089

## On the Existence of Pentacoordinated Nitrogen

Karl O. Christe,<sup>\*1a</sup> William W. Wilson,<sup>1a</sup> Gary J. Schrobilgen,<sup>1b</sup> Raman V. Chirakal,<sup>1c</sup>  
 and George A. Olah<sup>1d</sup>

Received September 3, 1987

The thermal decomposition of  $\text{NF}_4\text{HF}_2$  was studied by using  $^{18}\text{F}$ -labeled  $\text{HF}_2^-$ . The observed distribution of  $^{18}\text{F}$  among the decomposition products indicates that within experimental error the attack of  $\text{HF}_2^-$  on  $\text{NF}_4^+$  occurs exclusively on fluorine and not on nitrogen, contrary to the predictions based on bond polarities. These results confirm the previous suggestion that the lack of pentacoordinated nitrogen species is due mainly to steric reasons.

### Introduction

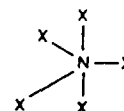
Hypervalency, hypercoordination, and formal expansion of the valence octet for first-row elements are and have been the subject of considerable interest and controversy.<sup>2</sup> Whereas hypercoordinated carbon<sup>3</sup> or boron<sup>4</sup> species are well-known, convincing experimental evidence has not been presented so far for the existence of hypercoordinated nitrogen.

It was speculated that pentacoordinated  $\text{NF}_5$  is formed either from  $\text{NF}_3\text{-F}_2$  by fission-fragment radiolysis at room temperature<sup>5</sup> or irradiation with 3-MeV bremsstrahlung<sup>6</sup> at  $-196^\circ\text{C}$  or from  $\text{NF}_4\text{AsF}_6$  by pyrolysis at  $175^\circ\text{C}$ .<sup>7</sup> However, all attempts have failed to confirm these speculations by either matrix isolation experiments,<sup>7,8</sup> low-temperature photolysis,<sup>9</sup> kinetic studies<sup>10</sup> or isotopic exchange studies.<sup>11</sup>

A second pentacoordinated nitrogen species that has been studied experimentally is  $\text{NH}_5$ . On the basis of hydrogen-deuterium exchange experiments between either molten  $\text{NH}_4^+$  salts and  $\text{LiD}$  or  $\text{ND}_4^+$  salts and  $\text{LiH}$ , the possible intermediacy of pentacoordinated  $\text{NH}_4\text{D}$  or  $\text{ND}_4\text{H}$  was postulated.<sup>12</sup> However, it was subsequently shown that the observed  $\text{H}_2$  to  $\text{D}_2$  ratios greatly exceeded those expected for the formation of an intermediate  $\text{NH}_4\text{D}$  or  $\text{ND}_4\text{H}$ , and a catalytic isotope exchange reaction of the formed  $\text{HD}$  gas must be involved.<sup>13</sup>

Theoretical calculations have been carried out for  $\text{NF}_5$ ,<sup>14,15</sup>  $\text{NH}_5\text{F}_2$ ,<sup>16</sup> and  $\text{NH}_5$ .<sup>12,17,18</sup> In all cases it has been found that the

pentacoordinated  $\text{NX}_5$  species are unstable with respect to decomposition to  $\text{NX}_3 + \text{X}_2$  and are less stable than the corresponding ion pairs  $\text{NX}_4^+\text{X}^-$ . Of the various geometries possible for a pentacoordinated  $\text{NX}_5$  species, the trigonal-bipyramidal  $D_{3h}$  structure with two symmetrical axial bonds, i.e.



was generally found to be most favorable. Interestingly, however, it was found for  $\text{NH}_5\text{F}_2$  that the  $D_{3h}$  geometry is only a saddle point and that the molecule is stabilized by relaxation to a  $C_{3v}$  structure that essentially is an ion pair  $\text{NH}_4^+\text{F}^-$  with only one F atom in the first coordination sphere and the second F atom at 2.00 Å from the nitrogen atom.<sup>16</sup> This behavior suggests that there is not enough space around nitrogen for five ligands and that steric reasons are mainly responsible for the nonexistence of a pentacoordinated nitrogen.<sup>19</sup>

In view of the previous failures of the experimentalists and the above conclusions by the theoreticians, the existence of a stable pentacoordinated nitrogen species is unlikely. This, however, would not preclude the possible existence of a pentacoordinate nitrogen species as a short-lived unstable intermediate, provided nitrogen could sterically accommodate five ligands. Consequently, we sought to obtain a conclusive answer to the question of whether nitrogen can sterically accommodate five ligands in its first coordination sphere.

### Experimental Section

A Teflon-FEP ampule equipped with a Kel-F valve was passivated with  $\text{F}_2$  and  $\text{NF}_4\text{PF}_6$  (0.854 mmol) and dry  $\text{CsF}^{20}$  (0.809 mmol) were added in the drybox. Fluorine-18 labeled HF was prepared by combining a  $\text{Ne}/[^{18}\text{F}]\text{F}_2$  mixture, which was accelerator produced under conditions previously described<sup>21</sup> except for using a 15-MeV beam, with 1 atmosphere of  $\text{H}_2$  at  $-196^\circ\text{C}$  in a 150-mL nickel can containing unlabeled anhydrous<sup>22</sup> HF (2.35 mmol). The  $\text{H}_2$  and Ne were pumped off at  $-196^\circ\text{C}$ , and the radioactivity of the HF was measured. The labeled HF was condensed at  $-196^\circ\text{C}$  into the Teflon reactor, and its contents were warmed first to room temperature. While the reactor was gradually warmed to  $100^\circ\text{C}$  over 1 h, the volatile products were pumped through a  $1/4$ -in. Teflon-FEP cold trap kept at  $-130^\circ\text{C}$ , followed by a soda lime scrubber and a second Teflon-FEP cold trap kept at  $-210^\circ\text{C}$ . The  $-130$

- (1) (a) Rocketdyne. (b) McMaster University. (c) Chedoke-McMaster Hospitals. (d) University of Southern California.
- (2) See for example: Arduengo, A. *Chem. Eng. News* 1983, 61 (Nov. 28), 3. Martin, J. C. *Science (Washington, D.C.)* 1983, 221, 509. Schleyer, P. v. R. *Chem. Eng. News* 1984, 62 (May 28), 4. Martin, J. C. *Chem. Eng. News* 1984, 62 (May 28), 4. Harcourt, R. D. *Chem. Eng. News* 1985, 63 (Jan. 21), 3.
- (3) Olah, G. A.; Klopman, G.; Schlossberg, R. H. *J. Am. Chem. Soc.* 1969, 91, 3261. Hogeveen, H.; Gaasbeek, C. J.; Bickel, A. F. *Recl. Trav. Chim. Pays-Bas* 1969, 88, 763.
- (4) Mesmer, R. E.; Jolly, W. L. *Inorg. Chem.* 1962, 1, 608. Kreevoy, M. M.; Hutchins, J. E. C. *J. Am. Chem. Soc.* 1972, 94, 6371. Olah, G. A.; Mo, Y. K.; Westerman, P. W.; Klopman, G. *J. Am. Chem. Soc.* 1972, 94, 7859.
- (5) Miller, A. R.; Tsukimura, R. R.; Velten, R. *Science (Washington, D.C.)* 1967, 688.
- (6) Goetschel, C. T.; Campanile, V. A.; Curtis, R. M.; Loos, K. R.; Wagner, C. D.; Wilson, J. N. *Inorg. Chem.* 1972, 11, 1696.
- (7) Solomon, I. J.; Keith, J. N.; Snelson, A. *J. Fluorine Chem.* 1972/73, 2, 129.
- (8) Christe, K. O.; Wilson, W. W., unpublished results.
- (9) Christe, K. O.; Schack, C. J.; Wilson, R. D. *Inorg. Chem.* 1976, 15, 1275.
- (10) Christe, K. O.; Wilson, R. D.; Goldberg, I. B. *Inorg. Chem.* 1979, 18, 2572.
- (11) Keith, J. N.; Solomon, I. J.; Sheft, I.; Hyman, H. *J. Inorg. Nucl. Chem. Suppl.* 1976, 143.
- (12) Olah, G. A.; Donovan, D. J.; Shen, J.; Klopman, G. *J. Am. Chem. Soc.* 1975, 97, 3559.
- (13) Johnson, R. W.; Holm, E. R. *J. Am. Chem. Soc.* 1977, 99, 8077.
- (14) Murrell, J. N.; Scollary, C. E. *J. Chem. Soc., Dalton Trans.* 1976, 818.
- (15) Peters, N. J. S. Dissertation, Princeton University, 1982.

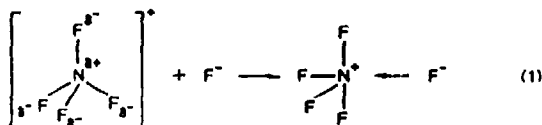
- (16) Keil, F.; Kutzelnigg, W. *J. Am. Chem. Soc.* 1975, 97, 3623.
- (17) Morosi, G.; Simonetta, M. *Chem. Phys. Lett.* 1977, 47, 396.
- (18) Gründler, W.; Schädler, H. D. *Z. Chem.* 1980, 20, 111.
- (19) Wallmeier, H.; Kutzelnigg, W. *J. Am. Chem. Soc.* 1979, 101, 2804.
- (20) Dewar, M. J. S.; Healy, E. *Organometallics* 1982, 1, 1705.
- (21) Christe, K. O.; Wilson, W. W.; Wilson, R. D. *Inorg. Chem.* 1980, 19, 1494.
- (22) Chirakal, R.; Firna, G.; Schrobilgen, G. J.; McKay, J.; Garnett, E. S. *Int. J. Appl. Radiat. Isot.* 1984, 35, 401.
- (23) Christe, K. O.; Wilson, W. W.; Schack, C. J. *J. Fluorine Chem.* 1978, 11, 71.

$^{\circ}\text{C}$  trap contained the HF and the  $-210^{\circ}\text{C}$  trap the  $\text{NF}_3$ , and the soda lime scrubber absorbed the  $\text{F}_2$ . The relative activity distribution, corrected for the elapsed time, was continuously monitored during the course of the experiment. The quantitative nature of the reaction was confirmed in a separate experiment by its material balance using unlabeled reagents under identical conditions.

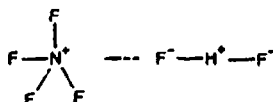
### Results and Discussion

A major drawback of the previously studied  $\text{NH}_4^+ - \text{H}^-$  system<sup>12</sup> is the unfavorable polarity of the N-H bonds. Since in  $\text{NH}_4^+$  the positive charge resides on the protons and the negative one on the nitrogen, the negatively charged  $\text{H}^-$  anion should attack on a proton ligand and not on the nitrogen as required for a pentacoordinated nitrogen transition state. This conclusion has been confirmed by an ab initio study, which showed that in the hydrogen abstraction reaction the pentacoordinated  $D_{3h}$  structure does not intervene either as an intermediate or a transition state. The  $\text{H}^-$  ion can abstract a proton from  $\text{NH}_4^+$  along a continuous downhill energy path.<sup>17</sup>

This drawback of unfavorable bond polarities can be overcome by the  $\text{NF}_4^+ - \text{F}^-$  system. In  $\text{NF}_4^+$  the N-F bonds have the desired polarity for an attack of  $\text{F}^-$  on nitrogen, i.e.



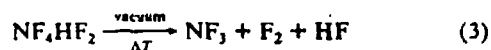
Since  $\text{NF}_4^+ \text{F}^-$  is unknown<sup>23</sup> and because in the solvents known to be compatible with  $\text{NF}_4^+$ , such as HF or halogen fluorides, the  $\text{F}^-$  forms complex fluoro anions, we have studied the attack of a complex fluoro anion on  $\text{NF}_4^+$ . The  $\text{HF}_2^-$  anion appeared to be the ideal candidate because of the low thermal stability of its  $\text{NF}_4^+$  salt<sup>20</sup> and its linear, highly polar structure presenting no additional steric hindrance compared to a free  $\text{F}^-$  anion, i.e.



The  $\text{NF}_4^+ \text{HF}_2^-$  salt can be generated from  $\text{NF}_4\text{PF}_6$  and  $\text{CsHF}_2$  in a minimal amount of anhydrous HF as a solvent.



The  $\text{NF}_4\text{HF}_2$ , which is stable at room temperature in an excess of HF, decomposes on removal of HF in a dynamic vacuum between 25 and  $100^{\circ}\text{C}$  with  $\text{NF}_3$  and  $\text{F}_2$  evolution.<sup>20</sup>



By the use of  $^{18}\text{F}$  labeled  $\text{HF}_2^-$  and a radioassay of the decom-

Table I. Distribution of  $^{18}\text{F}$  in the Reaction Products from the Pyrolysis of  $\text{NF}_4\text{F} \cdot 2.9\text{HF}$

product	found	$^{18}\text{F}$ activity, mCi	
		calcd for attack on	
		N	F
$\text{F}_2$	2.85	4.2	2.95
HF	8.2	6.1	8.55
$\text{CsPF}_6$	17.6	12.6	17.7
$\text{NF}_3$	$1.2 \times 10^{-3}$	6.3	0
tot. activity	28.6	29.2	29.2

position products, one then can distinguish between attack of  $\text{HF}_2^-$  on nitrogen or fluorine of  $\text{NF}_4^+$ . If there is no steric hindrance, i.e. if nitrogen can coordinate to five fluorine atoms, the  $\text{HF}_2^-$  should attack on nitrogen because of the more favorable Coulomb forces, and hence this should result in statistical scrambling of the  $^{18}\text{F}$  among  $\text{NF}_3$ ,  $\text{F}_2$ , and HF. If, however, nitrogen can coordinate to only four fluorine atoms, then  $\text{HF}_2^-$  must attack  $\text{NF}_4^+$  at a fluorine ligand. In this case all the activity should be found in  $\text{F}_2$  and HF and none in the  $\text{NF}_3$ . Since the  $\text{PF}_6^-$  anion can readily exchange with the labeled  $\text{HF}_2^-$  anion in HF solution, the  $\text{CsPF}_6$  residue which is left after completion of steps 2 and 3 should also contain a statistical amount of activity.

The results of our study are summarized in Table I. As can be seen, the  $^{18}\text{F}$  balance is excellent and the observed data are compatible only with attack of  $\text{HF}_2^-$  on the fluorine and not the nitrogen atom of  $\text{NF}_4^+$ . The fact that a small activity reading was observed for  $\text{NF}_3$  should not be interpreted as a small contribution of competing attack on nitrogen but is rather due to slight variation of the radiation background level and the associated difficulty in measuring relatively small radiation values.

In conclusion, it can be stated that within experimental error the  $\text{HF}_2^-$  attack on  $\text{NF}_4^+$  occurs exclusively on the fluorine atoms. Since the polarities of the bonds in both  $\text{NF}_4^+$  and  $\text{HF}_2^-$  would favor attack on nitrogen, the lack of attack on nitrogen is attributed to steric reasons. In view of the small size of fluorine and its ability to achieve maximum coordination numbers for most elements, the existence of pentacoordinated nitrogen species containing ligands other than fluorine must be judged even less likely, except for hydrogen, which has a smaller covalent radius than fluorine.

**Acknowledgment.** The work at both Rocketdyne and McMaster University was financially supported by the Air Force Astronautics Laboratory, Edwards AFB, and that at USC by the National Science Foundation. The authors would also like to thank Prof. J. M. Winfield for his efforts during the initial stage of this study, Dr. J. Kuehner and H. Harms for their assistance with the production of  $^{18}\text{F}$ , and Dr. S. Garnett for the use of the facilities of the Nuclear Medicine Department.

**Registry No.**  $\text{NF}_4\text{HF}_2$ , 71485-49-9;  $\text{F}_2$ , 7782-41-4; HF, 7664-39-3;  $\text{CsPF}_6$ , 16893-41-7;  $\text{NF}_3$ , 7783-54-2;  $\text{CsHF}_2$ , 12280-52-3;  $\text{NF}_4\text{PF}_6$ , 58702-88-8.

(23) Nikitin, I. V.; Rosolovskii, V. Ya. *Usp. Khim.* 1985, 54, 722.